ROYAUME DU MAROC
UNIVERSITE MOHAMMED V DE RABAT
FACULTE DE MEDECINE
ET DE PHARMACIE
RABAT

Year : 2021 **Thesis N°: 171**

CADAVERIC STUDY OF THE ENDOSCOPIC APPROACH OF THE CAVERNOUS SINUS

THESIS

Publicly submitted and defended on the : / /2021

BY

Mrs. Mouna YOUJILE
Born on September 21st, 1995 in Meknès

FOR THE DEGREE OF
Doctor of Medicine

Key Words : Cavernous sinus; Cadaveric study; Endoscopy

Jury Members:

Mr. Miloudi GAZZAZ Professor of Neurosurgery	**President**
Mr. Abas Cherif EL ASRI Professor of Neurosurgery	**Director**
Mr. Yasser ARKHA Professor of Neurosurgery	**Member**
Mr. Adil BELHACHMI Professor of Neurosurgery	**Member**
Mr. Mohamed ZALAGH Professor of OtoRhinoLaryngology	**Member**


قال تعالى في كتابه الكريم
وقل رب زدني علما
١٤٣٥

UNIVERSITE MOHAMMED V
FACULTE DE MEDECINE ET DE PHARMACIERABAT

DOYENS HONORAIRES :

1962 - 1969: Professeur Abdelmalek FARAJ
1969 - 1974: Professeur Abdellatif BERBICH
1974 - 1981: Professeur Bachir LAZRAK
1981 - 1989: Professeur Taieb CHKILI
1989 - 1997: Professeur Mohamed Tahar ALAOUI 1997 - 2003: Professeur Abdelmajid BELMAHI
2003 - 2013: Professeur Najia HAJJAJ - HASSOUNI

ADMINISTRATION :

Doyen :
Professeur Mohamed ADNAOUI

Vice-Doyen chargé des Affaires Académiques et estudiantines
Professeur Brahim LEKEHAL

Vice-Doyen chargé de la Recherche et de la Coopération
Professeur Taoufiq DAKKA

Vice-Doyen chargé des Affaires Spécifiques à la Pharmacie
Professeur Younes RAHALI

Secrétaire Général
Mr. Mohamed KARRA

Enseignant militaire

1 - ENSEIGNANTS-CHERCHEURS MEDECINS ET PHARMACIENS

PROFESSEURS DE L'ENSEIGNEMENT SUPERIEUR :

Décembre 1984

Pr. MAAOUNI Abdelaziz	Médecine Interne - **Clinique Royale**
Pr. MAAZOUZI Ahmed Wajdi	Anesthésie -Réanimation
Pr. SETTAF Abdellatif	Pathologie Chirurgicale

Décembre 1989

Pr. ADNAOUI Mohamed	Médecine Interne –**Doyen de la FMPR**
Pr. OUAZZANI Taïbi Mohamed Réda	Neurologie

Janvier et Novembre 1990

Pr. KHARBACH Aîcha	Gynécologie -Obstétrique
Pr. TAZI Saoud Anas	Anesthésie Réanimation

Février Avril Juillet et Décembre 1991

Pr. AZZOUZI Abderrahim	Anesthésie Réanimation
Pr. BAYAHIA Rabéa	Néphrologie
Pr. BELKOUCHI Abdelkader	Chirurgie Générale
Pr. BENSOUDA Yahia	Pharmacie galénique
Pr. BERRAHO Amina	Ophtalmologie
Pr. BEZAD Rachid	Gynécologie Obstétrique **Méd. Chef Maternité des Orangers**
Pr. CHERRAH Yahia	Pharmacologie
Pr. CHOKAIRI Omar	Histologie Embryologie
Pr. KHATTAB Mohamed	Pédiatrie
Pr. SOULAYMANI Rachida	Pharmacologie- **Dir. du Centre National PV Rabat**
Pr. TAOUFIK Jamal	Chimie thérapeutique

Décembre 1992

Pr. AHALLAT Mohamed	Chirurgie Générale **Doyen de FMPT**
Pr. BENSOUDA Adil	Anesthésie Réanimation
Pr. CHAHED OUAZZANI Laaziza	Gastro-Entérologie
Pr. CHRAIBI Chafiq	Gynécologie Obstétrique
Pr. EL OUAHABI Abdessamad	Neurochirurgie
Pr. FELLAT Rokaya	Cardiologie
Pr. JIDDANE Mohamed	Anatomie
Pr. ZOUHDI Mimoun	Microbiologie

Mars 1994

Pr. BENJAAFAR Noureddine	Radiothérapie
Pr. BEN RAIS Nozha	Biophysique
Pr. CAOUI Malika	Biophysique
Pr. CHRAIBI Abdelmjid	Endocrinologie et Maladies Métaboliques **Doyen de la FMPA**
Pr. EL AMRANI Sabah	Gynécologie Obstétrique
Pr. ERROUGANI Abdelkader	Chirurgie Générale - **Directeur du CHUIS**
Pr. ESSAKALI Malika	Immunologie

Enseignant militaire

Pr. ETTAYEBI Fouad	Chirurgie Pédiatrique
Pr. IFRINE Lahssan	Chirurgie Générale
Pr. RHRAB Brahim	Gynécologie –Obstétrique
Pr. SENOUCI Karima	Dermatologie

Mars 1994

Pr. ABBAR Mohamed*	Urologie **Inspecteur du SSM**
Pr. BENTAHILA Abdelali	Pédiatrie
Pr. BERRADA Mohamed Saleh	Traumatologie - Orthopédie
Pr. CHERKAOUI Lalla Ouafae	Ophtalmologie
Pr. LAKHDAR Amina	Gynécologie Obstétrique
Pr. MOUANE Nezha	Pédiatrie

Mars 1995

Pr. ABOUQUAL Redouane	Réanimation Médicale
Pr. AMRAOUI Mohamed	Chirurgie Générale
Pr. BAIDADA Abdelaziz	Gynécologie Obstétrique
Pr. BARGACH Samir	Gynécologie Obstétrique
Pr. EL MESNAOUI Abbes	Chirurgie Générale
Pr. ESSAKALI HOUSSYNI Leila	Oto-Rhino-Laryngologie
Pr. IBEN ATTYA ANDALOUSSI Ahmed	Urologie
Pr. OUAZZANI CHAHDI Bahia	Ophtalmologie
Pr. SEFIANI Abdelaziz	Génétique
Pr. ZEGGWAGH Amine Ali	Réanimation Médicale

Décembre 1996

Pr. BELKACEM Rachid	Chirurgie Pédiatrie
Pr. BOULANOUAR Abdelkrim	Ophtalmologie
Pr. EL ALAMI EL FARICHA EL Hassan	Chirurgie Générale
Pr. GAOUZI Ahmed	Pédiatrie
Pr. OUZEDDOUN Naima	Néphrologie
Pr. ZBIR EL Mehdi*	Cardiologie **Directeur HMI Mohammed V**

Novembre 1997

Pr. ALAMI Mohamed Hassan	Gynécologie-Obstétrique
Pr. BIROUK Nazha	Neurologie
Pr. FELLAT Nadia	Cardiologie
Pr. KADDOURI Noureddine	Chirurgie Pédiatrique
Pr. KOUTANI Abdellatif	Urologie
Pr. LAHLOU Mohamed Khalid	Chirurgie Générale
Pr. MAHRAOUI CHAFIQ	Pédiatrie
Pr. TOUFIQ Jallal	Psychiatrie **Directeur Hôp.Ar-razi Salé**
Pr. YOUSFI MALKI Mounia	Gynécologie Obstétrique

Novembre 1998

Pr. BENOMAR ALI	Neurologie **Doyen de la FM Abulcassis**
Pr. BOUGTAB Abdesslam	Chirurgie Générale
Pr. ER RIHANI Hassan	Oncologie Médicale

***Enseignant militaire**

Pr. BENKIRANE Majid*	Hématologie

Janvier 2000

Pr. ABID Ahmed*	Pneumo-phtisiologie
Pr. AIT OUAMAR Hassan	Pédiatrie
Pr. BENJELLOUN Dakhama Badr Sououd	Pédiatrie
Pr. BOURKADI Jamal-Eddine	Pneumo-phtisiologie
Pr. CHARIF CHEFCHAOUNI Al Montacer	Chirurgie Générale
Pr. ECHARRAB El Mahjoub	Chirurgie Générale
Pr. EL FTOUH Mustapha	Pneumo-phtisiologie
Pr. EL MOSTARCHID Brahim*	Neurochirurgie
Pr. TACHINANTE Rajae	Anesthésie-Réanimation
Pr. TAZI MEZALEK Zoubida	Médecine Interne

Novembre 2000

Pr. AIDI Saadia	Neurologie
Pr. AJANA Fatima Zohra	Gastro-Entérologie
Pr. BENAMR Said	Chirurgie Générale
Pr. CHERTI Mohammed	Cardiologie
Pr. ECH-CHERIF EL KETTANI Selma	Anesthésie-Réanimation
Pr. EL HASSANI Amine	Pédiatrie - **Directeur Hôp.Cheikh Zaid**
Pr. EL KHADER Khalid	Urologie
Pr. GHARBI Mohamed El Hassan	Endocrinologie et Maladies Métaboliques
Pr. MDAGHRI ALAOUI Asmae	Pédiatrie

Décembre 2001

Pr. BALKHI Hicham*	Anesthésie-Réanimation
Pr. BENABDELJLIL Maria	Neurologie
Pr. BENAMAR Loubna	Néphrologie
Pr. BENAMOR Jouda	Pneumo-phtisiologie
Pr. BENELBARHDADI Imane	Gastro-Entérologie
Pr. BENNANI Rajae	Cardiologie
Pr. BENOUACHANE Thami	Pédiatrie
Pr. BEZZA Ahmed*	Rhumatologie
Pr. BOUCHIKHI IDRISSI Med Larbi	Anatomie
Pr. BOUMDIN El Hassane*	Radiologie
Pr. CHAT Latifa	Radiologie
Pr. EL HIJRI Ahmed	Anesthésie-Réanimation
Pr. EL MAAQILI Moulay Rachid	Neuro-Chirurgie
Pr. EL MADHI Tarik	Chirurgie-Pédiatrique **Directeur Hôp. Des Enfants Rabat**
Pr. EL OUNANI Mohamed	Chirurgie Générale
Pr. ETTAIR Said	Pédiatrie - **Directeur Hôp. Univ. International (Cheikh Khalifa)**
Pr. GAZZAZ Miloudi*	Neuro-Chirurgie
Pr. HRORA Abdelmalek	Chirurgie Générale **Directeur Hôpital Ibn Sina**
Pr. KABIRI EL Hassane*	Chirurgie Thoracique
Pr. LAMRANI Moulay Omar	Traumatologie Orthopédie
Pr. LEKEHAL Brahim	Chirurgie Vasculaire Périphérique **V-D chargé Aff Acad. Est**.
Pr. MEDARHRI Jalil	Chirurgie Générale
Pr. MIKDAME Mohammed*	Hématologie Clinique

Enseignant militaire

Pr. MOHSINE Raouf	Chirurgie Générale
Pr. NOUINI Yassine	Urologie
Pr. SABBAH Farid	Chirurgie Générale
Pr. SEFIANI Yasser	Chirurgie Vasculaire Périphérique
Pr. TAOUFIQ BENCHEKROUN Soumia	Pédiatrie

<u>Décembre 2002</u>

Pr. AMEUR Ahmed*	Urologie
Pr. AMRI Rachida	Cardiologie
Pr. AOURARH Aziz*	Gastro-Entérologie
Pr. BAMOU Youssef*	Biochimie-Chimie
Pr. BELMEJDOUB Ghizlene*	Endocrinologie et Maladies Métaboliques
Pr. BENZEKRI Laila	Dermatologie
Pr. BENZZOUBEIR Nadia	Gastro-Entérologie
Pr. BERNOUSSI Zakiya	Anatomie Pathologique
Pr. CHOHO Abdelkrim*	Chirurgie Générale
Pr. CHKIRATE Bouchra	Pédiatrie
Pr. EL ALAMI EL Fellous Sidi Zouhair	Chirurgie Pédiatrique
Pr. FILALI ADIB Abdelhai	Gynécologie Obstétrique
Pr. HAJJI Zakia	Ophtalmologie
Pr. KRIOUILE Yamina	Pédiatrie
Pr. OUJILAL Abdelilah	Oto-Rhino-Laryngologie
Pr. RAISS Mohamed	Chirurgie Générale
Pr. SIAH Samir*	Anesthésie Réanimation
Pr. THIMOU Amal	Pédiatrie
Pr. ZENTAR Aziz*	Chirurgie Générale

<u>Janvier 2004</u>

Pr. ABDELLAH El Hassan	Ophtalmologie
Pr. AMRANI Mariam	Anatomie Pathologique
Pr. BENBOUZID Mohammed Anas	Oto-Rhino-Laryngologie
Pr. BENKIRANE Ahmed*	Gastro-Entérologie
Pr. BOULAADAS Malik	Stomatologie et Chirurgie Maxillo-faciale
Pr. BOURAZZA Ahmed*	Neurologie
Pr. CHAGAR Belkacem*	Traumatologie Orthopédie
Pr. CHERRADI Nadia	Anatomie Pathologique
Pr. EL FENNI Jamal*	Radiologie
Pr. EL HANCHI ZAKI	Gynécologie Obstétrique
Pr. EL KHORASSANI Mohamed	Pédiatrie
Pr. HACHI Hafid	Chirurgie Générale
Pr. JABOUIRIK Fatima	Pédiatrie
Pr. KHARMAZ Mohamed	Traumatologie Orthopédie
Pr. MOUGHIL Said	Chirurgie Cardio-Vasculaire
Pr. OUBAAZ Abdelbarre*	Ophtalmologie
Pr. TARIB Abdelilah*	Pharmacie Clinique
Pr. TIJAMI Fouad	Chirurgie Générale
Pr. ZARZUR Jamila	Cardiologie

<u>Janvier 2005</u>

Enseignant militaire

Pr. ABBASSI Abdellah	Chirurgie Réparatrice et Plastique
Pr. AL KANDRY Sif Eddine*	Chirurgie Générale
Pr. ALLALI Fadoua	Rhumatologie
Pr. AMAZOUZI Abdellah	Ophtalmologie
Pr. BAHIRI Rachid	Rhumatologie **Directeur Hôp. Al Ayachi Salé**
Pr. BARKAT Amina	Pédiatrie
Pr. BENYASS Aatif*	Cardiologie
Pr. DOUDOUH Abderrahim*	Biophysique
Pr. HAJJI Leila	Cardiologie (mise en disponibilité)
Pr. HESSISSEN Leila	Pédiatrie
Pr. JIDAL Mohamed*	Radiologie
Pr. LAAROUSSI Mohamed	Chirurgie Cardio-vasculaire
Pr. LYAGOUBI Mohammed	Parasitologie
Pr. SBIHI Souad	Histo-Embryologie Cytogénétique
Pr. ZERAIDI Najia	Gynécologie Obstétrique

AVRIL 2006

Pr. ACHEMLAL Lahsen*	Rhumatologie
Pr. BELMEKKI Abdelkader*	Hématologie
Pr. BENCHEIKH Razika	O.R.L
Pr. BOUHAFS Mohamed El Amine	Chirurgie - Pédiatrique
Pr. BOULAHYA Abdellatif*	Chirurgie Cardio - Vasculaire. **Directeur Hôpital Ibn Sina Marr.**
Pr. CHENGUETI ANSARI Anas	Gynécologie Obstétrique
Pr. DOGHMI Nawal	Cardiologie
Pr. FELLAT Ibtissam	Cardiologie
Pr. FAROUDY Mamoun	Anesthésie Réanimation
Pr. HARMOUCHE Hicham	Médecine Interne
Pr. IDRISS LAHLOU Amine*	Microbiologie
Pr. JROUNDI Laila	Radiologie
Pr. KARMOUNI Tariq	Urologie
Pr. KILI Amina	Pédiatrie
Pr. KISRA Hassan	Psychiatrie
Pr. KISRA Mounir	Chirurgie - Pédiatrique
Pr. LAATIRIS Abdelkader*	Pharmacie Galénique
Pr. LMIMOUNI Badreddine*	Parasitologie
Pr. MANSOURI Hamid*	Radiothérapie
Pr. OUANASS Abderrazzak	Psychiatrie
Pr. SAFI Soumaya*	Endocrinologie
Pr. SOUALHI Mouna	Pneumo - Phtisiologie
Pr. TELLAL Saida*	Biochimie
Pr. ZAHRAOUI Rachida	Pneumo - Phtisiologie

Octobre 2007

Pr. ABIDI Khalid	Réanimation médicale
Pr. ACHACHI Leila	Pneumo phtisiologie
Pr. AMHAJJI Larbi*	Traumatologie orthopédie
Pr. AOUFI Sarra	Parasitologie
Pr. BAITE Abdelouahed*	Anesthésie réanimation
Pr. BALOUCH Lhousaine*	Biochimie-chimie

Enseignant militaire

Pr. BENZIANE Hamid*	Pharmacie clinique
Pr. BOUTIMZINE Nourdine	Ophtalmologie
Pr. CHERKAOUI Naoual*	Pharmacie galénique
Pr. EL BEKKALI Youssef*	Chirurgie cardio-vasculaire
Pr. EL ABSI Mohamed	Chirurgie générale
Pr. EL MOUSSAOUI Rachid	Anesthésie réanimation
Pr. EL OMARI Fatima	Psychiatrie
Pr. GHARIB Noureddine	Chirurgie plastique et réparatrice
Pr. HADADI Khalid*	Radiothérapie
Pr. ICHOU Mohamed*	Oncologie médicale
Pr. ISMAILI Nadia	Dermatologie
Pr. KEBDANI Tayeb	Radiothérapie
Pr. LOUZI Lhoussain*	Microbiologie
Pr. MADANI Naoufel	Réanimation médicale
Pr. MARC Karima	Pneumo phtisiologie
Pr. MASRAR Azlarab	Hématologie biologique
Pr. OUZZIF Ez zohra*	Biochimie-chimie
Pr. SEFFAR Myriame	Microbiologie
Pr. SEKHSOKH Yessine*	Microbiologie
Pr. SIFAT Hassan*	Radiothérapie
Pr. TACHFOUTI Samira	Ophtalmologie
Pr. TAJDINE Mohammed Tariq*	Chirurgie générale
Pr. TANANE Mansour*	Traumatologie-orthopédie
Pr. TLIGUI Houssain	Parasitologie
Pr. TOUATI Zakia	Cardiologie

Mars 2009

Pr. ABOUZAHIR Ali*	Médecine interne
Pr. AGADR Aomar*	Pédiatrie
Pr. AIT ALI Abdelmounaim*	Chirurgie Générale
Pr. AKHADDAR Ali*	Neuro-chirurgie
Pr. ALLALI Nazik	Radiologie
Pr. AMINE Bouchra	Rhumatologie
Pr. ARKHA Yassir	Neuro-chirurgie **Directeur Hôp.des Spécialités**
Pr. BELYAMANI Lahcen*	Anesthésie Réanimation
Pr. BJIJOU Younes	Anatomie
Pr. BOUHSAIN Sanae*	Biochimie-chimie
Pr. BOUI Mohammed*	Dermatologie
Pr. BOUNAIM Ahmed*	Chirurgie Générale
Pr. BOUSSOUGA Mostapha*	Traumatologie-orthopédie
Pr. CHTATA Hassan Toufik*	Chirurgie Vasculaire Périphérique
Pr. DOGHMI Kamal*	Hématologie clinique
Pr. EL MALKI Hadj Omar	Chirurgie Générale
Pr. EL OUENNASS Mostapha*	Microbiologie
Pr. ENNIBI Khalid*	Médecine interne
Pr. FATHI Khalid	Gynécologie obstétrique
Pr. HASSIKOU Hasna*	Rhumatologie
Pr. KABBAJ Nawal	Gastro-entérologie
Pr. KABIRI Meryem	Pédiatrie

Enseignant militaire

Pr. KARBOUBI Lamya	Pédiatrie
Pr. LAMSAOURI Jamal*	Chimie Thérapeutique
Pr. MARMADE Lahcen	Chirurgie Cardio-vasculaire
Pr. MESKINI Toufik	Pédiatrie
Pr. MESSAOUDI Nezha*	Hématologie biologique
Pr. MSSROURI Rahal	Chirurgie Générale
Pr. NASSAR Ittimade	Radiologie
Pr. OUKERRAJ Latifa	Cardiologie
Pr. RHORFI Ismail Abderrahmani*	Pneumo-Phtisiologie

Octobre 2010

Pr. ALILOU Mustapha	Anesthésie réanimation
Pr. AMEZIANE Taoufiq*	Médecine Interne **Directeur ERSSM**
Pr. BELAGUID Abdelaziz	Physiologie
Pr. CHADLI Mariama*	Microbiologie
Pr. CHEMSI Mohamed*	Médecine Aéronautique
Pr. DAMI Abdellah*	Biochimie- Chimie
Pr. DARBI Abdellatif*	Radiologie
Pr. DENDANE Mohammed Anouar	Chirurgie Pédiatrique
Pr. EL HAFIDI Naima	Pédiatrie
Pr. EL KHARRAS Abdennasser*	Radiologie
Pr. EL MAZOUZ Samir	Chirurgie Plastique et Réparatrice
Pr. EL SAYEGH Hachem	Urologie
Pr. ERRABIH Ikram	Gastro-Entérologie
Pr. LAMALMI Najat	Anatomie Pathologique
Pr. MOSADIK Ahlam	Anesthésie Réanimation
Pr. MOUJAHID Mountassir*	Chirurgie Générale
Pr. ZOUAIDIA Fouad	Anatomie Pathologique

Decembre 2010

Pr. ZNATI Kaoutar	Anatomie Pathologique

Mai 2012

Pr. AMRANI Abdelouahed	Chirurgie pédiatrique
Pr. ABOUELALAA Khalil*	Anesthésie Réanimation
Pr. BENCHEBBA Driss*	Traumatologie-orthopédie
Pr. DRISSI Mohamed*	Anesthésie Réanimation
Pr. EL ALAOUI MHAMDI Mouna	Chirurgie Générale
Pr. EL OUAZZANI Hanane*	Pneumophtisiologie
Pr. ER-RAJI Mounir	Chirurgie Pédiatrique
Pr. JAHID Ahmed	Anatomie Pathologique

Février 2013

Pr. AHID Samir	Pharmacologie
Pr. AIT EL CADI Mina	Toxicologie
Pr. AMRANI HANCHI Laila	Gastro-Entérologie
Pr. AMOR Mourad	Anesthésie-Réanimation
Pr. AWAB Almahdi	Anesthésie-Réanimation
Pr. BELAYACHI Jihane	Réanimation Médicale

Enseignant militaire

Pr. BELKHADIR Zakaria Houssain	Anesthésie-Réanimation
Pr. BENCHEKROUN Laila	Biochimie-Chimie
Pr. BENKIRANE Souad	Hématologie
Pr. BENSGHIR Mustapha*	Anesthésie Réanimation
Pr. BENYAHIA Mohammed*	Néphrologie
Pr. BOUATIA Mustapha	Chimie Analytique et Bromatologie
Pr. BOUABID Ahmed Salim*	Traumatologie orthopédie
Pr. BOUTARBOUCH Mahjouba	Anatomie
Pr. CHAIB Ali*	Cardiologie
Pr. DENDANE Tarek	Réanimation Médicale
Pr. DINI Nouzha*	Pédiatrie
Pr. ECH-CHERIF EL KETTANI Mohamed Ali	Anesthésie Réanimation
Pr. ECH-CHERIF EL KETTANI Najwa	Radiologie
Pr. ELFATEMI NIZARE	Neuro-chirurgie
Pr. EL GUERROUJ Hasnae	Médecine Nucléaire
Pr. EL HARTI Jaouad	Chimie Thérapeutique
Pr. EL JAOUDI Rachid*	Toxicologie
Pr. EL KABABRI Maria	Pédiatrie
Pr. EL KHANNOUSSI Basma	Anatomie Pathologique
Pr. EL KHLOUFI Samir	Anatomie
Pr. EL KORAICHI Alae	Anesthésie Réanimation
Pr. EN-NOUALI Hassane*	Radiologie
Pr. ERRGUIG Laila	Physiologie
Pr. FIKRI Meryem	Radiologie
Pr. GHFIR Imade	Médecine Nucléaire
Pr. IMANE Zineb	Pédiatrie
Pr. IRAQI Hind	Endocrinologie et maladies métaboliques
Pr. KABBAJ Hakima	Microbiologie
Pr. KADIRI Mohamed*	Psychiatrie
Pr. LATIB Rachida	Radiologie
Pr. MAAMAR Mouna Fatima Zahra	Médecine Interne
Pr. MEDDAH Bouchra	Pharmacologie
Pr. MELHAOUI Adyl	Neuro-chirurgie
Pr. MRABTI Hind	Oncologie Médicale
Pr. NEJJARI Rachid	Pharmacognosie
Pr. OUBEJJA Houda	Chirugie Pédiatrique
Pr. OUKABLI Mohamed*	Anatomie Pathologique
Pr. RAHALI Younes	Pharmacie Galénique **Vice-Doyen à la Pharmacie**
Pr. RATBI Ilham	Génétique
Pr. RAHMANI Mounia	Neurologie
Pr. REDA Karim*	Ophtalmologie
Pr. REGRAGUI Wafa	Neurologie
Pr. RKAIN Hanan	Physiologie
Pr. ROSTOM Samira	Rhumatologie
Pr. ROUAS Lamiaa	Anatomie Pathologique
Pr. ROUIBAA Fedoua*	Gastro-Entérologie
Pr. SALIHOUN Mouna	Gastro-Entérologie
Pr. SAYAH Rochde	Chirurgie Cardio-Vasculaire
Pr. SEDDIK Hassan*	Gastro-Entérologie

Enseignant militaire

Pr. ZERHOUNI Hicham	Chirurgie Pédiatrique
Pr. ZINE Ali*	Traumatologie Orthopédie

AVRIL 2013

Pr. EL KHATIB MOHAMED KARIM*	Stomatologie et Chirurgie Maxillo-faciale

MARS 2014

Pr. ACHIR Abdellah	Chirurgie Thoracique
Pr. BENCHAKROUN Mohammed*	Traumatologie- Orthopédie
Pr. BOUCHIKH Mohammed	Chirurgie Thoracique
Pr. EL KABBAJ Driss*	Néphrologie
Pr. EL MACHTANI IDRISSI Samira*	Biochimie-Chimie
Pr. HARDIZI Houyam	Histologie- Embryologie-Cytogénétique
Pr. HASSANI Amale*	Pédiatrie
Pr. HERRAK Laila	Pneumologie
Pr. JEAIDI Anass*	Hématologie Biologique
Pr. KOUACH Jaouad*	Génycologie-Obstétrique
Pr. MAKRAM Sanaa*	Pharmacologie
Pr. RHISSASSI Mohamed Jaafar	CCV
Pr. SEKKACH Youssef*	Médecine Interne
Pr. TAZI MOUKHA Zakia	Génécologie-Obstétrique

DECEMBRE 2014

Pr. ABILKACEM Rachid*	Pédiatrie
Pr. AIT BOUGHIMA Fadila	Médecine Légale
Pr. BEKKALI Hicham*	Anesthésie-Réanimation
Pr. BENAZZOU Salma	Chirurgie Maxillo-Faciale
Pr. BOUABDELLAH Mounya	Biochimie-Chimie
Pr. BOUCHRIK Mourad*	Parasitologie
Pr. DERRAJI Soufiane*	Pharmacie Clinique
Pr. EL AYOUBI EL IDRISSI Ali	Anatomie
Pr. EL GHADBANE Abdedaim Hatim*	Anesthésie-Réanimation
Pr. EL MARJANY Mohammed*	Radiothérapie
Pr. FEJJAL Nawfal	Chirurgie Réparatrice et Plastique
Pr. JAHIDI Mohamed*	O.R.L
Pr. LAKHAL Zouhair*	Cardiologie
Pr. OUDGHIRI NEZHA	Anesthésie-Réanimation
Pr. RAMI Mohamed	Chirurgie Pédiatrique
Pr. SABIR Maria	Psychiatrie
Pr. SBAI IDRISSI Karim*	Médecine préventive, santé publique et Hyg.

AOUT 2015

Pr. MEZIANE Meryem	Dermatologie
Pr. TAHIRI Latifa	Rhumatologie

Enseignant militaire

PROFESSEURS AGREGES :

JANVIER 2016

Pr. BENKABBOU Amine	Chirurgie Générale
Pr. EL ASRI Fouad*	Ophtalmologie
Pr. ERRAMI Noureddine*	O.R.L
Pr. NITASSI Sophia	O.R.L

JUIN 2017

Pr. ABI Rachid*	Microbiologie
Pr. ASFALOU Ilyasse*	Cardiologie
Pr. BOUAITI El Arbi*	Médecine préventive, santé publique et Hyg.
Pr. BOUTAYEB Saber	Oncologie Médicale
Pr. EL GHISSASSI Ibrahim	Oncologie Médicale
Pr. HAFIDI Jawad	Anatomie
Pr. MAJBAR Mohammed Anas	Chirurgie Générale
Pr. OURAINI Saloua*	O.R.L
Pr. RAZINE Rachid	Médecine préventive, santé publique et Hyg.
Pr. SOUADKA Amine	Chirurgie Générale
Pr. ZRARA Abdelhamid*	Immunologie

MAI 2018

Pr. AMMOURI Wafa	Médecine interne
Pr. BENTALHA Aziza	Anesthésie-Réanimation
Pr. EL AHMADI Brahim	Anesthésie-Réanimation
Pr. EL HARRECH Youness*	Urologie
Pr. EL KACEMI Hanan	Radiothérapie
Pr. EL MAJJAOUI Sanaa	Radiothérapie
Pr. FATIHI Jamal*	Médecine Interne
Pr. GHANNAM Abdel-Ilah	Anesthésie-Réanimation
Pr. JROUNDI Imane	Médecine préventive, santé publique et Hyg.
Pr. MOATASSIM BILLAH Nabil	Radiologie
Pr. TADILI Sidi Jawad	Anesthésie-Réanimation
Pr. TANZ Rachid*	Oncologie Médicale

NOVEMBRE 2018

Pr. AMELLAL Mina	Anatomie
Pr. SOULY Karim	Microbiologie
Pr. TAHRI Rajae	Histologie-Embryologie-Cytogénétique

NOVEMBRE 2019

Pr. AATIF Taoufiq*	Néphrologie
Pr. ACHBOUK Abdelhafid*	Chirurgie réparatrice et plastique
Pr. ANDALOUSSI SAGHIR Khalid	Radiothérapie
Pr. BABA HABIB Moulay Abdellah*	Gynécologie-Obstétrique
Pr. BASSIR RIDA ALLAH	Anatomie
Pr. BOUATTAR TARIK	Néphrologie
Pr. BOUFETTAL MONSEF	Anatomie
Pr. BOUCHENTOUF Sidi Mohammed*	Chirurgie-Générale

Enseignant militaire

Pr. BOUZELMAT HICHAM*	Cardiologie
Pr. BOUKHRIS JALAL*	Traumatologie-Orthopédie
Pr. CHAFRY BOUCHAIB*	Traumatologie-Orthopédie
Pr. CHAHDI HAFSA*	Anatomie pathologique
Pr. CHERIF EL ASRI ABAD*	Neuro-chirurgie
Pr. DAMIRI AMAL*	Anatomie Pathologique
Pr. DOGHMI NAWFAL*	Anesthésie-Réanimation
Pr. ELALAOUI SIDI-YASSIR	Pharmacie-Galénique
Pr. EL ANNAZ HICHAM*	Virologie
Pr. EL HASSANI MOULAY EL MEHDI*	Gynécologie-Obstétrique
Pr. EL HJOUJI ABDERRAHMAN*	Chirurgie Générale
Pr. EL KAOUI HAKIM*	Chirurgie Générale
Pr. EL WALI ABDERRAHMAN*	Anesthésie-Réanimation
Pr. EN-NAFAA ISSAM*	Radiologie
Pr. HAMAMA JALAL*	Stomatologie et Chirurgie Maxillo-faciale
Pr. HEMMAOUI BOUCHAIB*	O.R.L
Pr. HJIRA NAOUFAL*	Dermatologie
Pr. JIRA MOHAMED*	Médecine interne
Pr. JNIENE ASMAA	Physiologie
Pr. LARAQUI HICHAM*	Chirurgie-Générale
Pr. MAHFOUD TARIK*	Oncologie Médicale
Pr. MEZIANE MOHAMMED*	Anesthésie-Réanimation
Pr. MOUTAKI ALLAH YOUNES*	Chirurgie Cardio-Vasculaire
Pr. MOUZARI YASSINE*	Ophtalmologie
Pr. NAOUI HAFIDA*	Parasitologie-Mycologie
Pr. OBTEL MAJDOULINE	Médecine préventive, santé publique et Hyg.
Pr. OURRAI ABDELHAKIM*	Pédiatrie
Pr. SAOUAB RACHIDA*	Radiologie
Pr. SBITTI YASSIR*	Oncologie Médicale
Pr. ZADDOUG OMAR*	Traumatologie-Orthopédie
Pr. ZIDOUH SAAD*	Anesthésie-Réanimation

Enseignant militaire

2 - ENSEIGNANTS-CHERCHEURS SCIENTIFIQUES

PROFESSEURS DE L'ENSEIGNEMENT SUPERIEUR :

Pr. ABOUDRAR Saadia	Physiologie
Pr. ALAMI OUHABI Naima	Biochimie-chimie
Pr. ALAOUI KATIM	Pharmacologie
Pr. ALAOUI SLIMANI Lalla Naïma	Histologie-Embryologie
Pr. ANSAR M'hammed	Chimie Organique et Pharmacie Chimique
Pr. BARKIYOU Malika	Histologie-Embryologie
Pr. BOUHOUCHE Ahmed	Génétique Humaine
Pr. BOUKLOUZE Abdelaziz	Applications Pharmaceutiques
Pr. DAKKA Taoufiq	Physiologie **Vice-Doyen chargé de la Rech. et de la Coop.**
Pr. FAOUZI Moulay El Abbes	Pharmacologie
Pr. IBRAHIMI Azeddine	Biologie moléculaire/Biotechnologie
Pr. OULAD BOUYAHYA IDRISSI Mohammed	Chimie Organique
Pr. RIDHA Ahlam	Chimie
Pr. TOUATI Driss	Pharmacognosie
Pr. ZAHIDI Ahmed	Pharmacologie

PROFESSEURS HABILITES :

Pr. BENZEID Hanane	Chimie
Pr. CHAHED OUAZZANI Lalla Chadia	Biochimie-chimie
Pr. DOUKKALI Anass	Chimie Analytique
Pr. EL JASTIMI Jamila	Chimie
Pr. KHANFRI Jamal Eddine	Histologie-Embryologie
Pr. LYAHYAI Jaber	Génétique
Pr. OUADGHIRI Mouna	Microbiologie et Biologie
Pr. RAMLI Youssef	Chimie
Pr. SERRAGUI Samira	Pharmacologie
Pr. TAZI Ahnini	Génétique
Pr. YAGOUBI Maamar	Eau, Environnement

Mise à jour le 05/03/2021
KHALED Abdellah
Chef du Service des Ressources Humaines
FMPR

***Enseignant militaire**

Dedications

To my parents:

My every achievement and success, I owe to you. You are my source of strength and faith. Many lifetimes won't be enough to repay you, and no words can ever encompass the love I hold for you.

To my brother:

I haven't always been kind, and more often than not you were a thorn in my side, but you were always quick to forgive, and the first to apologize. I hope that through the many years to come, you'll remain my confidant, and partner in crime.

To my aunts, Fatima and Nacira:

You were there at every success and failure, my own personal cheering squad, ever constant in your support and belief in me. No words are enough to express how dear you are, and no material goods could be enough of a repayment.

To Salma Sbai, Aziza Ouhadi, Fatima Zahra El Garah, and Mouad Semmouri:

I've met each of you at different stages of my journey, and since then life has seen to take us on separate paths, but know that even If I don't reach out as much as I should, you're always in my thoughts, and my affection for you burns constantly in my heart.

To my support group, Mylissa, Vera, Karmen, Zeyad, Risha, and Atifa:

Ever ready with kind words and unending support, you've grown to be my rock in this turbulent life, my family aboard, every single one of you is precious to me.

To my grandmother:

You live on in my heart.

Acknowledgments

To our mentor and President

Dr GAZZAZ Miloudi

Professor of Neurosurgery

We are deeply honored by having you as a president of the jury of this thesis,

and wish to express our heartfelt gratitude and appreciation.

We dearly hope that this work will meet with your approval.

To our mentor and advisor

Dr EL ASRI Abad Cherif

Professor of Neurosurgery

We wish to extend our sincere gratitude and appreciation.

This study couldn’t have been accomplished without your continuous support, patience and guidance.

We could not have imagined a better mentor and adviser.

To our mentor and jury member

Dr ARKHA Yasser

Professor of Neurosurgery

It is a great privilege to have you on our thesis' jury.

We'd like to express our special thanks for your encouragement and warm reception, which shall always be remembered.

We hope that this study will gain your approval.

To our mentor and jury member

Dr BELHACHMI Adil

Professor of Neurosurgery

We would like to thank you for honoring us by agreeing to judge this thesis.

Please accept our sincere gratitude and appreciation.

Your encouragement and kind words were deeply treasured.

To our mentor and jury member

Dr ZALAGH Mohamed

Professor of Otolaryngology

We are deeply grateful for having you as a member of the jury of our thesis.

Please accept the assurances of our high esteem and respect.

List of abbreviations

Abbreviations

Ant : Anterior

Car : Carotid

CCF : Carotid cavernous fistula

Clin : Clinoid

CN : Cranial nerve

CS : Cavernous sinus

CSCH : Cavernous sinus cavernous hemangioma

Fiss : Fissure

For : Foramen

ICA : Internal carotid artery

ILT : Inferolateral Trunk.

Impress : Impression

MHT : Meningohypophseal Trunk

Orb. : Orbital

PA : Pituitary adenoma

Pet : Petrous

Sup : Superior

Trig : Trigeminal.

List of illustrations

List of figures

List of tables

Summary

Introduction

The cavernous sinuses are paired interconnected venous plexuses that lay within the anteromedial portion of the middle cranial fossa, situated on either side of the sella.

Dubbed an ‘anatomical jewelry box’, each sinus houses vital neurovascular structures, among which are the cavernous carotid artery with its branches, the sympathetic plexus, the IIIrd, IVth, VIth cranial nerves, and the first and second branches of the trigeminal nerve.

Aside from this crucial network, the CS represents a critical region for its close connection with other structures, including the orbit, the nasopharynx, the posterior cranial fossa, and the infratemporal fossa through different foramina, fissures, and canals, and for its communication with various venous channels.

Cavernous sinus surgery has always represented a surgical challenge. Early surgery, using a craniotomic approach, was marked by great difficulty and high morbidity, which made the CS be considered by many surgeons as a surgical ‘no man’s land’.

The recent introduction of the endoscope in the trans-sphenoidal surgery of pituitary adenomas led to a wider exposure of the sellar and parasellar areas (1), allowing a panoramic and angled view, and the expansion of surgical corridors, as well as a higher rate of resection with no significant additional morbidity in case of CS invasion (2).

In this study, we describe the frequent lesions that can affect the CS, emphasizing the imaging characteristics of each one, and investigate the endoscopic anatomy of this structure on three fresh human cadavers, as well as review the different endoscopic endonasal approaches.

Anatomical Remarks

Although the anatomy of the CS has been substantially chronicled in literature, the sinus remains a challenging and unfamiliar place for many neurosurgeons. In the following chapter, rather than describing the anatomy of this area, we will try to make some observations on anatomical landmarks which may be useful in understanding surgical strategy.

The paired cavernous sinuses are located centrally within the skull, on each side of the sella and body of the sphenoid bone. Each sinus is a four-walled structure with an oblique converging shape, extending from the lower surface of the anterior clinoid process and from the posterior edge of the superior orbital fissure to the posterior clinoid process above the junction of the petrous apex with the body of the sphenoid bone (3).

The walls of the CS, minus the medial one, are formed of two dural layers: the external meningeal layer and the internal periosteal layer (figure 1). The superior wall (or the roof) faces the basal cisterns, the lateral wall faces the temporal lobe and the posterior wall faces the posterior cranial fossa. The medial wall is bordered by the sella turcica, the pituitary gland, and the sphenoid bone (Figure 2). It may be divided into two parts, sellar (superior part) and spheroidal (inferior wall), both of which are formed by one dural layer: the meningeal layer in the sellar part, and the periosteal layer in the inferior wall. It should be noted that the medial and lateral walls merge inferiorly at the superior margin of the maxillary nerve in a ‘keel-like’ formation (4). Each CS communicates with its counterpart by way of intercavernous sinuses, which are found between the two layers covering the anterior, posterior, and inferior surfaces of the sella.

Four cranial nerves are related directly to the CS. The oculomotor nerve (CN III), the trochlear nerve (CN IV), and the ophthalmic branch of the trigeminal nerve (V1) are contained in the reticularis membrane that forms the lateral wall of the CS. While the maxillary branch of the trigeminal nerve (V1) lie inferior to the junction of the lateral and medial walls (5). The abducens nerve (CN VI) penetrates the posterior wall of the CS after leaving Dorello’s canal, and unlike the other cranial nerves, courses centrally in the CS inferolateral to the horizontal segment of the ICA and medial to the ophthalmic nerve to reach the superior orbital fissure. The venous lake of the CS is additionally penetrated by the ICA, its branches and the associated sympathetic plexus (figure 3).

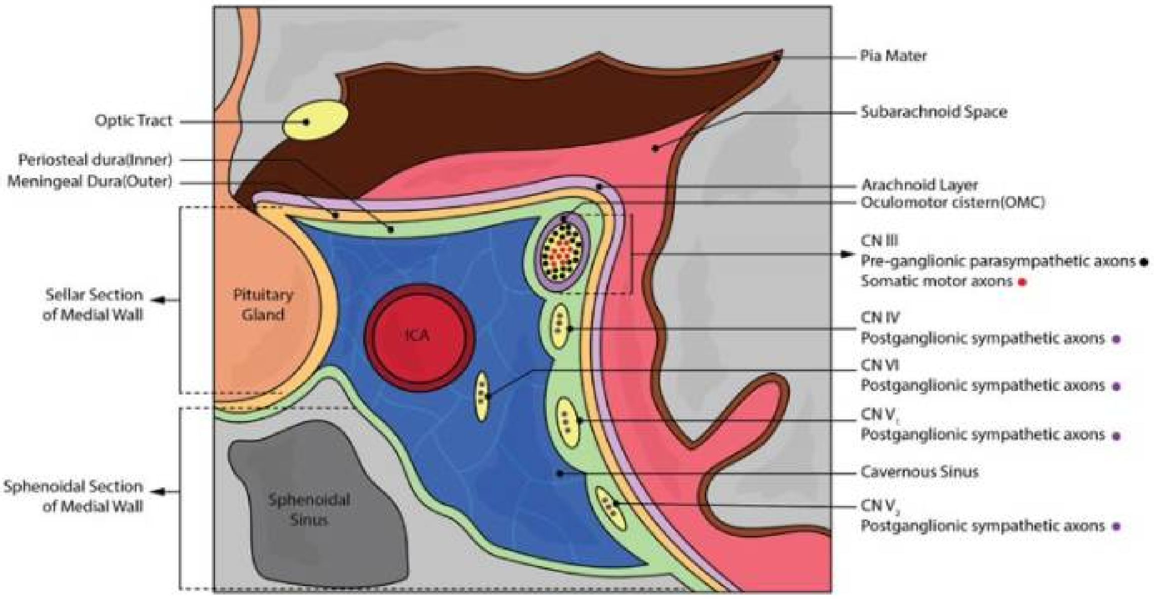

Figure 1: coronal section of the CS showing the close spatial relationships between its neurovascular structures and the different dural layers forming its walls (6)

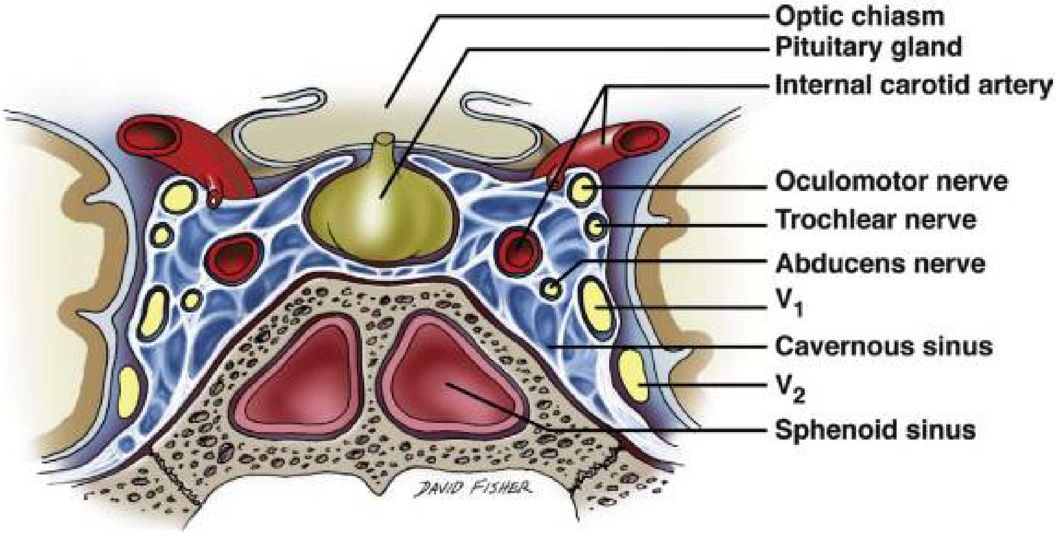

Figure 2: schematic drawing of a coronal section through the CS and the sella turcica: (3)

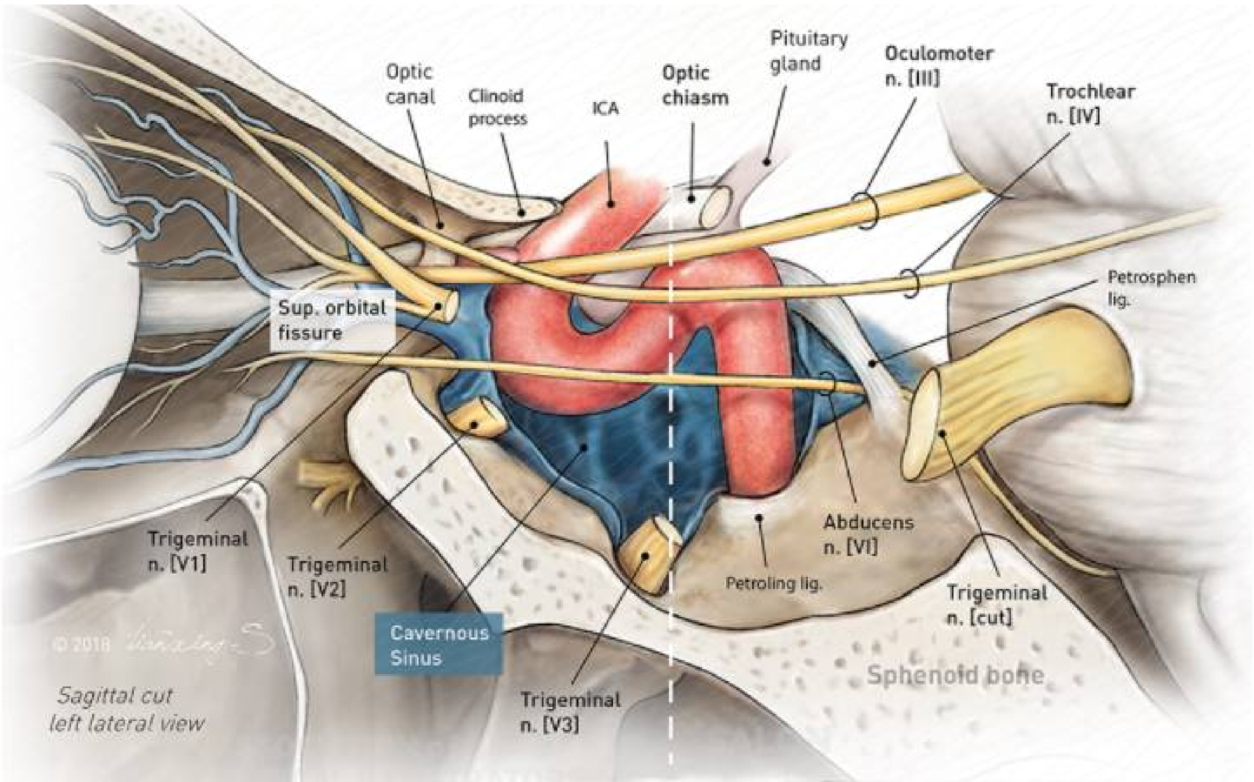

Figure 3: schematic drawing of sagittal section of the CS : (7)

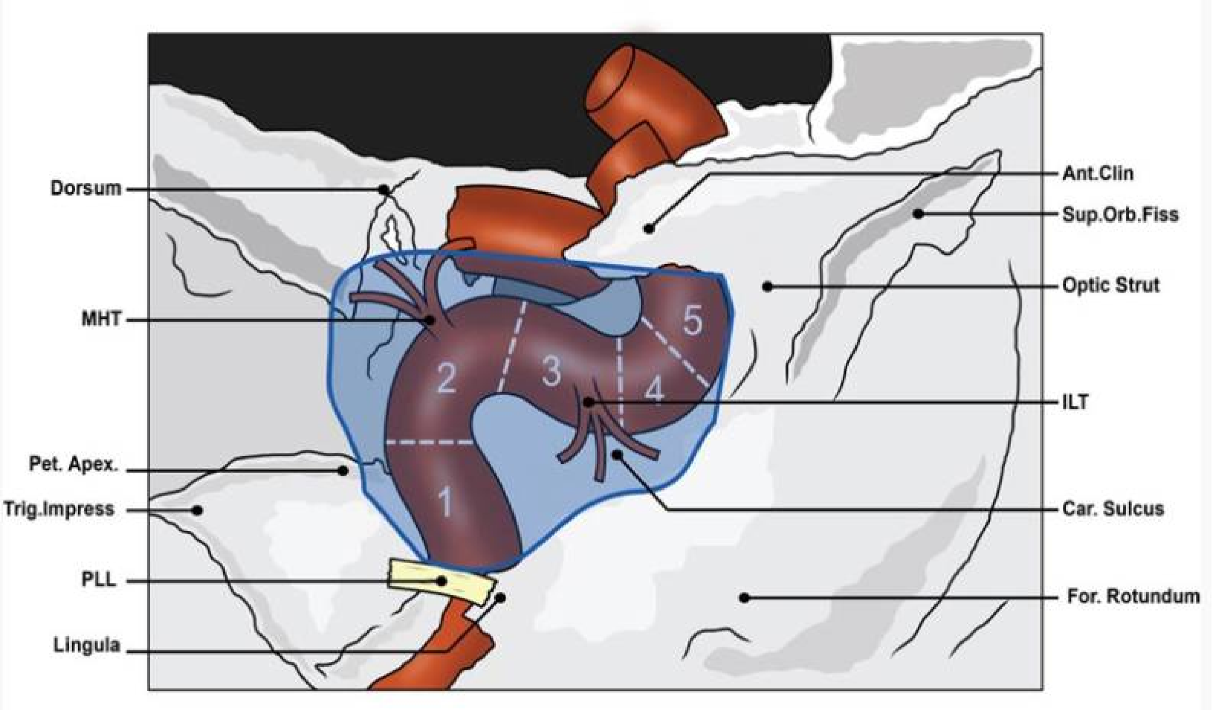

Figure 4: a diagram showing the course of the intracavernous ICA and its different segments– (1) Posterior vertical segment (2) Posterior Genu (3) Horizontal Segment (4) Anterior Genu (5) Anterior Vertical : (6).

1. The intracavernous ICA:

The cavernous ICA is an S-shaped vessel that begins where the petrous segment of the ICA passes between the cartilaginous foramen lacerum below and the petrolingual ligament above to become intracavernous, and ends when it perforates the superior wall of the CS medial to the upper surface of the anterior clinoid process (4). During its course through the CS, it gives rise to two main branches: the meningohypophyseal trunk originating medially from the posterior genu and the inferolateral trunk arising from the middle or lateral surface of the horizontal segment (figure 4).

Alfieri and Jho (8) proposed a subdivision of the ICA based on surgical perspective obtained through endonasal endoscopic route. On the posterior wall of the sphenoidal sinus, two divisions of the cavernous ICA can be recognized by their bony protuberances: caudally, the paraclival protuberance and cranially, the parasellar protuberance. The paraclival ICA segment can be further subdivided into two parts: the lacerum segment caudally, corresponding to the extracavernous portion of the vessel, and the trigeminal segment rostrally, the intracavernous portion of the artery. A landmark leading to the lacerum segment is the vidian canal, which is located inferomedial to the foramen lacerum.

The parasellar carotid protuberance is a C- shaped with the convexity of the C facing anterolaterally. It covers four segments of the ICA in a caudal-to-rostral orderthe hidden segment; the inferior horizontal segment; the anterior vertical segment, and the superior horizontal segment. The hidden segment is the posterior bend of the ICA and is located at the level of the posterior sellar floor. It is named thus for it cannot be seen by this endoscopic anteroinferior approach. The inferior horizontal segment is anterior to the hidden segment, at the level of the sella floor. It appears short due to the perspective view, but is the longest segment of the cavernous ICA.

The anterior vertical segment is located lateral to the anterior wall of the sella and corresponds to the most convex portion of the C- shaped ICA. The superior horizontal segment includes the clinoidal segment of the ICA as well the subarachnoid segment. The clinoidal segment courses medially to the optic strut, is anchored by the proximal and distal dural ring and continues in the subarachnoid portion of the vessel.

2. The cavernous sinus' compartments:

Miranda et al (9) developed an endonasal classification of the venous spaces of the CS based on the intracavernous course of the carotid artery, leading to the description of four virtual compartments: superior, posterior, inferior, and lateral.

The superior compartment of the CS (figure 5) is located above the horizontal cavernous ICA and posterior to the anterior genu. It is bordered by the roof of the CS superiorly and laterally: the ventral surface of the paraclinoidal ICA anterolaterally, and the dura of the oculomotor triangle posterolaterally.

The posterior compartment of the CS (figure 6) is located posterior to the short ascending cavernous ICA (posterior vertical and posterior genu) and anterior to the lateral petroclival dura, forming the posterior wall of the CS. The transition between the short vertical and horizontal segments of the cavernous ICA marks the transition between the superior and posterior compartments.

The inferior compartment of the CS (figure 7) lies below the horizontal intracavernous ICA and anterior to the short vertical segment. The anterior wall of the CS forms the anterior wall of this space. The lateral compartment of the CS (figure 8) lies lateral to the anterior genu and horizontal ICA segments. The proximal dural ring, the maxillary strut (along with the V2 prominence) marks the superior and the inferior limits of this compartment respectively.

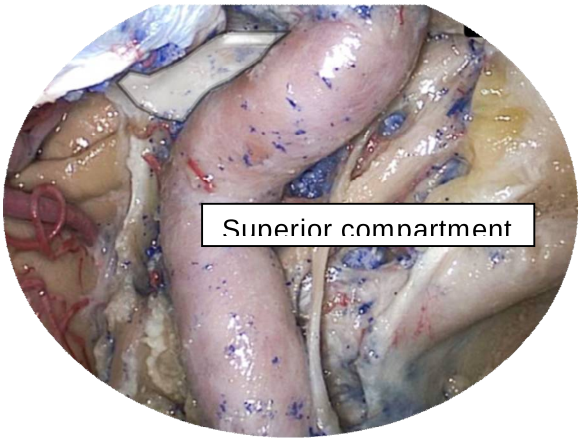

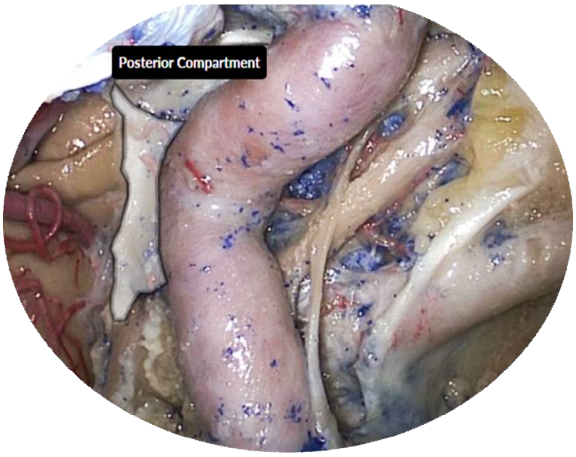

Figure 5: location of the superior compartment in relation to the ICA: (9)

Figure 6: location of the posterior compartment in relation to the ICA: (9)

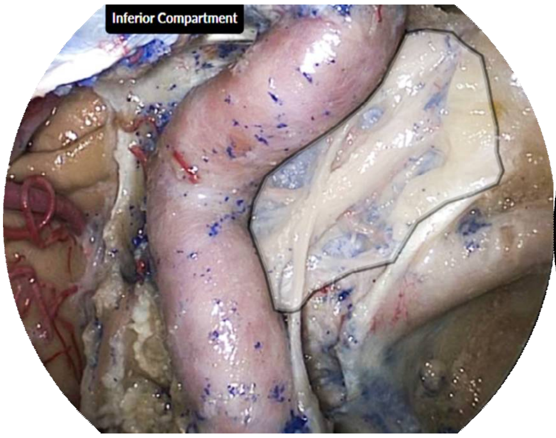

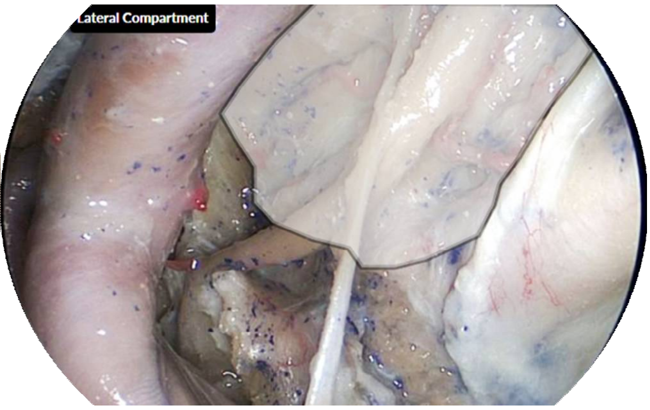

Figure 7: location of the inferior compartment in relation to the ICA (9)

Figure 8: location of the lateral compartment in relation to the ICA (9)

Lesions of the cavernous sinus

A. Epidemiology:

Recent studies on the incidence of CS syndrome are few. An analysis of 151 cases from Los Angeles in 1996 (10) showed that 59% of patients were men. The age on onset varied depending on the cause with the average being 39 years, with a range of 15- 72 years. Tumors were the most frequent cause of CS syndrome (30%), with two-thirds of tumors being malignant, followed by trauma (24%), and inflammation (23%).

In a 2017 study of 73 cases in Northern India (11), 64% of patients were men. The average age was 44 years, with a range of 11- 70 years. Tumors were still the most frequent cause of CS syndrome (28.8%), but fungal infections took second place as the most common cause (24.6%). A higher prevalence of Tolosa-Hunt syndrome at 23.2% was also noted. Headache (97.2%) was the most common presenting symptom, followed by binocular diplopia (90.4%), ptosis (68.4%), and facial numbness (56.2%).

B. Clinical symptoms : cavernous sinus syndrome :

CS syndrome is a constellation of clinical signs that refers to the presence of a lesion within or adjacent to the CS. This includes ophthalmoplegia, facial sensory loss, Horner syndrome, diplopia, chemosis and proptosis.

Ophtalmoplegia is a result of the compromise of the CN III, IV, or VI. In the case of an isolated lesion of the oculomotor nerve, the palsy manifests by a characteristic “down and out” position of the eye, ptosis and mydriasis (figure 9). Isolated CN IV and VI palsies mainly translate as vertical and horizontal diplopia, respectively, as well as esotropia in case of a CN VI lesion. Horner syndrome consists of unilateral ptosis, an ipsilateral miotic but normally reactive pupil, and sometimes ipsilateral facial anhidrosis, all of which occur from damage to the sympathetic plexus accompanying the cavernous ICA. Facial sensory loss is caused by the involvement of the first and second divisions of the trigeminal nerve. (6)

Other symptoms such as signs of intracranial hypertension, retro-orbital pain, headache, disturbances of the hypothalamic-pituitary axis and seizures could also manifest due to a possible mass effect. Various combinations of these symptoms can occur, and the onset can be acute or insidious, all depending on the specific etiology and affected structures. They are usually unilateral but can also be bilateral such in the case of neoplastic pathology.

Ishikawa (12) is the most commonly used system for the classification of the CS syndrome, determined by the investigation of serial topographical sections of human CS and clinical findings. It divides the CS into three portions: anterior, middle, and posterior, separated by the locations of the intracranial orifice of the optic canal and the entry of the maxillary nerve into the CS. Subsequent studies (13) (14) found that when using the newer classification, anterior CS lesions were found to be due to inflammation, while posterior CS lesions were due to malignancies, thus suggesting that this scheme can help in throwing light on the underlying etiology and its localization.

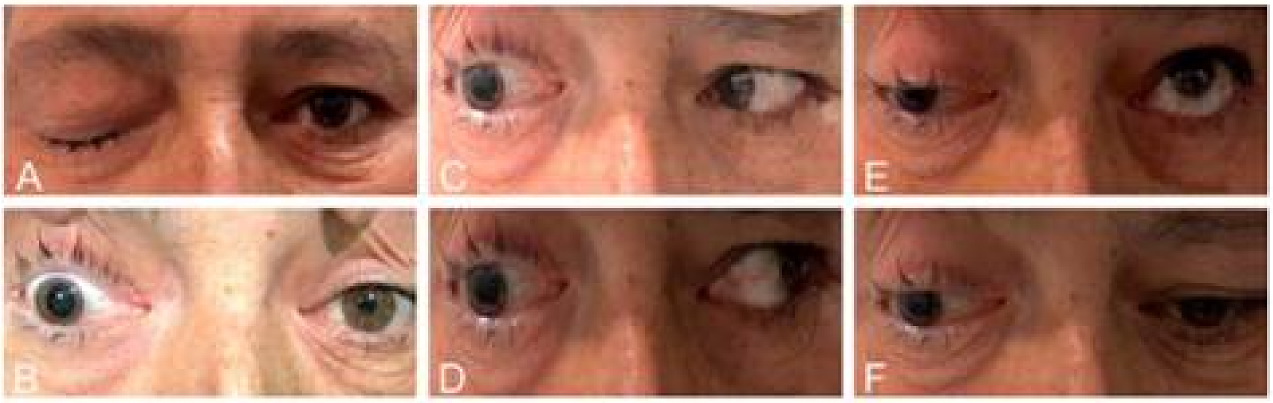

Figure 9: Ocular manifestations of CSS: right ptosis (A), absent right pupillary response (B), limited adduction (C) adduction (D), supraduction (E), and infraduction (F) of the right eye (15)

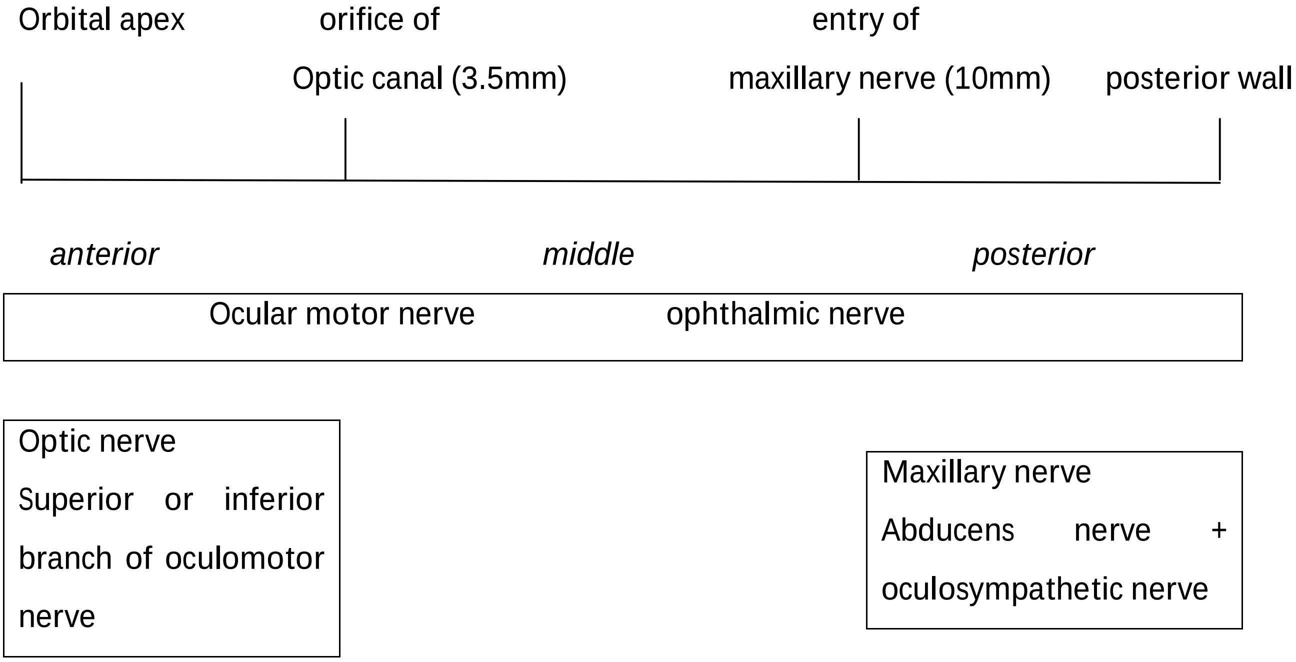

Figure 10: Ishikawa classification (13)

C. Pathology :

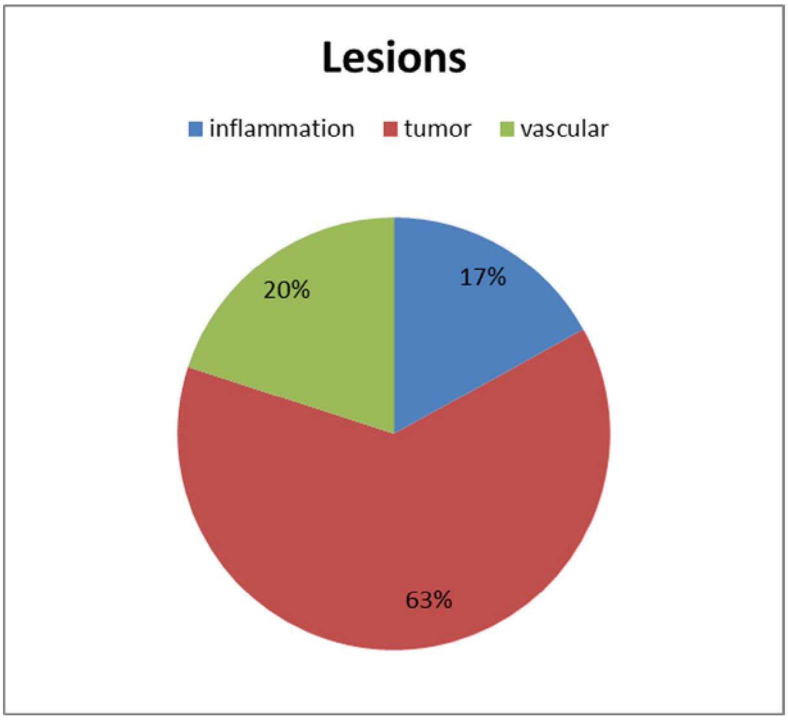

Figure 11: a pie chart of lesions of the CS as found in a study of a series of 126 patients (16):

1. Neoplastic :

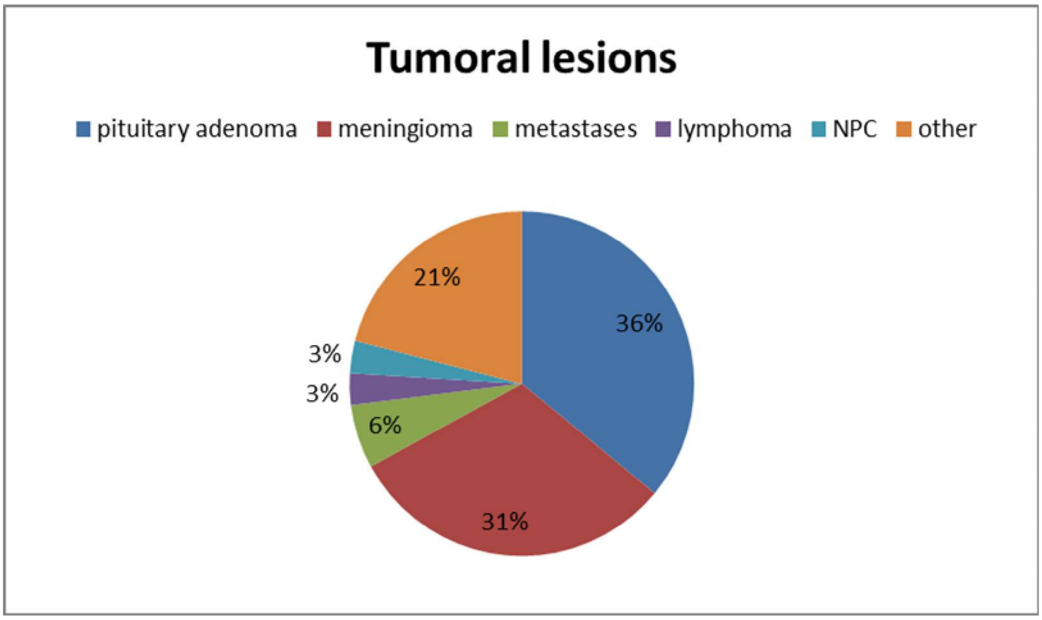

Figure 12: a pie chart of tumoral lesions of the CS as found in a study of a series of 126 patients (16):

1.1. Pituatary adenoma :

Involvement of the CS occurs in 6 to 10 % of all patients with PAs (17), with macroadenomas (≥1 cm in diameter) showing the most tendency toward invasion. This parasellar extension concerns the medial wall of the CS, and it could be explained by the hypothesis of the path of least resistance. While the mean thickness varied, the medial wall was always found to be the thinnest among the CS walls, with the thickness decreasing from inferior to superior, and from anterior to posterior. In some studies, the presence of defects has also been reported (18). Invasion of the medial wall of the CS could also be explained by the biological properties of the tumor. Overexpression of collagenase (particularly MMP 9 and MMP 2) was linked to invasive PAs, regardless of their size, type or status. In light of findings of different immunohistochemical analysis, pointing out collagen IV as the main component of the extracellular matrix of the medial wall, it all suggests the role of MMPs in the invasion process via their proteolytic activity. In addition, abundant expression of MMP 9 was also correlated with angiogenesis, which is a key factor in tumor invasiveness. Considering these associations, MMPs are promising biomarkers for detecting PAs invasiveness (19).

1.2. Meningioma:

Meningiomas are frequent CS lesions, representing 41% of all CS tumors (20). 80%–90% of them are slow-growing benign tumors. Female sex and advanced age – peak being in the 5th through the 7th decade– are two risk factors for their development (21).

These tumors arise from arachnoid cap cells in the dural walls of the CS (mainly the lateral wall) or from the adjacent dura with extension to the CS. They can project laterally from the lateral dura of the CS, grow between the two dural layers of the lateral wall, or invade the CS proper. In the latter case, meningiomas can encase the cavernous ICA, often causing its narrowing –which is a characteristic that can be helpful in distinguishing a meningioma from a PA–or invade the vessel’s wall (22). Meningiomas originating from the dural walls of the CS could extend to the Meckel cave, the sella, and to the anterior, middle, or infratemporal fossae, with a growth rate of 0.02 to 0.24 cm per year (20).

1.3. Schwannoma (nerve sheath tumor)

Schwannomas are benign and slow growing nerve sheath tumors arising from differentiated Schwann cells. When originating in the CS, they most commonly arise from the trigeminal nerve and from the oculomotor nerve to a lesser extent. Only a few cases were reported about CS schwannomas arising from the abducens nerve (to our knowledge, only 16 cases have been reported since 1982 (23)) and the sympathetic plexus around the ICA (with only one reported case in the literature (24)).

Most CS Schwannomas occur in patients in their 5th and 6th decades, with no gender predilection. In case of multiple Schwannomas at an earlier age, the diagnosis of neurofibromatosis type 2 should be suspected.

1.4. Lymphoma :

Lymphoma can involve the CS as a primary lymphomatous lesion (25), or as a secondary lesion part of systemic disease. In the latter case, lymphoma (often non-Hodgkin lymphoma) can be a result of either direct extension from adjacent structures, such as the marrow of surrounding bones or the nasopharynx, or of hematogenous or perineural spread. Lymphomas may also occur as unilateral or bilateral lesions (26). Burkitt lymphoma (27), diffuse large B-cell lymphoma (28), T-cell lymphoblastic lymphoma (29), diffuse small B-cell lymphoma (30), and chronic lymphocytic leukemia (31) have all been reported to involve the CS in the literature.

1.5. Metastases:

Metastasis to the CS can occur in approximately 1% of patients with metastatic cancer (32). It can be secondary to hematogenous spread or direct extension from bony or soft tissue metastases. Head and neck cancers are the most common ones to metastasize to the CS. Distant tumors with known CS metastatic involvement are lung, breast, renal and gastric malignancies (17). The presence of CS lesion with a history of a known primary neoplasm should suggest the diagnosis. However, CS syndrome may occasionally be the only symptom of an occult malignancy (33). Aggressive features such as rapid growth or bone destruction are frequent characteristics of a metastatic lesion.

1.6. Nasopharyngeal carcinoma :

NPC is endemic in North Africa and Southeast Asia (34). The male-to-female ratio is 3:1 and it is most common in patients in their 5th and 6th decades of life (35).

This tumor is the most common extracranial malignancy to invade the CS (17), with an invasion rate of 17.9% (36). This involvement is frequently the initial clinical presentation of the tumor (37). It can occur by direct extension through different foramens at the skull base, as seen in 25–35% of cases (38), or by perineural tumor spread. They can also spread to the CS through the foramen lacerum, petroclival synchondrosis, or along the carotid canal (39).

1.7. Cavernous hemongioma :

Cavernous hemangiomas of the CS are benign vascular tumors, formed by sinusoidal vascular channels that contain slow-flowing or stagnant blood, and are lined by a pseudo capsule. They are distinct from cavernous angiomas which are vascular malformations and are encountered most commonly in the brain parenchyma (40). CSCHs can be distinguished into two subtypes: type A CSCHs are characterized by a large number of thin-walled sinusoidal vessels with little connective tissue. This type is important to consider prior to biopsy or resection due to their propensity to profusely bleed. Type B CSCHs are characterized by fewer sinusoidal vessels and more interconnective tissue and as such, they are associated with a lesser risk of intraoperative bleeding (41).

CSCHs constitute 2–3 % of all CS tumors (40) and they occur more commonly in middle-aged women. They usually do not cause the narrowing of ICA, in contrast to meningiomas.

2. Vascular :

2.1. ICA aneurysm:

ICA aneurysms which involve the CS constitute 2%– 9% of all intracranial aneurysms (42), and around 5% of giant aneurysms (>2.5 cm) (43). Most of them are idiopathic, but they can be traumatic, iatrogenic, or infectious in etiology. Unruptured, they are often asymptomatic and found incidentally at imaging, most often in women older than 50 years. When symptomatic, these aneurysms manifest mostly by way of diplopia, headaches, or retroorbital pain owing to mass effect (44). Rupture rarely occurs, in which case it should be considered a surgical emergency, for it can result in direct CCF, massive epistaxis if there is erosion into the sphenoid sinus, subarachnoid hemorrhage if there is extension into the subarachnoid space through the dural ring, and cerebral infarction (45).

2.2. Carotid cavernous fistula:

CCF is an abnormal arterial to venous communication between the carotid artery and the veins of the CS, which can be direct or indirect (or dural) (46). Direct CCFs (Barrow type A) are high-flow fistulas that occur when the ICA ruptures into the CS. The clinical manifestations tend to be dramatic. It is frequently traumatic in origin, but may also be iatrogenic, or caused by the rupture of an ICA aneurysm or Ehlers–Danlos syndrome type IV (47).

Indirect CCFs are typically low-flow fistulas that occur when the cavernous arterial branches drain into the CS. They are further divided into 3 types: Barrow type B involves meningeal branches of the ICA; Barrow type C involves meningeal branches of the external carotid artery, while Type D includes meningeal branches of both the internal and external carotid arteries (48). Dural CCFs are most commonly seen in elderly individuals with an insidious onset of visual disturbance and progressive chemosis (49). They are the result of hypertension, fibromuscular dysplasia, Ehlers–Danlos type IV, and dissection of the ICA (46).

2.3. Cavernous sinus thrombosis:

CS thrombosis often occurs as a complication of bacterial or fungal sepsis involving the paranasal sinuses, oral cavity, the orbits, facial soft tissues, or the skull base. It may also be aseptic in origin, and result from traumatic injury, surgery, vascular lesion or tumor growth. Other risk factors of CS thrombosis include immunosuppression, thrombophilia and obesity (17).

3. Inflammatory/infectious:

3.1. Sarcoidosis :

Sarcoidosis is an inflammatory multisystem disorder of unknown etiology, which is characterized by the formation of noncaseating granulomas. It is most common among young and middle-aged adults, with a slightly higher incidence among women (40). CS involvement often occurs as part of systemic disease. However, it can also be an isolated finding in patients with no evidence of intrathoracic or systemic disease (50).

3.2. Tuberculosis :

Tuberculomas account for 10–30% of all intracranial masses in developing countries (51), with them being mostly located in the cerebral or cerebellar hemispheres, and rarely in the brainstem, cerebellopontine angle, hypothalamic region, Meckel's cave, pituitary gland, and intraventricular spaces (52). The involvement of CS is exceptional, with only 18 cases having been reported in previous literature (53) (54), three of which were in the pediatric age group. Twelve cases were diagnosed based on operative removal of the lesion and resultant histopathology; AFB smear and culture for M. tuberculosis reported negative in all of them. The rest were diagnosed by revealing evidence of tuberculosis at extra-CNS sites.

3.3. Tolosa hunt syndrome :

Tolosa-Hunt syndrome describes a non-specific and chronic granulomatous inflammation in the anterior CS and/or superior orbital fissure. It is a rare disorder, with an estimated annual incidence of one case per million per year (55). The average age of onset is 41 years, with no male-female predisposition (56). It tends to have spontaneous remissions and recurrences, with episodes recurring every few months or years (57). A quick and dramatic response to the administration of corticosteroid therapy is a characteristic of these episodes, which could last up to 8 weeks if not treated (58).

3.4. Invasive fungal infection :

Aspergillus and Mucormycosis are the most commonly involved invasive fungal species (59). They can spread to the CS via hematogenous dissemination from the lungs, but most often by direct extension from the paranasal sinuses and orbits. Invasive fungal infection is divided into 3 subtypes depending on histologic criteria (60): The acute invasive (fulminant) occurs in case of immunocompromise and is characterized by a painless, necrotic black nasal septal or palatal ulcer that rapidly evolves into CS syndrome and ICA thrombosis, leading to a high mortality rate. The chronic invasive and chronic granulomatous invasive subtypes typically occur in immunocompetent patients, although diabetes mellitus and steroid therapy are risk factors.

D. Imaging features of the cavernous sinus’ lesions:

The CS can be affected by a wide variety of vascular, neoplastic, and inflammatory pathologies; however, they often have similar and overlapping clinical features. Imaging plays a crucial role in the characterization of the nature of the lesion and in defining its relationship to neurovascular structures and extension to surrounding tissues, which is essential in determining the appropriate mode of treatment. MRI with and without contrast is the imaging modality of choice for assessment of the CS, offering higher soft-tissue contrast resolution compared to CT, while CT and digital subtraction angiography may be useful in certain cases such as vascular pathology.

1. Imaging of the tumoral lesions:

1.1. Pituatary adenomas :

On MRI, PA is seen as a mass expanding the sella, hypointense on T1-weighted sequences, hyperintense on T2-weighted imaging, and hypoenhancing in comparison to the normal pituitary gland when visible (figure 14). The lesion may be heterogeneous, reflecting cystic and/or necrotic areas (17) (64). Among several radiological classifications to predict the likelihood of CS invasion by

Pituitary adenomas, that of Knosp et al (61) (figure 13) is the most widely used. It divides the cavernous space into 4 venous compartments by drawing 3 lines (medial tangent, intercarotid line and lateral tangent) between the supraclinoid ICA and intracavernous ICA on coronal MRI imaging (table 1).

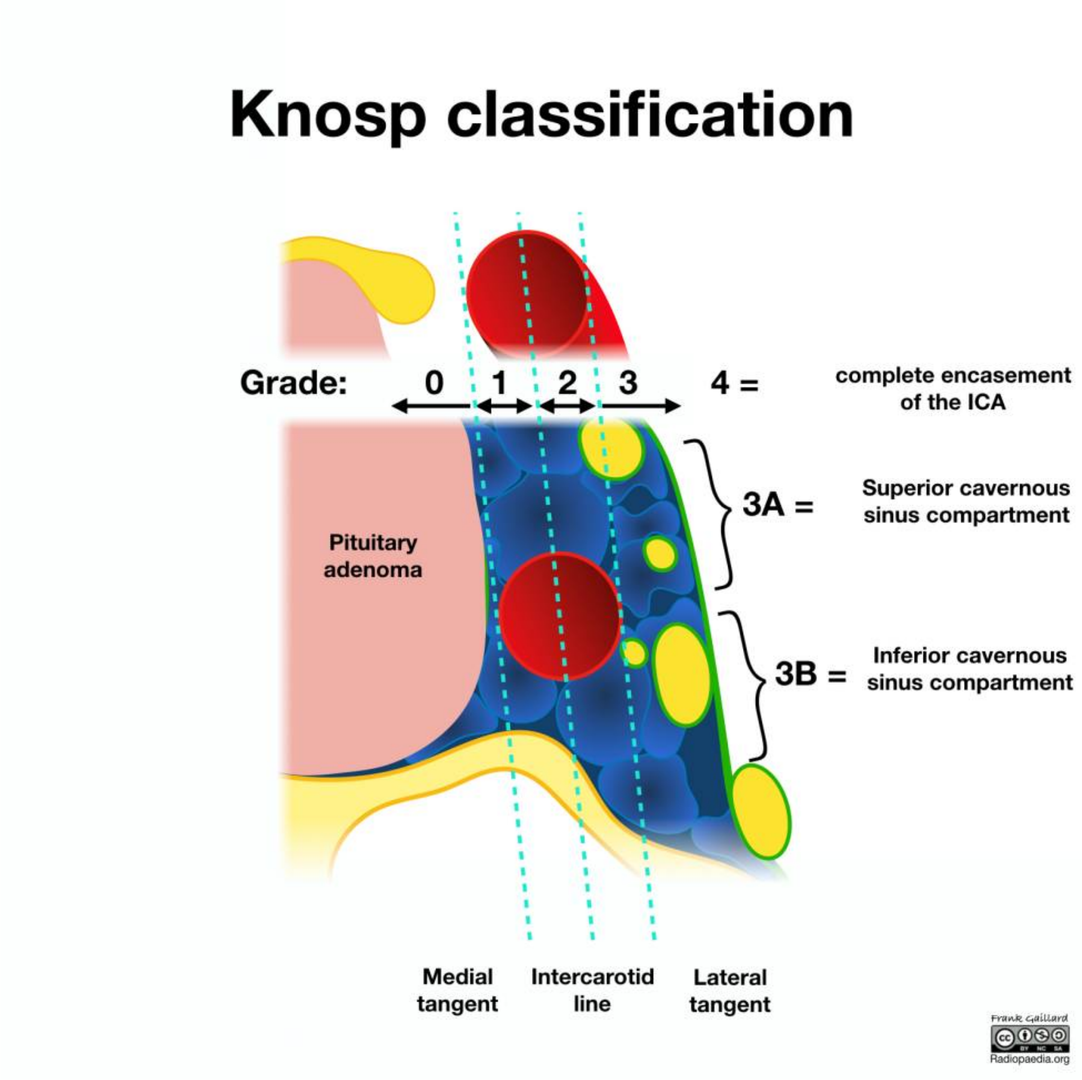

Figure 13: Knosp et al classification : (62)

Grade 0	- Medial to medial tangent	No invasion	- predictive GTR: 83% - predictive endocrinological remission: 88%
Grade 1	- extension to the space between the medial tangent and the intercarotid line	No invasion	- predictive GTR: 71% - predictive endocrinological remission: 60%
Grade 2	- extension to the space between the intercarotid line and the lateral tangent	Possible invasion	- predictive GTR: 83% - predictive endocrinological remission: 88%
Grade 3A	- extension lateral to the lateral tangent, above the intracavernous ICA	Probable invasion	- predictive GTR: 85% - predictive endocrinological remission: 67%
Grade 3B	- extension lateral to the lateral tangent, below the intracavernous ICA		- predictive GTR: 64% - predictive endocrinological remission: 0%
Grade 4	- total encasement of intracavernous ICA	Definite invasion	- predictive GTR: 0% - predictive endocrinological remission: 0%

Table I: knosp classification and surgical correlation: (63)

Although classification systems based on preoperative imaging play an important role as predicting tools, intraoperative findings remain the golden standard for the diagnosis of PAs invasion.

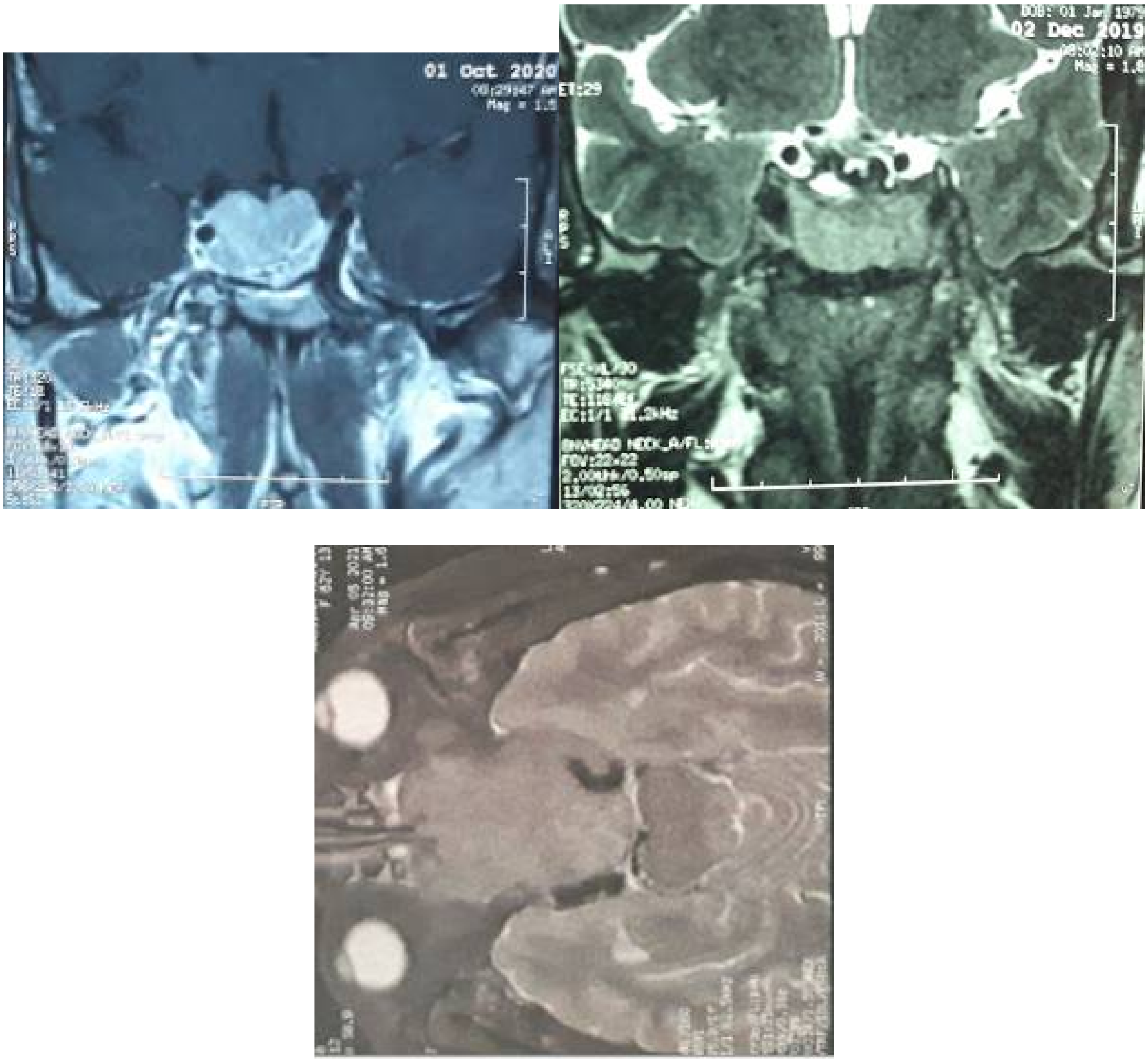

Figure 14: MRI images of Pituitary adenoma with CS invasion. (A) coronal T1 weighted with gado. (B) coronal T2 weighted image. (c) axial MRI image

1.2. Meningioma:

On MRI, meningiomas are isointense to gray matter on T1- and T2-weighted MR images with intense homogenous enhancement. Although usually homogeneous in appearance, tumor heterogeneity can be seen due to calcification, tumor-associated vascularity, cystic areas, and, rarely, hemorrhage. A broad-based dural attachment and dural tail sign are characteristic. Luminal narrowing of the ICA can be seen, a feature that differentiates a meningioma from a pituitary adenoma. On CT, The presence of calcifications and adjacent hyperostosis should suggest the diagnosis (17) (64) (Figure 15).

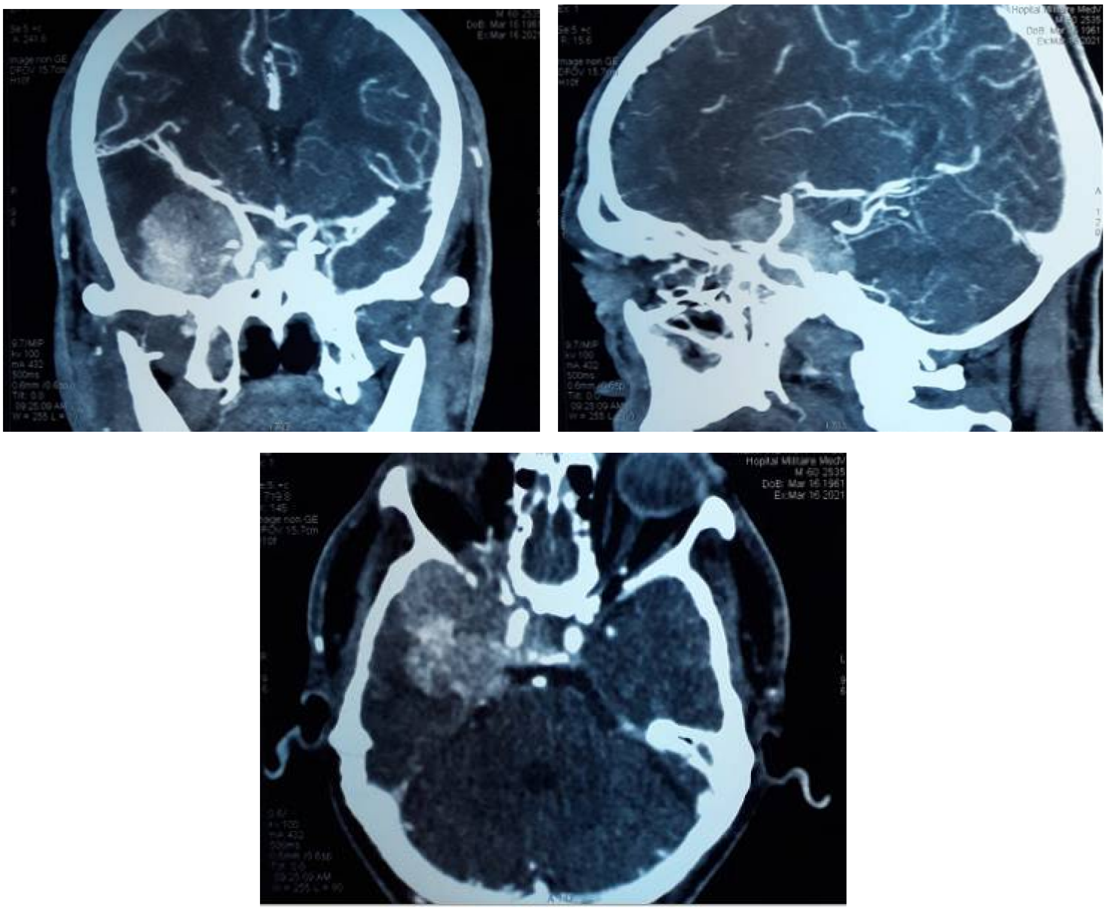

Figure 15: (A—C) angio CT scan of a meningioma of the right CS extending to the middle cerebral fossa. (A) coronal plane (B) sagittal plane (C) axial image

Based on the preoperative MR and CT findings, Hirsch et al proposed (65) a classification of CS meningiomas to predict the ease of surgical resection, and as such, assist surgeons in planning treatment. Depending on their relationship to the cavernous carotid artery in imagery, meningiomas were classified into five categories (table 2).

Grade I	- tumor involve 1 region of the CS without involving the ICA
Grade II	- tumor involve multiple areas of the CS, with no ICA encasement
Grade III	- ICA encased without narrowing
GradeIV	- ICA encased and narrowed
Grade V	- bilateral CS invasion

Table II: Sekhar-Hirsh grading system, the modified radiological classification, is based on the encasement of the ICA and the extent of the tumor (93)

1.3. Schwannoma :

MRI imaging is the modality of choice for the diagnosis of these tumors. They are seen as iso- or hypointense on T1-weighted images with strong enhancement and hyperintense on T2-weighted images. They are well-defined enhancing masses, with or without cystic components. These nerve sheath tumors often follow the expected course of the involved nerve, having an ovoid shape when restricted to the CS, and a dumbbell shape when they extend beyond it into the posterior cranial fossa, the orbit, or the infratemporal fossa (17) (64). (figure 16)

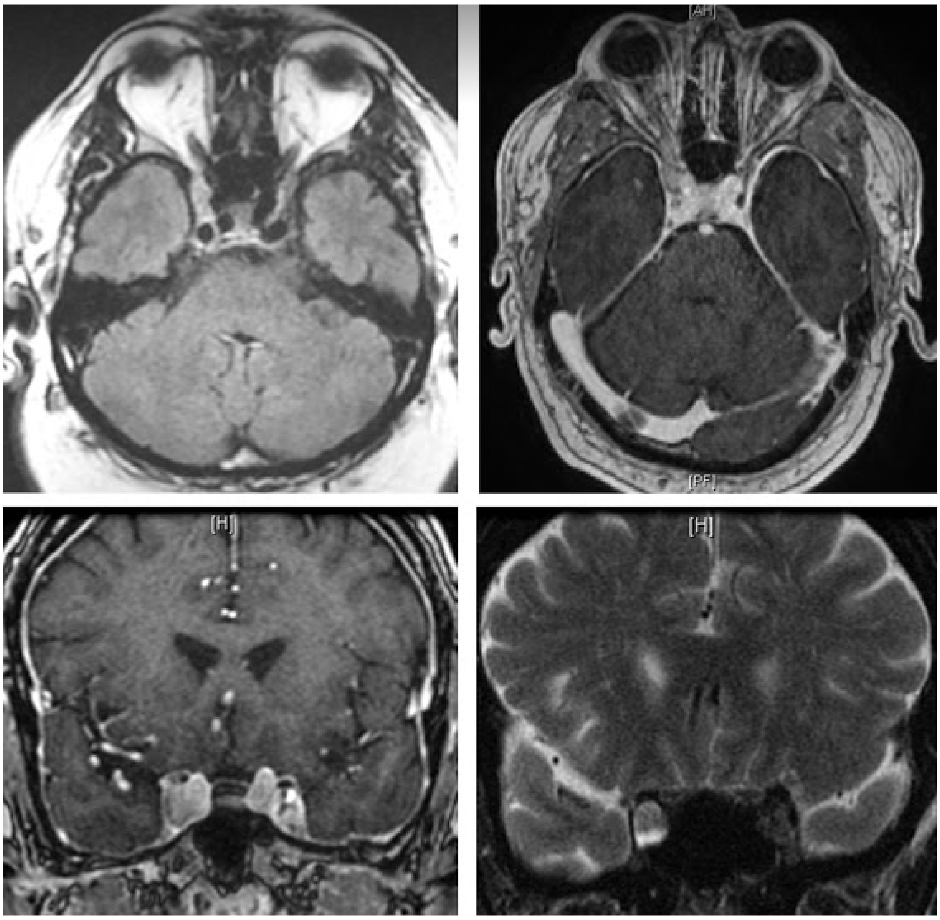

Figure 16: MR images of CS Schwannoma arising from the 3^{rd} cranial nerve. (A-B) axial T1 and T2 weighted images. (C-D) coronal T1 and T2 weighted MR images

1.4. Lymphoma :

At MRI, lymphomatous lesions often are hypointense on T2 weighted imaging and show diffusion restriction due to their hypercellularity, while they demonstrate hyperdense attenuation on non-contrast CT. PET plays an essential role in evaluating the extent of systemic disease involvement. Lymphoma enlarges the CS without compressing the ICA and typically extends through the skull base foramina (17) (64). (figure 17)

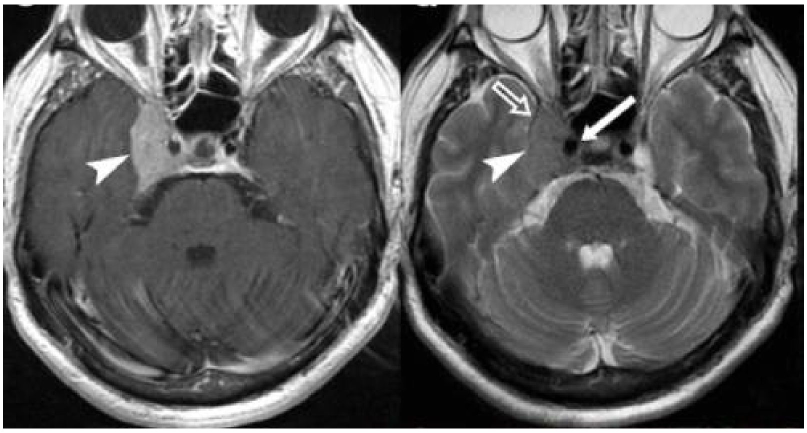

Figure 17: imaging of lymphoma. Axial CE T1W and T2 weighted MR images shows homogeneous contrast enhancement of the tumor (arrowhead). (67)

1.5. Metastases :

The imaging appearance of metastatic involvement of the CS is nonspecific, with outward bowing of the lateral wall and an enhancing mass in CS. There may be additional lesions depending on the primary tumor. Metastatic lesions often have a rapid growth rate (17) (64).

1.6. Cavernous hemangioma :

At MRI, cavernous hemangiomas are characterized by a hyperintense signal on T2- weighted sequences, and as a result, are often misdiagnosed as schwannomas. Dynamic contrast-enhanced T1-weighted MR images show characteristic homogenous and progressive“fill-in” of contrast agent. Scintigraphic imaging after administration of 99mTc pertechnetate–labeled red blood cells offers high sensitivity and specificity for diagnosis, initially showing an area of photopenia followed by increased activity on delayed blood pool images. Digital subtraction angiography may be useful by showing hypertrophic branches from the external carotid artery and ICA. (17) (64) (figure 18)

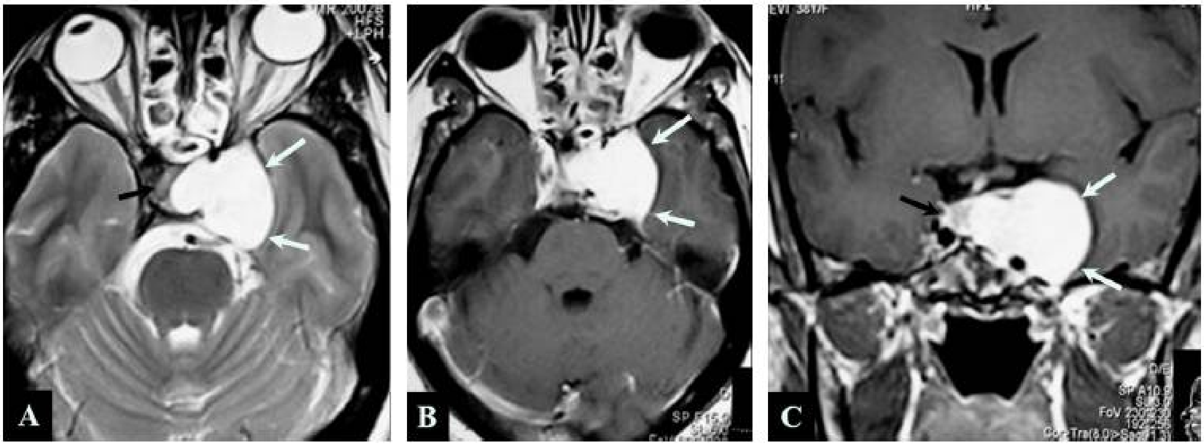

Figure 18: imaging of Hemangioma: MR images show homogeneous mass (white arrows) involving
the left CS. it is hyperintense on axial T2-weighted images (A) with intense homogeneous contrast-enhancement on axial and coronal contrast-enhanced T1-weighted images (B and C). (59)

2. Imaging of vascular lesions:

2.1. ICA Aneurysm :

On CT, cavernous ICA aneurysms are mildly hyperattenuating compared with brain tissue, and can show peripheral calcifications or central calcifications in the case of thrombosed aneurysms. On MRI, the signal intensity can be highly variable depending on the flow dynamics within the sac and the extent of thrombosis. Non-thrombosed aneurysms demonstrate a flow loss on traditional spin-echo (SE) sequences, whereas thrombosis may result in high T1 signal and variable T2 signal. CTA, MRA, or conventional angiography plays an important role in verifying contiguity with the ICA and confirming the diagnosis (17) (64). (figure 19)

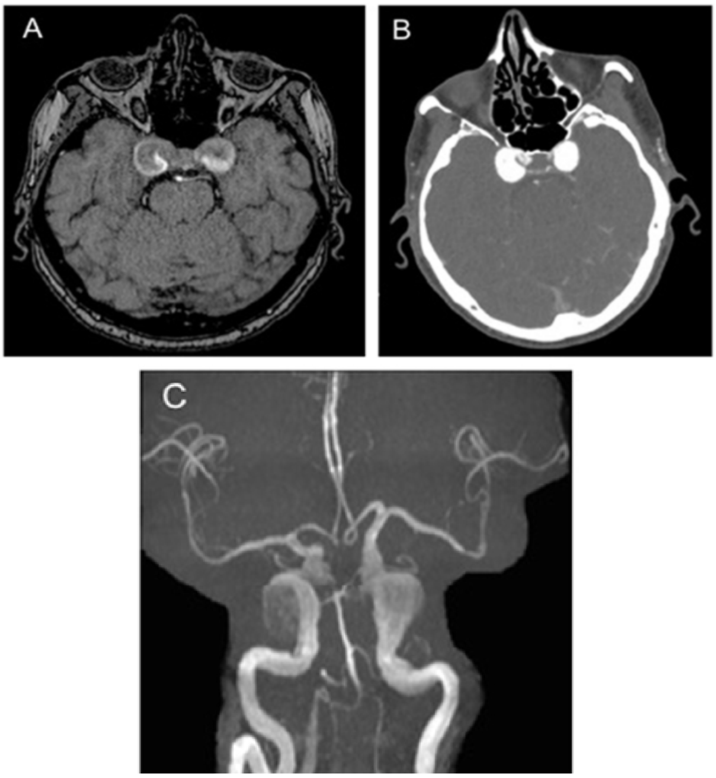

Figure 19: imaging bilateral CS aneurysms.**(A)** T1-weighted axial MRI imaging **(B)** Brain CT angiography **(C)** MRI angiography (68)

2.2. Carotid cavernous fistula :

Futures of CCF at MRI include intense enhancement of an enlarged CS, associated with a dilated superior ophthalmic vein, infiltration/edema of the orbital fat, and bulky extraocular muscles. Digital subtraction angiography remains the gold standard, demonstrating shunting from the ICA or its branches to the CS. CT angiography has been shown to be as good as digital subtraction angiography and better than MR angiography in the detection of CCFs. (17) (64) (figure 21)

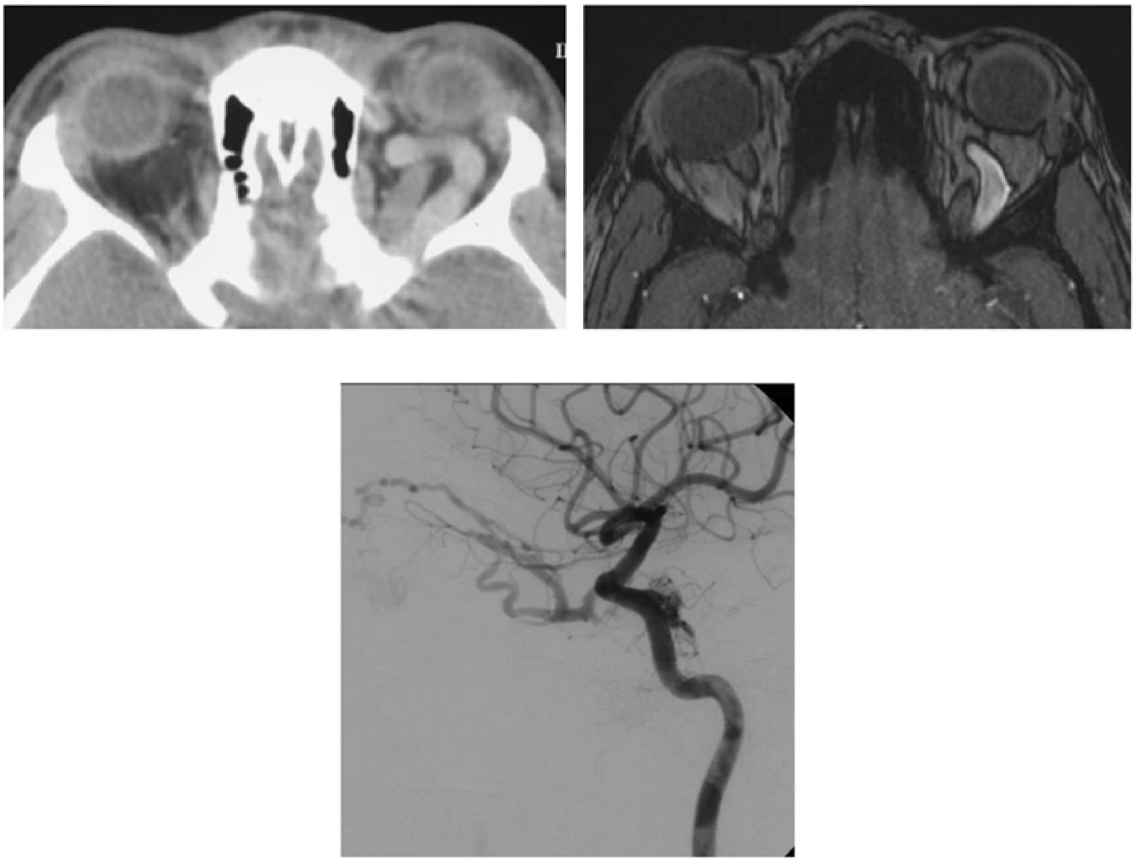

Figure 20: imaging of Carotid-cavernous fistula: Axial CT scan (left) and postcontrast MR image (right) show dilated left superior ophthalmic vein in a patient with a left-sided, anteriorly draining, CCF. Selective left internal carotid arteriogram (lateral view) shows a dural CCF with drainage both anteriorly and posteriorly (69)

2.3. Cavernous sinus thrombosis :

Imaging signs of CS thrombosis include an enlarged CS, a convex configuration of the lateral wall, filling defects within the sinus, engorged or thrombosed superior ophthalmic vein which manifests as a loss of its flow void, ipsilateral retro-orbital fat stranding, bulky extraocular muscles, and exophthalmos. T1 and T2 signal intensity depends on the stage of thrombus evolution. Sub-acute thrombus produces high signal intensity on T1 and T2 weighted images while thrombi in the acute stage produce an isointense signal. Contrast-enhanced images can be useful in the acute stages, as the thrombus will be seen as a filling defect with surrounding rim enhancement. (17) (64) (figure 21)

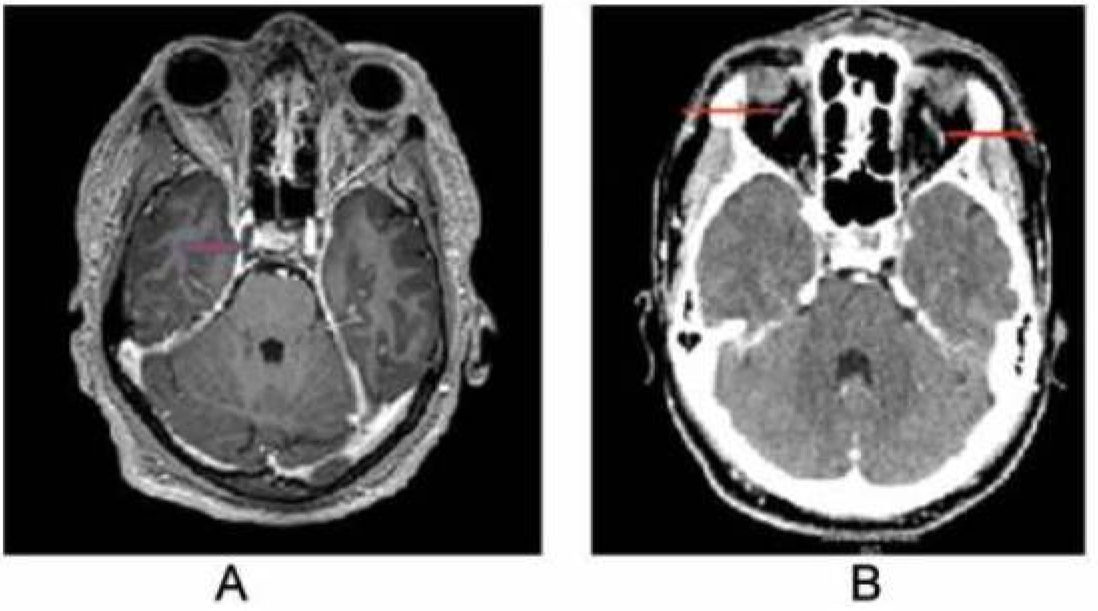

Figure 21: imaging of CS thrombosis: (A) T1-weighted with gadolinium MR image showing non- opacification of the right CS. (B) Contrast-enhanced brain CT showing bilateral engorged thrombosed superior ophthalmic veins. (70)

3. Imaging of inflammatry/infectious conditions:

3.1. Tolosa hunt syndrom :

MRI shows an enlarged CS with abnormal soft tissue which is isointense to gray matter on T1 weighted imaging and variable hypo- or hyperintense signal on T2 weighted MR images. The cavernous ICA may show mild narrowing due to the inflammatory process. More importantly, imaging plays an essential role in showing a lack of disease outside of CS, superior orbital fissure, and orbital apex region, and in ruling out mimics. (17) (64)

3.2. Sarcoidosis :

Imaging signs of CS sarcoidosis are nonspecific and include masslike enhancement of the CS and adjacent dural thickening. Clues to the diagnosis include the involvement of CNS such as multiple dural based lesions, pachymeningitis or leptomeningeal enhancement, thickeneing of cranial nerves, and thickening with enhancement of hypothalamus/pituitary stalk. There may also be a thickening and enhancing of extraocular muscles and infiltrative enhancing soft tissue in the retrobulbar fat. (17) (64) (figure 22)

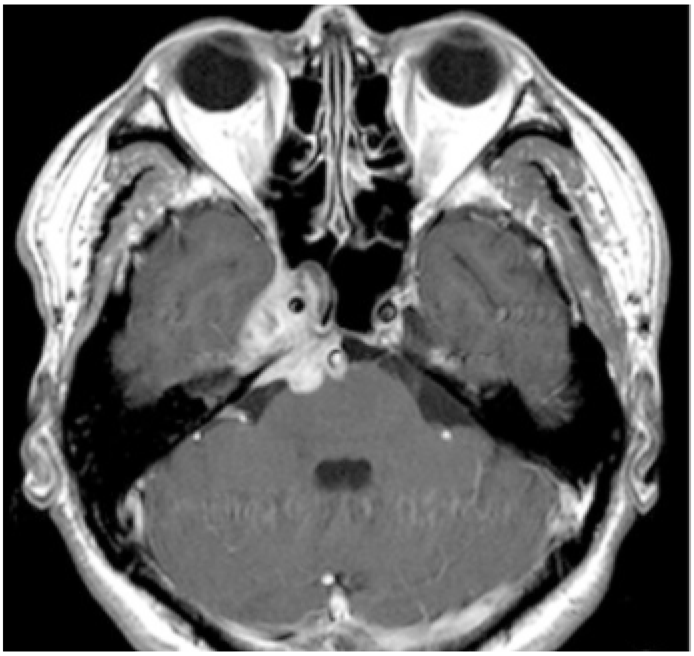

Figure 22: imaging ofCS Sarcoidosis: Gadolinium-enhanced MR image_showing the mass extended toward the middle fossa laterally and to the sphenoid sinus anteriorly (71)

3.3. Tuberculosis :

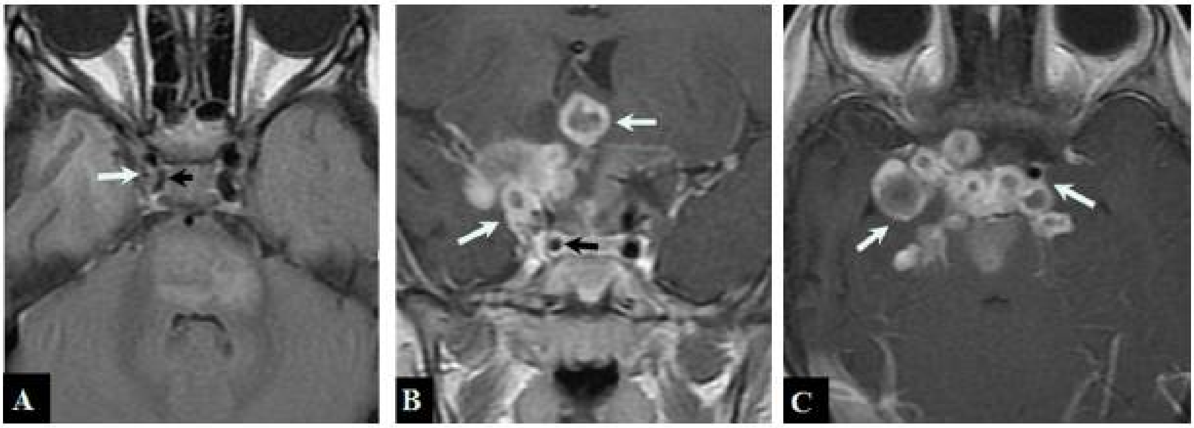

Figure 23: imaging of CS Tuberculosis: MR images showing isointense soft tissue (white arrow) in the right CS on axial FLAIR image (A). Contrast-enhanced images (B and C) show multiple ring-enhancing lesions (white arrows) in basal cisterns with the involvement of the right CS. (59)

3.4. Inavsive fungal infection :

CT is particularly useful to evaluate bone destruction, often showing an associated paranasal sinus disease; whereas MR imaging is useful to demonstrate soft tissue anomalies. On MRI, fungal infection shows as a low signal on both T1-and T2-weighted imaging which is attributed to the ferromagnetic elements related to fungal metabolism. Other secondary imaging features include CS thrombosis and stenosis or mycotic pseudoaneurysm of the intracavernous ICA. The infection may extend into the subdural space and cause the development of subdural abscesses. (17) (64)

Materials and methods

Three artery-injected head adult cadavers were studied, and a bilateral endoscopic endonasal approach to the CS was performed (n = 6) at the Skull Base Laboratory at Weill Cornell Medical College in New York USA (figure 24). The selection criteria were: (1) age of 18 years or older, (2) no history of head trauma or craniofacial surgery, and (3) dissection of corpses that had already been autopsied or during autopsy (dissection was done after the evaluation and permission of the forensic medicine doctors).

Figure 24: Skull Base Laboratory at Weill Cornell Medical College in New York USA

Dissection was performed using Karl Storz 0° and 30°, 4 mm, 18 cm rod lens rigid endoscope (Karl Storz and Co., Tuttlingen, Germany). The endoscope was connected to a light source via a fiber optic cable and to a full HD camera. The video camera was connected to a 31-inch monitor. We used the Karl Storz Kassam-Snydermann endoscopic surgical set as surgical instrumentation. The cadaveric specimen was placed in a supine position with the head in a neutral position and 10–15° adducted toward the left shoulder.

❖ Dissection technique:

By introducing the endoscope into the right nostril, the choana was identified in the posteroinferior end of the nasal cavity, at the end of the tail of the inferior turbinate, and medially to the vomer. Then we redirected rostrally the 0-degree endoscope along the sphenoethmoidal recess, where the sphenoid ostium is usually exposed nearly 15 mm superior to the choana, between the superior turbinate and the nasal septum. A middle turbinectomy allowed a wider exposure and a more comfortable surgical corridor. We removed the mucosa (laterally and medially) to expose the sphenoid sinus floor and anterior wall and the rostrum medially.

In the aim of performing a binostril approach, the posterior part of the nasal septum was resected. In this way, the entire sphenoid sinus floor and the Ostia were exposed. A similar procedure was performed from the left nostril, except that the left middle turbinate was lateralized. The anterior and inferior walls of the sphenoid sinus were removed using a high-speed drill or 2-mm Karrison rongeur. In this stage of dissection, care must be taken not to injure the vidian nerve (the sphenopalatine nerve) and the sphenopalatine artery. The latter is located in the inferolateral corner to the sphenoid sinus and 1 cm anterior to the rear end of the tail of the middle turbinate in 90% of cases. All septae in the sphenoid sinus must be resected by punch or diamond drill to expose the sellar floor and its anatomic landmarks. Lateral septae generally point to the opticocarotid recess, which is the reason why these are good anatomic landmarks during dissection.

Planum sphenoidal is located superior and above the sella floor. The optic protuberances were identified on both sides laterally to the planum sphenoidal. Laterally to the sellar fossa, the carotid protuberance was identified with its two parts: superiorly the sellar carotid protuberance and inferiorly the clival carotid protuberance. Between the optic and carotid protuberance, the opticocarotid recess, which represents the base of the anterior clinoid processes, was identified. The thin bone of the sellar fossa was easily fractured by a sharp dissector or a diamond drill to expose the sellar dura. To access the parasellar region, the extended endoscopic endonasal transsphenoidal approach facilitated by removing the superior and middle turbinate and posterior ethmoidectomy allowed the exposition of the inferior portion of the CS.

The exposition of the lateral wall of the CS required using the endonasal ethmoido-pterygo-sphenoidal approach. During this procedure, the uncinate process wasresected. Then after identifying the ethmoid bulla, the anterior and then the posterior ethmoidal cells were exposed and removed. The medial wall of the CS was exposed by a 30°endoscope introduced through the contralateral nostril (contralateral endoscopic endonasal transsphenoidal approach) (72).

Results

1. Parasellar ICA:

Two segments are distinguished along the parasellar ICA: cavernous and paraclinoidal. The cavernous ICA is the continuation of the paraclival ICA. It can be subdivided from proximal to distal into the short vertical segment (corresponding to the posterior vertical and posterior genu), horizontal segment, anterior genu and anterior vertical (figure 25). The paraclinoidal ICA begins as the artery emerges from the CS, which is marked by the middle clinoid when present. It extends at the roof of the CS, between the proximal and distal dural rings, bordered by the lateral optic-carotid recess superolateraly (figure 26) (9).

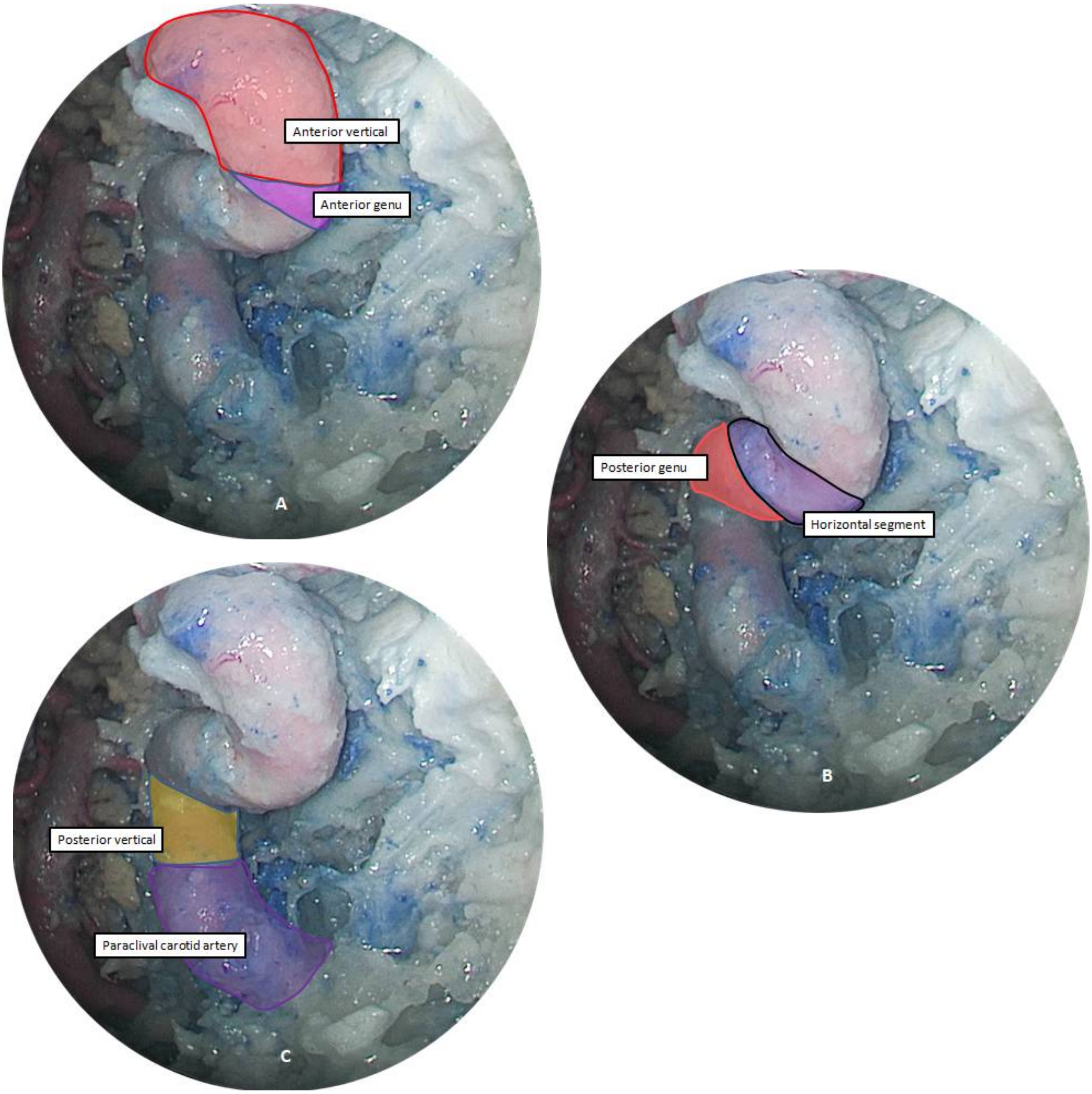

Figure 25: representation of the segments of the parsellar ICA. A: highlighting the anterior vertical segment (which transition into the paraclinoidal ICA as it emerges from the CS) and the anterior genu. B: highlighting the horizontal and posterior genu segment of the ICA. C: highlighting the posterior vertical segment which is a continuation of the paraclival carotid artery.

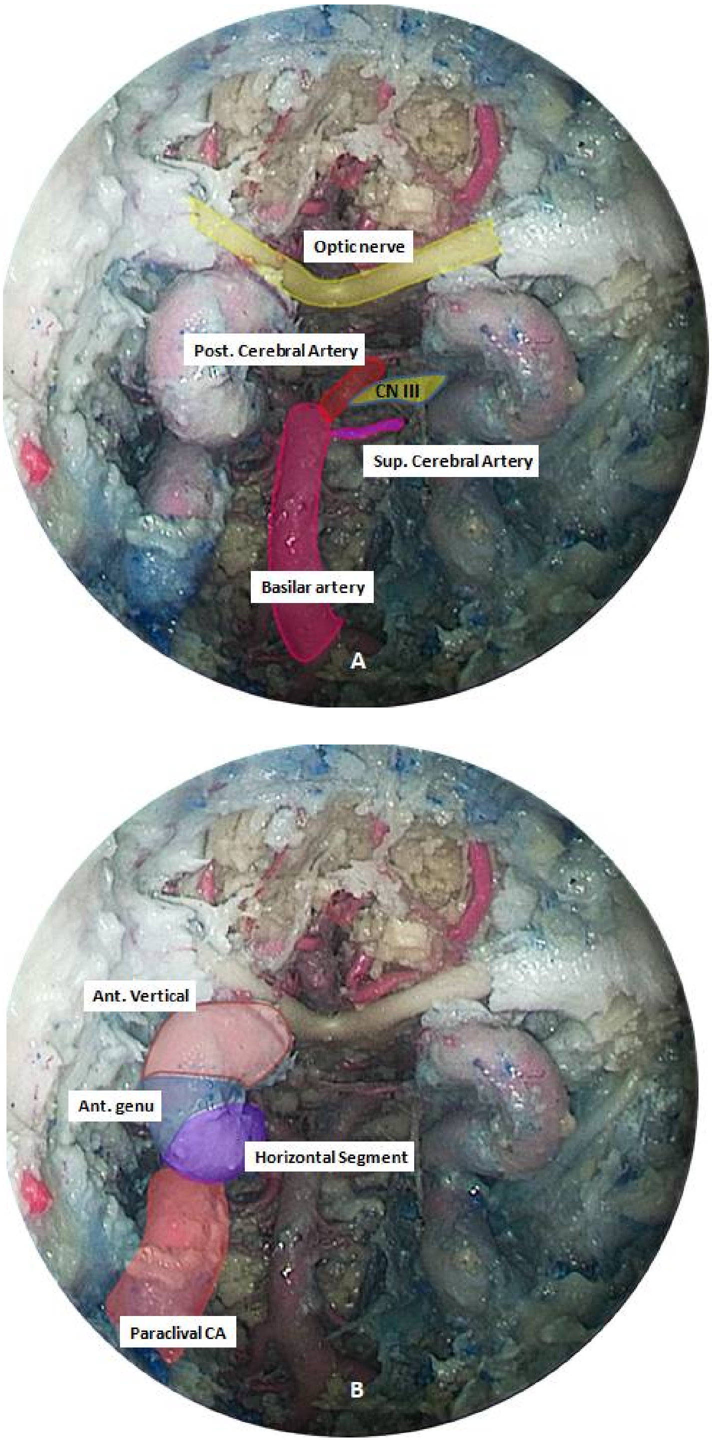

Figure 26: Endonasal perspective of the exposed parasellar region.

A: neurovascular relationships in the parasellar region

B: representation of the segments of the ICA.

2. Superior compartment of the CS:

The roof of this compartment is marked by the interclinoidal ligament which extends from the posterior to the anterior clinoid process. Medial and anterior to this dural band, the paraclinoidal ICA runs, while the oculomotor nerve courses just lateral and posterior. The oculomotor nerve (CN III) runs in the lateral wall of this compartment, in between the two dural layers. This interdural segment, filled with CSF, is defined as the oculomotor cistern. The nerve courses anteriorly and upwards into the most superior aspect of the lateral wall of the CS, and emerges laterally to the anterior genu of the ICA (figure 27) (9).

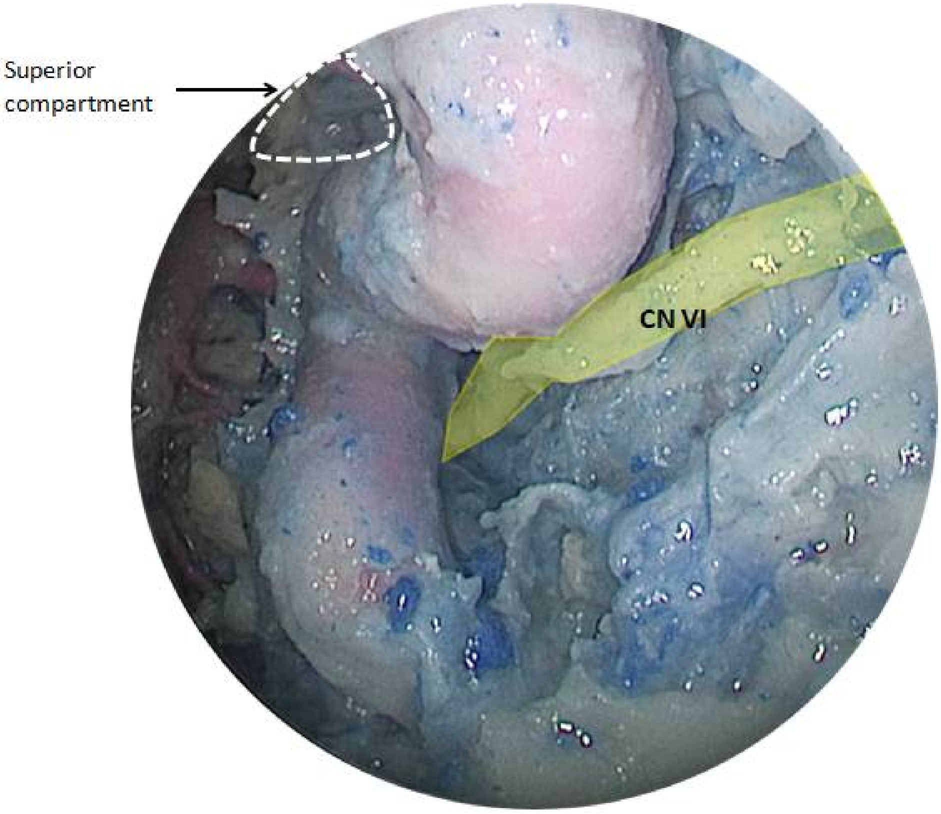

Figure 27: location of the superior compartment in relation to the ICA:

❖ Surgical Nuances

The removal of the anterior wall of the CS allows the exploration of the superior compartment which facilitates the lateral displacement of the carotid artery and direct section within this area. The tumors invading this compartment are more likely to extend to the medial wall of the CS and consequently are easily approached through this wall. In this case, gentle medial-to-lateral ICA mobilization is performed with the suction shaft while a second surgical instrument is used to remove the tumor.

This dissection can be performed with 0-degree endoscopes, but the use of angled scopes maximizes visualization, especially of the dorsal aspect of the anterior genu of the ICA. The portion of the oculomotor nerve located laterally to the anterior genu of the ICA is the most vulnerable and is not an area easily accessible from a medial to lateral trajectory (9).

3. Posterior compartment of the CS:

The MHT originates from the posterior genu of the ICA. This vessel may further branch into the tentorial artery, the inferior hypophyseal artery, and the dorsal meningeal, although these 3 vessels may also arise directly from the ICA. The inferior hypophyseal artery travels in a lateromedial trajectory toward the dura covering the sellar floor, while the dorsal meningeal artery takes a posterior and inferomedial trajectory toward the dura of the dorsum sella. The CN VI runs at the most inferior portion of this compartment as it passes through Dorello’s canal to enter the CS, just behind the ICA, after losing the dural layer protecting it. It lies above the most medial aspect of the petrous apex and is bordered posteriorly by the petro-sphenoidal ligament (9) (figure 28)

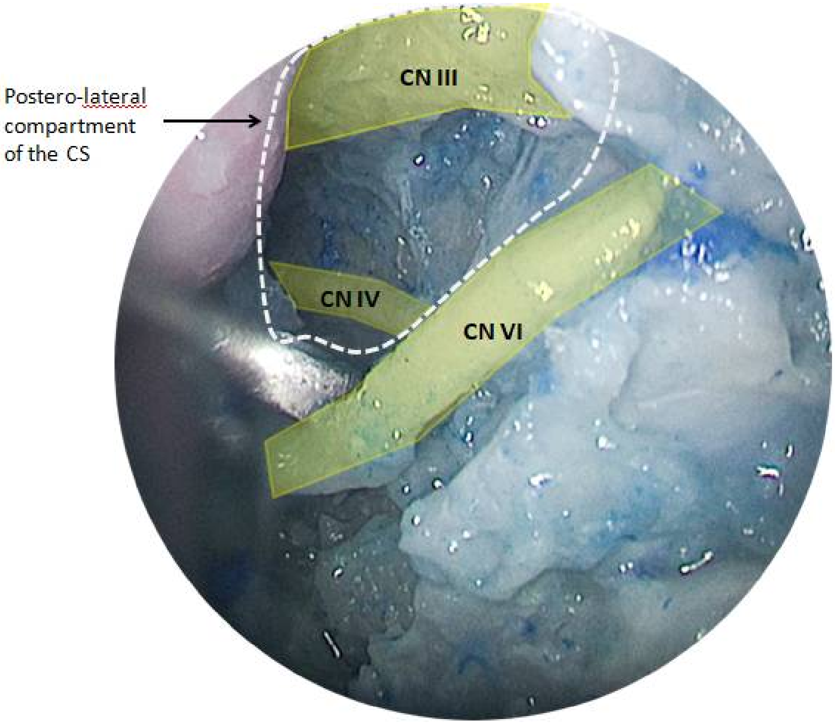

Figure 28: exposure of the postero-lateral compartment of the CS by pushing the abducens nerve downwards by the dissector:

❖ Surgical Nuances

Lateral mobilization of the short vertical and posterior genu segments of the ICA is needed to gain access posterior to the cavernous ICA. Coagulation and transection of the inferior hypophyseal artery may be necessary. The presence of the abducens nerve at the floor of this compartment is marked by the short vertical segment of the ICA, and can be confirmed by electrostimulation (9).

4. Inferior compartment of the CS:

In this compartment the sympathetic plexus courses along the short vertical and the horizontal segments of the ICA. Located medially to the abducens nerve, it runs an oblique route from the surface of the ICA to join the sixth cranial nerve. The latter lay just inferior and lateral to the horizontal segment of the ICA, at the transition between the inferior and lateral compartments (figure 29) (9).

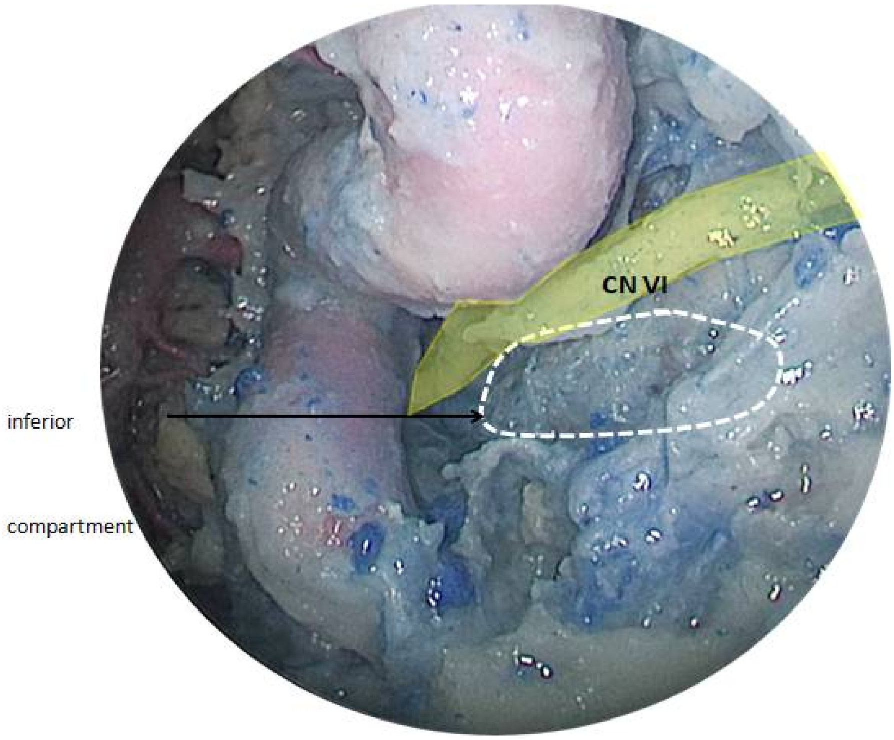

Figure 29: location of the inferior compartment in relation to the ICA and the abducens nerve:

❖ Surgical Nuances

Maxillary nerve entering the foramen rotundum and the inferior wall of the CS extending laterally to the CS anterior are anatomical landmarks that enable the extension of the opening of the dura laterally and inferior to the anterior genu and horizontal ICA, and in front of the short vertical ICA segment. Intraoperative echo Doppler is very useful in identifying the trajectory of the ICA before opening the dura, which is performed using a right-angled knife with a blunt tip. The sympathetic plexus runs medial to the abducens nerve. Electrical stimulation can help the identification of the abducens nerve lateral, inferior, and parallel to the horizontal ICA and enable its distinction from the sympathetic nerve (9).

5. Lateral compartment of the CS:

We identify the oculomotor (figure 30), trochlear nerves (figure 31), the first division of the trigeminal nerve (figure 32), as well as the abducens nerve which is located at the transition point between the inferior and lateral compartments. Arising from the horizontal segment of the horizontal, the arterial branches of the inferolateral trunk run from medial to lateral where they distribute along the lateral wall of the CS (9).

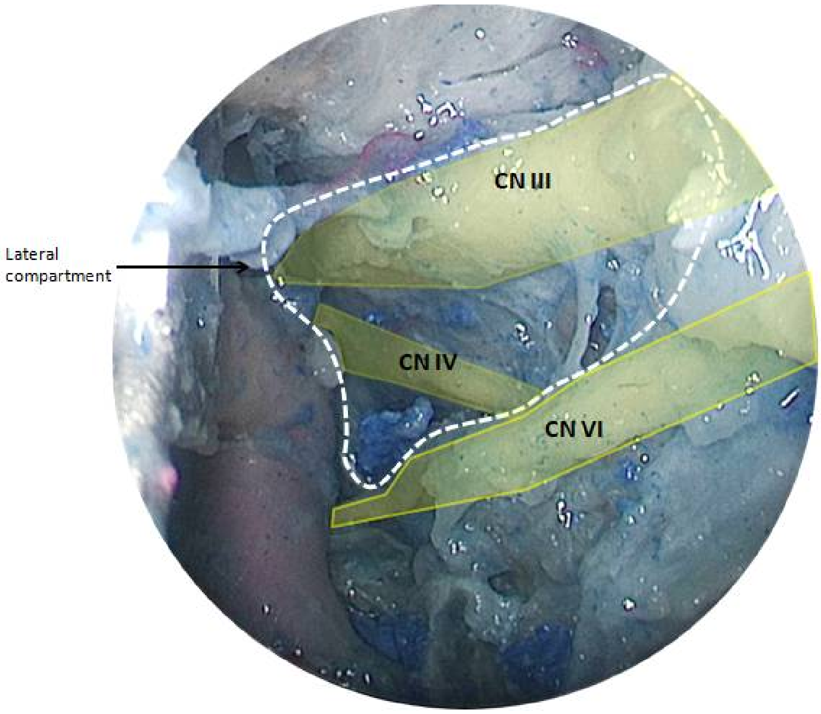

Figure 30: exposure of the lateral compartment of the CS after lateralization of the horizontal segment of the ICA by the dissector

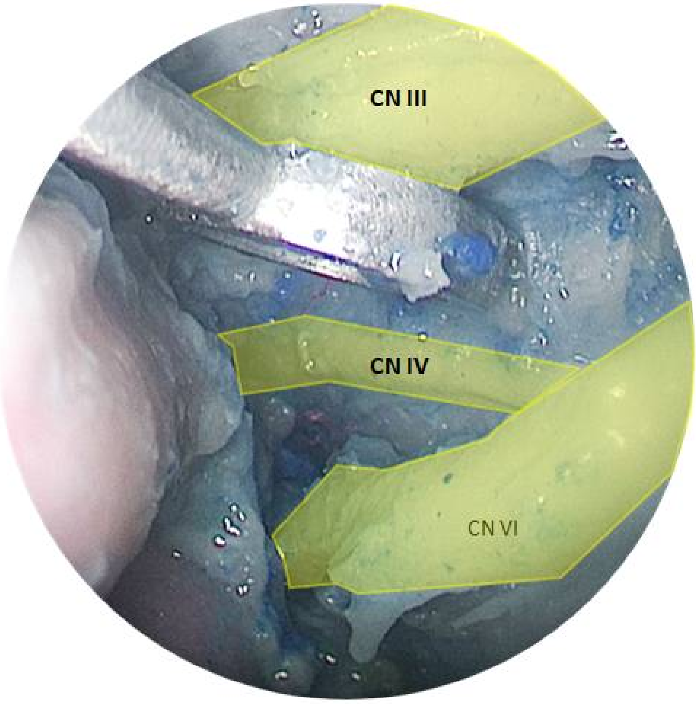

Figure 31: exposure of the course of the trochlear nerve by pushing the oculomotor nerve upwards by the dissector

Figure 32: exposure of the first division of the maxillary nerve by dissection of the lateral wall of the CS:

❖ Surgical Nuances

Tumors in this compartment commonly involve the lateral wall of the CS, in which case complete resection can risk CN injury. Surgical access requires exposure of the anterior wall of the CS, paraclinoidal ICA and the anterior genu segment of the cavernous ICA laterally up to the superior orbital fissure. The dura is opened in front of the anterior genu segment of the cavernous ICA, starting from the inferior compartment and advancing superiorly and anteriorly with a blunt tip, right-angled knife. The extent of the exposure can be marked by the optic and maxillary struts, superiorly and inferiorly, respectively. An echo-Doppler device and neuronavigation can be used to enable accurate mapping of the carotid artery. A surgical corridor needs to be developed between the anterior genu/ horizontal ICA and the CNs in the lateral wall of the CS.

To mobilize (from lateral to medial) the cavernous ICA and paraclinoidal ICA, the lateral aspect of the proximal ring requires partial sectioning. Coagulation and division may prove to be necessary in case of an encounter of the arterial branches of the inferolateral trunk. Tumors can be carefully removed between the cavernous ICA and CNs with the assistance of electrostimulation to identify the oculomotor, trochlear, and especially abducens nerves (9).

Discussion

A. Instrumentation:

1. Endoscopic equipment and instruments:

The endoscopic endonasal approach employs a 0-degree endoscope (figure 33), 4-mm in diameter (or 2.7-mm for narrow nostrils), and 18-cm (for nasal stage) or 30 cm (for sellar stage) in length (Karl Storz Endoscopy, Tuttlingen, Germany) (figure 34). Angled endoscopes (30° and 45°) can be used to achieve a larger visual field in the parasellar area. A digital endoscopic 3-CCD FullHD video camera (35) connected to the endoscope provides clear endoscopic images and the capacity for digital archiving. A cleaning system with pedal control is used to reduce the necessity of removing the telescope from the nasal cavity to clean the lens every time vision becomes unclear (75).

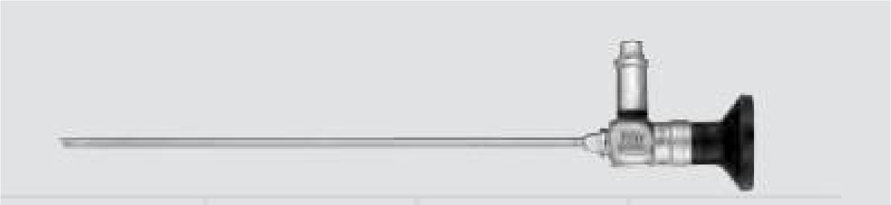

Figure 33: Karl Storz HOPKINS 0 degree rigid telescope: (73)

Figure 34: karl storz basic set including monitor, camera control unit, light source & light cable (73)

Figure 35: Karl storz 3-CCD FullHD video camera (74)

At the end of the approach phase and during the tumor removal phase, some authors (106) use a mechanical holder for the endoscope to allow the surgeon to work with both hands. The camera zoom allows a close-up view of anatomical features of better definition and the positioning of the endoscope further away from the surgical field, reducing the risk of contamination of the tip of the telescope. Surgical instruments must be in order so that they may be inserted parallel to the endoscope and must be equipped with variously angled tips in order to provide vision at corners (77). We employed a high-speed electric micro drill to open bone (Anspach, Palm Beach Gardens, Florida, USA) (figure 36). It is equipped with an extra-long, low-profile handpiece (3–4mm diameter, 15 cm long, and 20° angle attachment), and a diamond burr of small diameter (2–4 mm).

Figure 36: **ANSPACH EG1 High Speed Electric System (178)**

Instruments used for the standard endoscopic transsphenoidal approach (Karl Storz Endoscopy, Tuttlingen, Germany) can be used for extended approaches. Specifically designed skull base instrumentation has been developed, equipped with variously shaped and longer tips, offering a deeper access to pathological material and enabling more effective dissection.

2. Technical Adjuncts:

Although much success has been achieved in the field of endoscopic endonasal surgery, there remains a need for image-guided systems, providing information for midline orientation and trajectory, and offering precision in defining the extent of planum removal. Echo-Doppler (figure 37) enable the precise localization of the ICA before the incision of the CS wall and its visualization within the tumor stroma, as well as allow maximum navigation of the operative field (76).

Figure 37: mizuho vascular Doppler systems. (79)

Modern neuronavigation (figure 38) systems using a magnetic field, termed magnetic digitizers, help the identification of the lesion and its location relative to crucial neural structures and decide on the optimal trajectory. They are especially suitable for endoscopy by allowing more continuous navigation and avoiding interruptions due to the body of the surgeon and/or the endoscope itself coming between the pointer and the optic system.

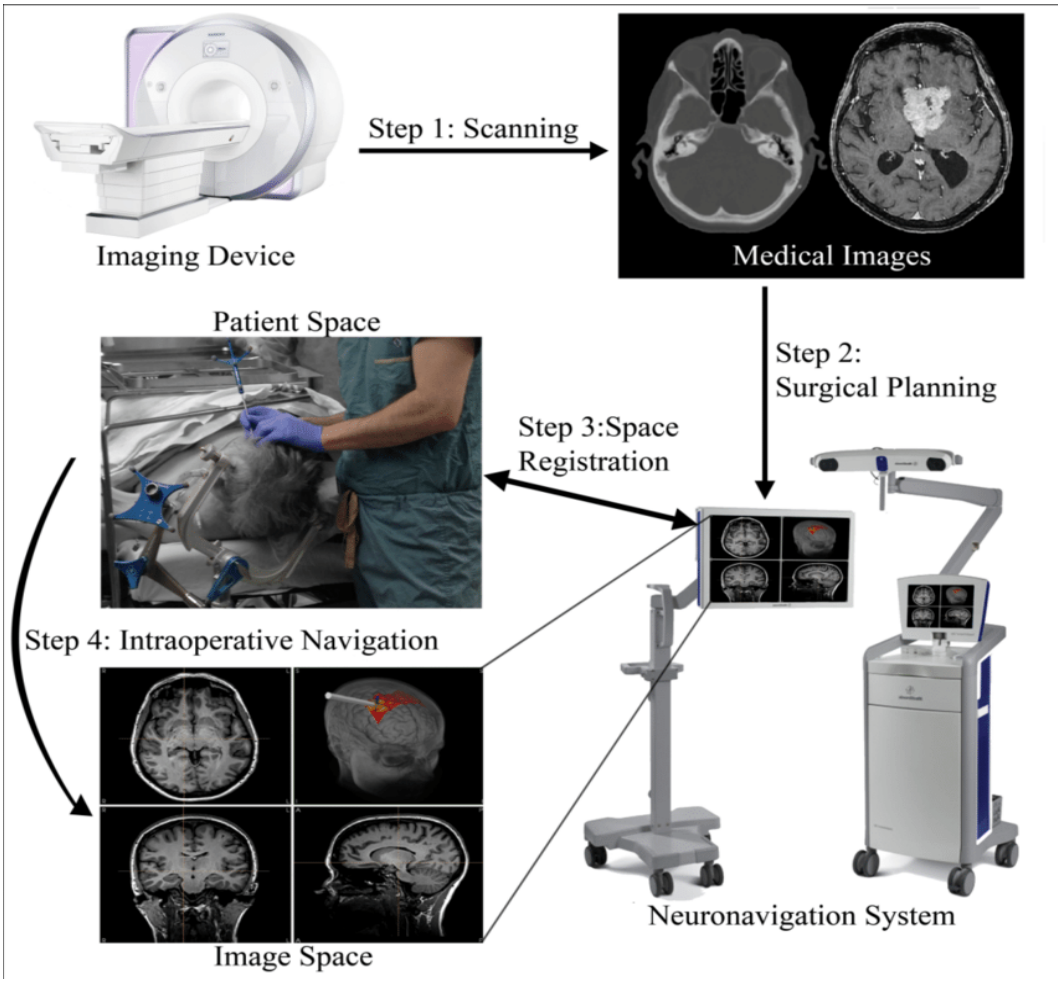

Figure 38: workflow of traditional neuronavigation (80)

Intraoperative MRI or CT scans are useful additions to surgery, providing a more objective assessment of the resection level of a tumor and its relationship with surrounding tissues.

B. Indications:

A wide variety of lesions can involve the CS. The most commonly encountered is pituitary adenoma invading the medial wall of the CS, followed by meningiomas extending into the CS or arising from its walls. Primary tumors arising within the CS are rare and include lymphoma, schwannoma, hemangioma, and chondrosarcoma.

Based on the general surgical rule of removing extradural tumors by an extradural approach, many authors (81) believe that endoscopic endonasal CS surgery should be used in case of lesions with an extradural location. In the case of Macroadenoma, the presence and extent of CS involvement are defined during surgical planning. The Knosp-Steiner classification provides a useful determination of the extent of tumor invasion relative to the ICA. If complete tumor resection is a surgical goal, the presence of tumor within the lateral CS may indicate a transpterygoid approach for lateral exposure (82).

The use of an extradural approach allows the avoidance of any brain manipulation, and access to the CS through its medial wall in its sellar or sphenoidal part which is devoid of any cranial nerves, and surgical proceeding through surgical corridors with no or low risk of cranial nerve damage. In the case of intradural growth, a craniotomic approach or a combined or multistaged craniotomic and endoscopic approach would be preferred.

C. Surgical techniques:

Tumors involving the cavernous sinus might be approached by different surgical techniques: the midline transsphenoidal endoscopic approach (MTea), the ethmoid- pterygoidsphenoidal endoscopic approach (EPSea) and only occasionally the trans- maxillopterygoid endoscopic approach (TMPea) (figure 39).

The selected approach depends on the compartments involved by the tumor. An MTea is more adapted to lesions invading the medial and posterosuperior compartments. When located in the anteroinferior and lateral compartments or invading the entirety of the CS, tumors are best approached by the EPSea. Otherwise, a tumor extending from the lateral compartment through the foramen rotundum to the pterygo- maxillary fossa need the use of the TMPea.

Figure 39: Illustration depicting the endoscopic endonasal approaches to the CS. (A) Transsphenoidal transsellar approach. (B) Transethmoidal transsphenoidal parasellar approach. (C) Transmaxillary transpterygoid approach. (82)

1. Positioning and preparation of the patient:

Surgery is performed under general anesthesia using orotracheal intubation. The periumbilical skin is routinely prepared for future harvest of a free fat graft. Preoperatively, 4% cocaine is applied to cottonoid pledgets to prepare the nasal cavity (figure 40). As indicated by certain authors, as Th. Schwartz a lumbar puncture or lumbar drain with intrathecal fluorescein administration is used to assist in detecting intraoperative cerebrospinal fluid leaks (CSF).

In the extended approaches, a 3-point Mayfield–Kees skeletal fixation is used, and the patient's head is turned 10°–15° toward the surgeon, who is usually on the right side of the patient.

It is recommended that the neck be extended or flexed for approximately 10°–15° during surgery. The extension is necessary for suprasellar approaches, which require a more anterior trajectory so that the endoscope and surgical instruments will not hit the patient's chest.

It is useful for delineating the extent of tumors and their relationship to the carotid artery with magnetic resonance imaging (MRI) and computed tomography angiography.

The oropharynx is packed with moist gauze to prevent blood and secretions from the operative site to reach the stomach.

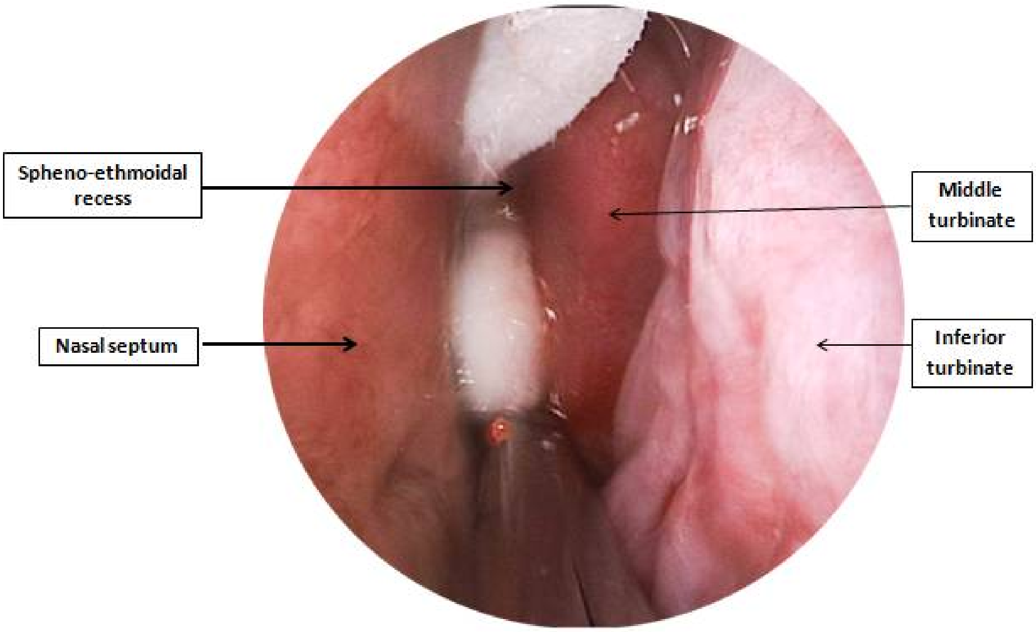

Figure 40: preoperative preparation of the nasal cavity by applying cotton soaked with naphazolin in the sephenoethmoidal recess

2. Approaches:

2.1. Midline Transsphenoidal Endoscopic Approach

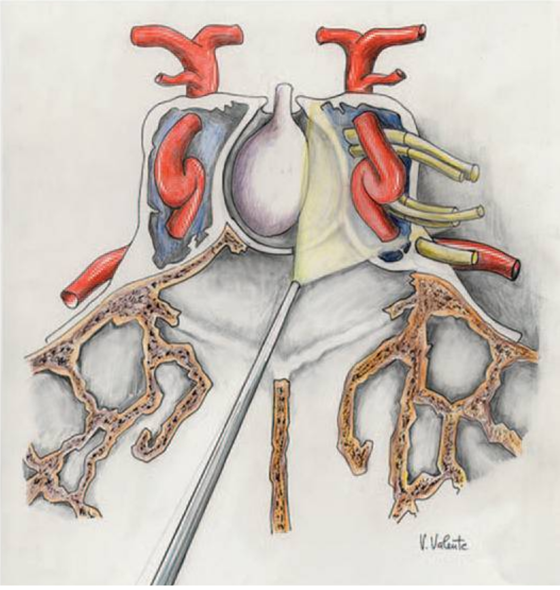

Figure 41: schematic drawing of the transsphenoidal endoscopic approach: (83)

The transsphenoidal transsellar approach (figure 41) to the CS has substantial overlap with the endoscopic approach for resection of pituitary tumors, and is used to completely remove a pituitary adenoma that has invaded the CS. The surgical procedure can be divided into 3 stages: approach phase, tumor removal and closure.

2.1.1. Stage I: Approach Phase

With the use of a 0-degree endoscope, the inferior margin of the middle turbinate is followed toward the nasopharynx to expose the posterior nasal cavity and the choana. The lateral dislocation of the middle (figure 42) and upper turbinate allows identification of the sphenoethmoidal recess and the sphenoid ostium which sometimes is hidden by the superior turbinate (figure 43).

Figure 42: Lateralization of the Middle turbinate

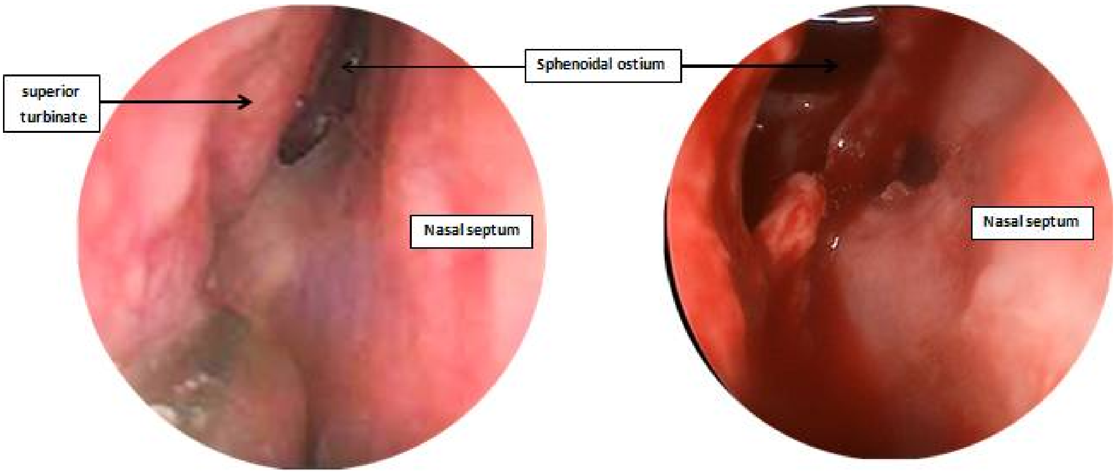

Figure 43: exposure of the right sphenoidal ostium after the removal of the inf 1/3 of the sup turbinate

A posterior septectomy (figure 44) is performed to permit a 2-nostril, 4-handed surgical technique and greater maneuverability of surgical instruments, by coagulation of the posterior nasal mucosa from 5mm above the choana superiorly to the sphenoid ostium, and extending the coagulated area to the corresponding portion of the nasal septum (1–5–2 cm circa) (75). The shaver is very useful in this stage of surgery and allows a bloodless exposure of the sphenoethmoidal recess.

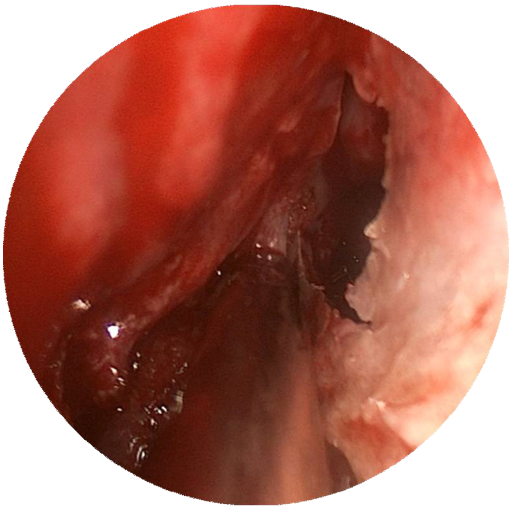

Figure 44: Removal of the posterior part of the nasal septum:

The anterior sphenoidotomy is begun by progressive enlargement of the sphenoid ostium to access the contralateral one or by drilling the sphenoidal rostrum. This sphenoidotomy (figure 45) should be wide, extending from the roof to the floor of the sphenoid sinus vertically and exceeding the sphenoidal ostia laterally . All the sphenoidal septa have to be removed. The sphenoidal mucosa may be preserved because the wide opening of the natural ostia avoids the risk of postoperative mucocele; preserving the mucosa permits a faster postoperative stabilization of the sphenoid cavity with a decreased incidence of sphenoidal inflammatory sequels (4).

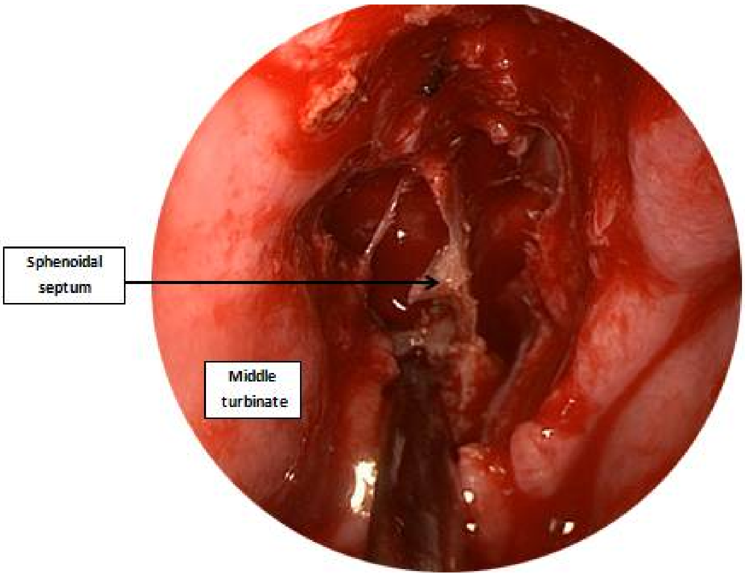

Figure 45: opening of the sphenoid sinus:

The recognition of some landmarks is important for the correct orientation and bone opening: the sellar floor is at the center, the sphenoethmoid planum above it and the clival indentation below; the bony prominences of the optic nerve above and the intracavernous carotid artery (ICA) below are identified lateral to the sellar floor, between them, the lateral opto-carotid recess, molded by pneumatization of the optic strut of the anterior clinoid process.

The opening of the sellar floor (figure 46) is performed using a drill and is enlarged using the Kerrison rongeur. It should be wide, from the superior to the inferior intercavernous sinus and from one cavernous sinus to the other. The bone overlying the invaded cavernous sinus must be carefully removed (figure 47) from the optic- carotid recess to the paraclival carotid protuberance vertically and 1 cm laterally to the sella, exposing the main bulge of the parasellar carotid artery.

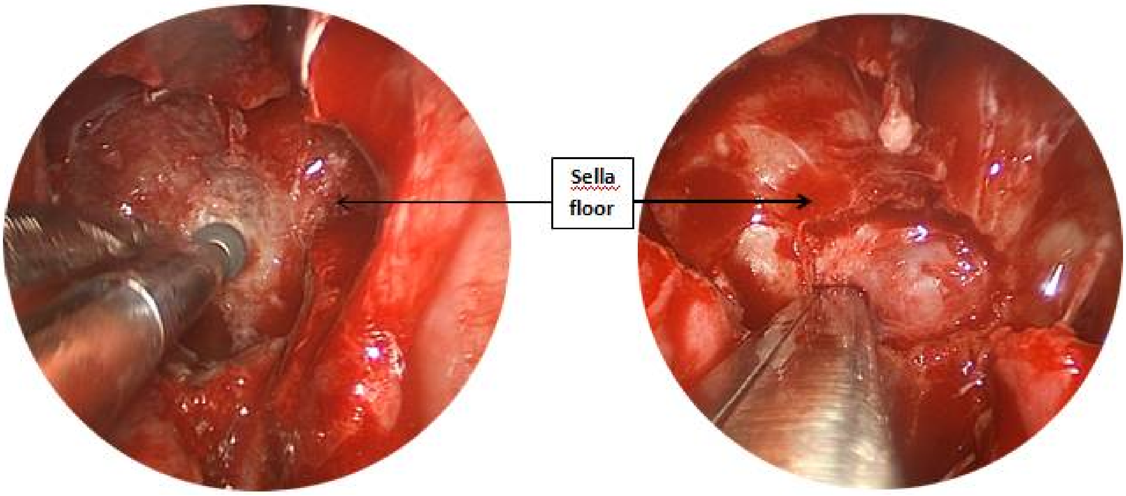

Figure 46: Opening of sella floor with drill and enlargement with Kerisson

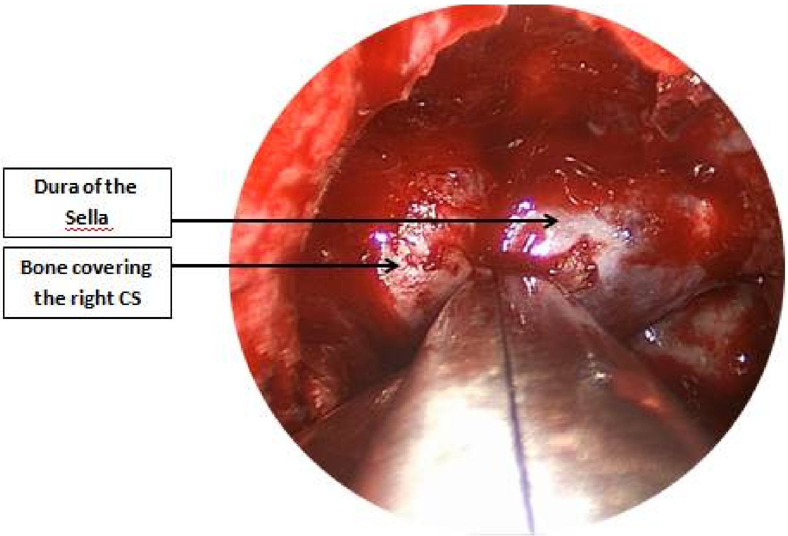

Figure 47: removal of the anterior and inferior wall of the left CS

2.1.2. Stage II: Exposure of the CS and tumor removal.

The dural opening (figure 48), in a cruciate fashion, starts in the sellar area, and the sellar part of the tumor is resected first. Then the lateral wall of the sella is explored with the use of an angled ring curette bent in a “hockey-stick” configuration. A defect is frequently encountered by palpation alone which indicates the site of CS invasion (82). Then we enlarge the defect of the medial wall created by the tumor itself, or more rarely, make an incision in the medial wall in a safe area (which is normally located in the posterior two-thirds of the medial wall). Recognition of this ‘safe’ area requires identification of the bulge of the tumor and accurate mapping of the course of the ICA by using direct vision, micro-Doppler, and neuronavigation (4).

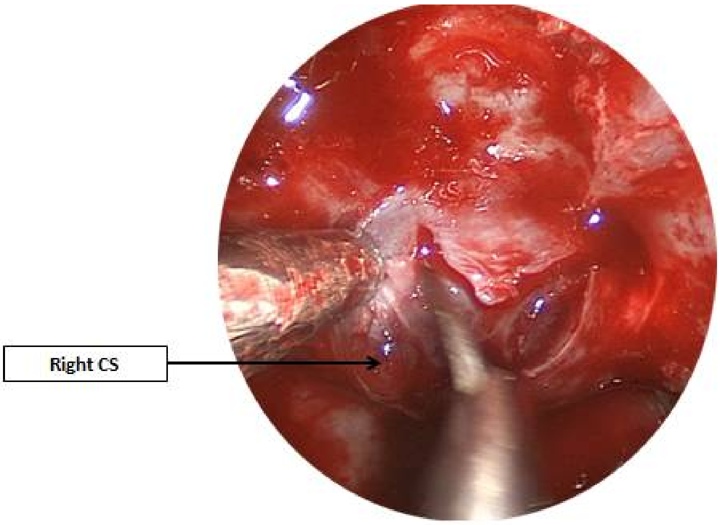

Figure 48: opening of the dura of the sella:

Switching from a 0-degree endoscope to a 30° angled one allows the visualization beyond the edge of the sellar opening to identify residual lesions within the cavernous sinus (figure 49) without risk of neural damage. Because the bone has been removed over the CS, the carotid can be gently retracted laterally to increase the exposure of the contents of these compartments.

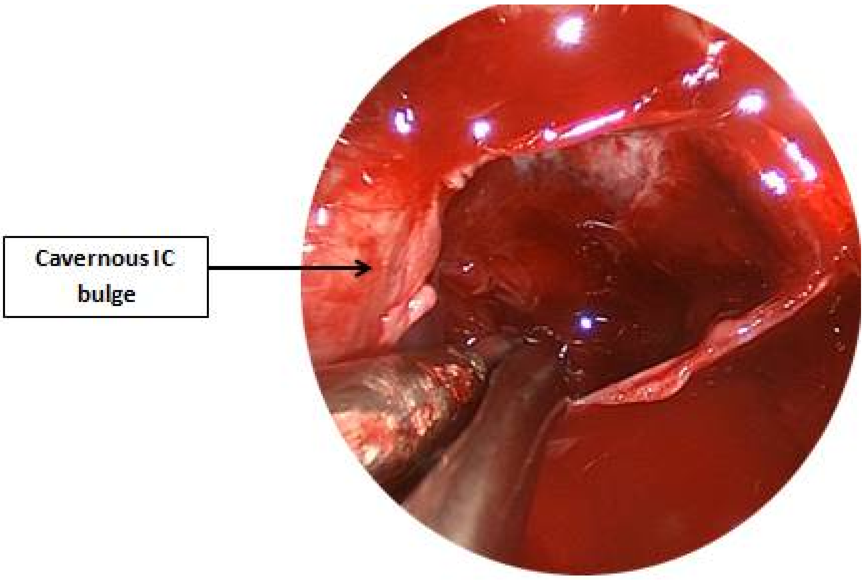

Figure 49: Removal of the right intracavernous part of the Macroadenoma:

2.1.3. Stage III: Exploration and Closure:

At the end of the removal phase, a free-hand exploration into the surgical field using angled 30° and 45° optic scopes is recommended. Once the tumor has been resected, increased venous bleeding may be encountered, which usually responds to packing with cottonoid and application of thrombin-soaked gel foam.

Whenever a CSF leak is detected or suspected, a multilayer repair is performed by applying autologous fat in the cavity, a piece of bone or cartilage (if available) extradurally, and a mucoperiosteal flap across (from the middle turbinate or from the septum) (81) . To have a viable graft the mucosa should be removed and the graft should be applied directly over the bleeding surface (figure 50). Finally, the middle turbinate is returned to its original position. Nasal packing is not routinely required.

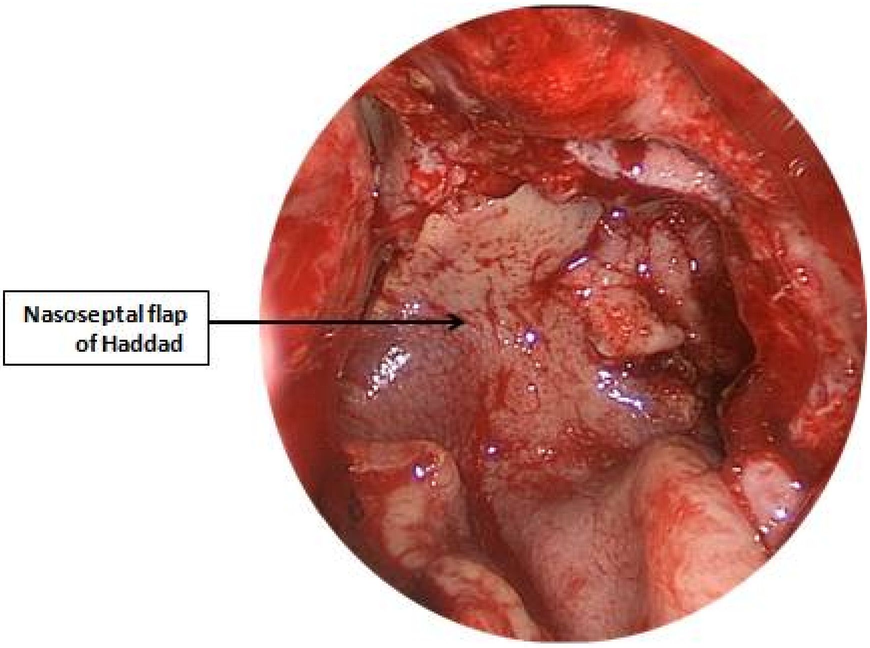

Figure 50: Closure using a left nasoseptal flap

2.2. Lateral approach to the CS: Ethmoido- Pterygo- Sphenoidal Endoscopic Approach (EPSea).

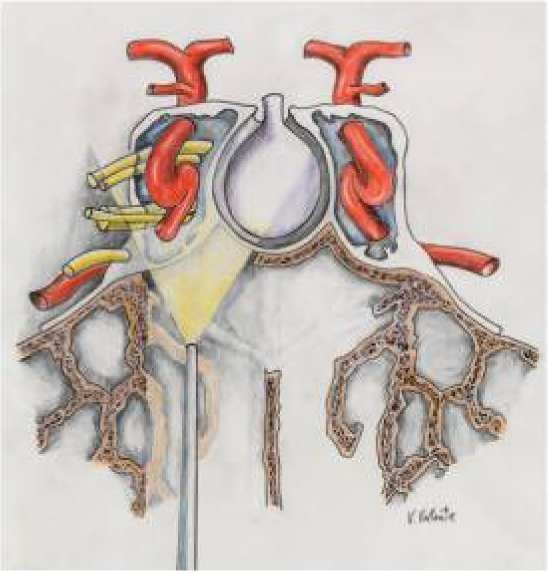

Figure 51: schematic drawing of the ethmoido-pteyro-sphenoidal_endoscopic approach: (83)

EPSea (figure 51) is reserved for tumors invading the anteroinferior and/or the lateral compartments or the entirety of the CS. This procedure is the most versatile, allowing total exposition of the cavernous sinus with the possibility of simultaneous direct control of all of its compartments. The procedure can be schematically divided into 3 stages.

2.2.1. Stage I: the approach to the parasellar area:

It requires an ethmoidal route through a middle turbinectomy (figure 52-53) and complete monolateral ethmoidectomy (figure 54), followed by the sphenoidotomy. The medial portion of the posterior wall of the maxillary sinus is therefore resected to expose the posterior wall of the maxillary antrum and the vertical process of the palatine bone. After coagulation or clipping of pterygopalatine artery in the foramen, the vertical process is drilled out and the medial pterygoid process exposed (84). Its resection allows reaching the inferolateral portion of the CS.

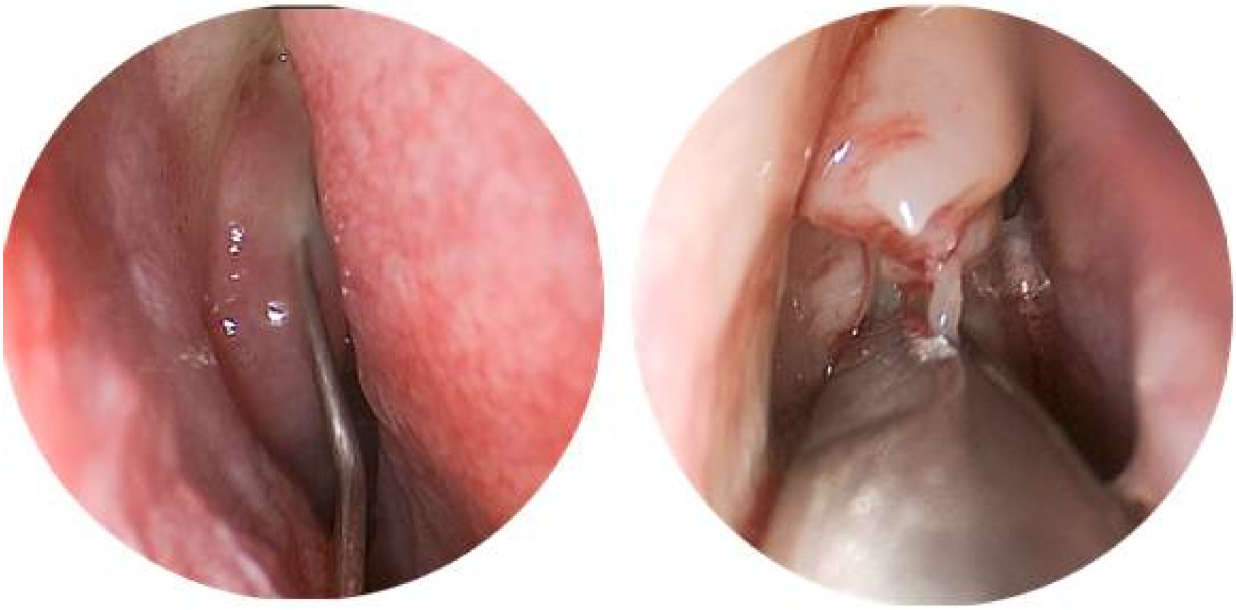

Figure 52: Infiltration and middle turbinectomy:

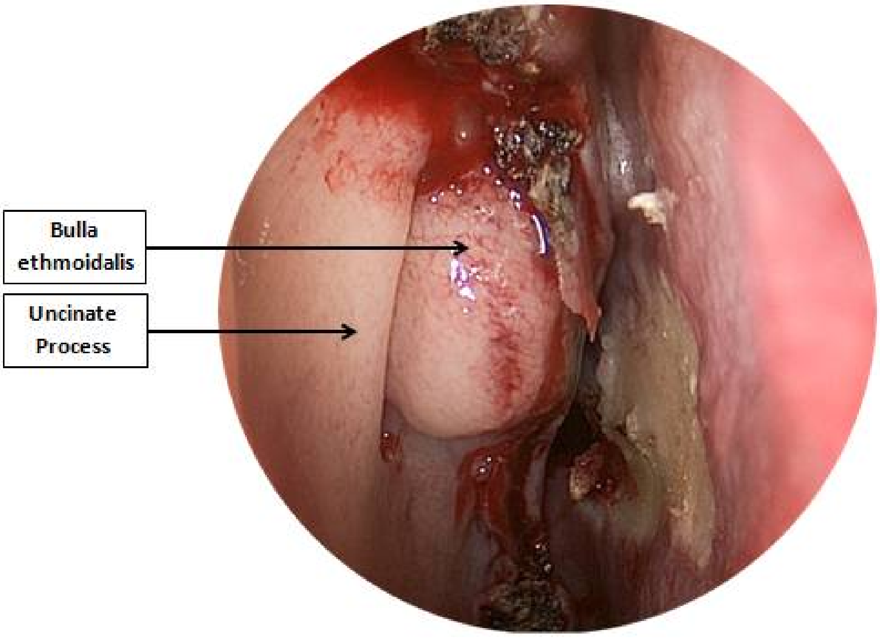

Figure 53: Bulla and uncinate process after removal of the Middle turbinate

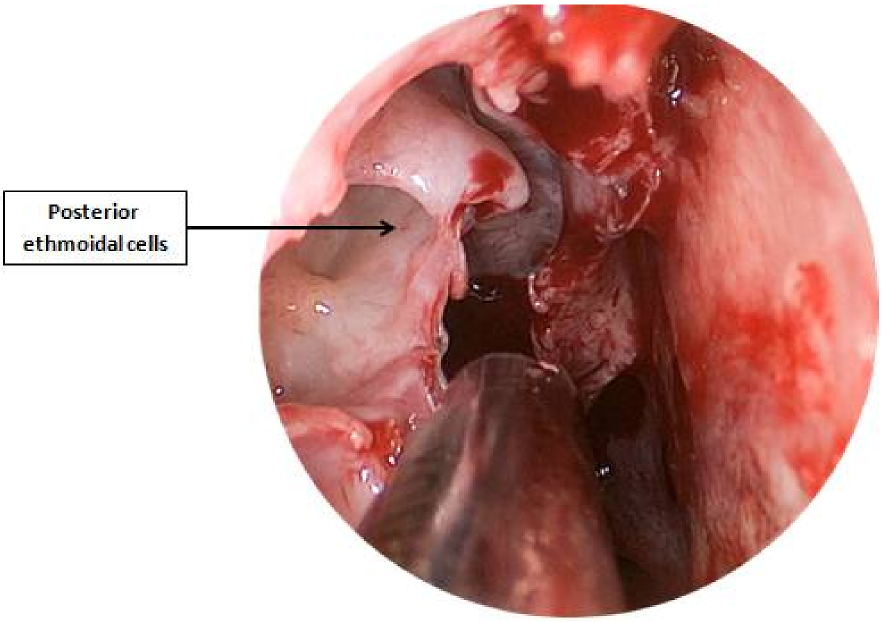

Figure 54: Posterior ethmoidectomy.

2.2.2. Stage II: Opening of the CS and Removal of the Tumor

We divide the opening phase into two steps: removal of the bone in front of the CS, and opening of its dura. To expose the anterior CS (figure 55), a quadrilateral-shaped bone should be removed (posterolateral wall of the sphenoid sinus) located between the optic-carotid recess and the paraclival carotid protuberance medially, and the orbital apex (figure 56) and the trigeminal nerve protuberance laterally. It's mandatory to mark the vidian canal on the floor of the sphenoidal sinus as a landmark (it indicates the junction of the horizontal, petrosal part of the carotid artery with the ascending paraclival segment of the vessel) and, therefore, is a guide to the inferior portion of the cavernous sinus (figure 57) (4).

The use of neuronavigation and echo-Doppler probe allows a safe opening of the inferior cavernous sinus wall (or sphenoidal part of the medial wall) by locating a safe area away from the carotid artery which is usually displaced by the tumor.

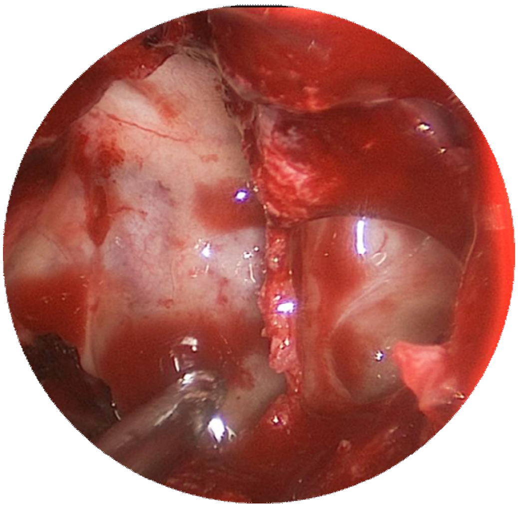

Figure 55: Exposure of sella floor and the anteroinferior wall of the right CS

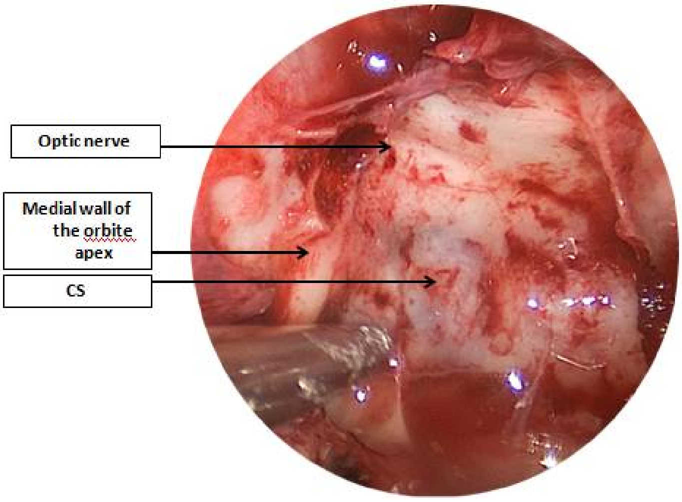

Figure 56: exposure of the CS and medial wall of the orbital apex:

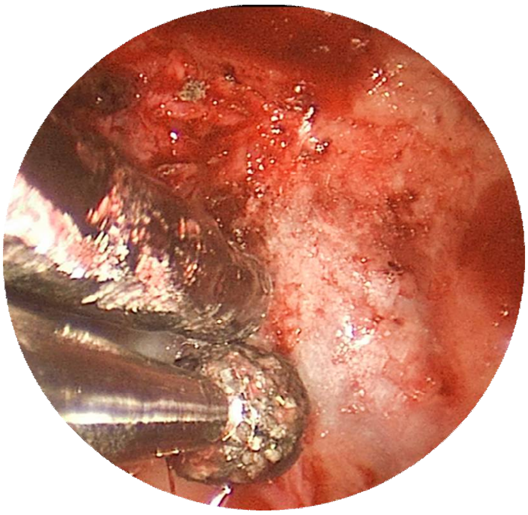

Figure 57: Drilling of the lateral part of anteroinferior wall of the CS

2.2.3. The last stage

Similar to the previous approach, it consists of a final exploration through 30 and 45° angled endoscopes and closure of the surgical defect. Bleeding from the CS is usually not significant and can be controlled with hemostatic absorbable material.

2.3. Pterygo- Maxillary Endoscopic Approach (PMea)

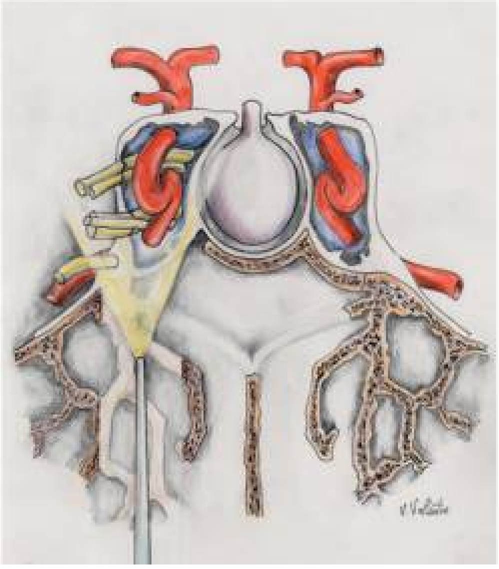

Figure 58: schematic drawing of the petrygo-maxillary endoscopic approach: (83)

The transmaxillary transpterygoid approach (figure 58) is used to gain exposure to lesions of the lateral CS or tumor extending into the pterygomaxillary fossa. It is the combination of an EPSea and an endoscopic medial maxillectomy.

The procedure starts with a sphenoethmoidotomy ipsilateral to the CS involved, followed by resection of the inferior turbinate. Then the vertical portion of the maxillary bone is drilled out and the medial wall of the maxillary sinus is removed (figure 59), allowing a wide exposition of the lateral and posterior wall of the maxillary sinus.

The nasolacrimal duct is transected immediately below the lacrimal sac in order to maintain its patency. The outline of the vidian canal can be identified on the floor of the sphenoid sinus. Careful drilling anteriorly along the superomedial surface of the canal allows preservation of the nerve and associated sphenopalatine ganglion while drilling posteriorly along this same tract leads to the petrous ICA and the foramen lacerum, located below the level of the CS (82). The posterior bone of the maxillary sinus is removed up to the course of the infraorbital nerve, and the periostium of the pterygomaxillary fossa is exposed. The landmarks are the vidian canal with the vidian nerve medially marking the paraclival portion of the ICA; laterally and inferiorly, the maxillary artery and the pterygoid muscles, and superiorly, the infraorbital nerve and the maxillary division following which, by passing through the foramen rotundum, makes it possible to arrive in the inferolateral compartment of the CS (4).

After taking of sphenoid sinus mucosa, and bone removal over the anterior CS proceeds as described previously. Once the CS is entered, the abducens nerve may be identified in the lateral side of the carotid artery. The CN (3rd, 4th, and V1th) within the lateral wall and are less prone to direct injury.

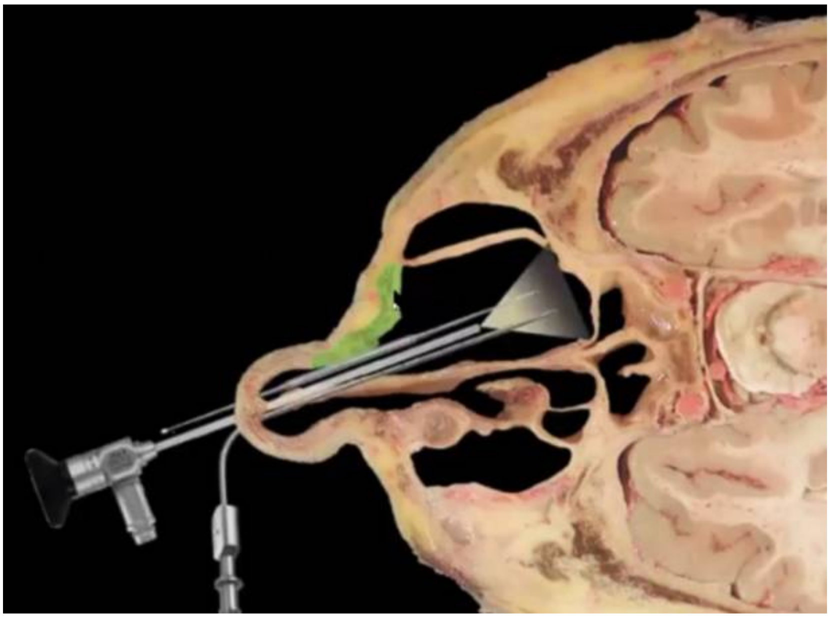

Figure 59: endoscopic medial maxillectomy:

3. Reconstruction:

In all cases with substantial venous bleeding, the addition of intrathecal fluorescein as a surgical adjunct may significantly improve the chance of detecting an intraoperative CSF leak. In the midline approach, whenever a CSF leak is detected or suspected, a multilayer repair is performed by applying autologous fat in the cavity, a piece of bone, or cartilage (if available) extradurally and a mucoperiosteal flap across (figure 60) (from the middle turbinate or from the septum) (81). In the transethmoidal transsphenoidal parasellar approach only the dura of the anterior CS typically opens, and the application of hemostatic agents such as FloSeal (Baxter, Deerfield, IL) may be sufficient closure. Defects resulting from the transmaxillary transpterygoid approach may extend far laterally into the pneumatized sphenoid bone, which predisposes to postoperative CSF leak if the closure is not adequate (82).

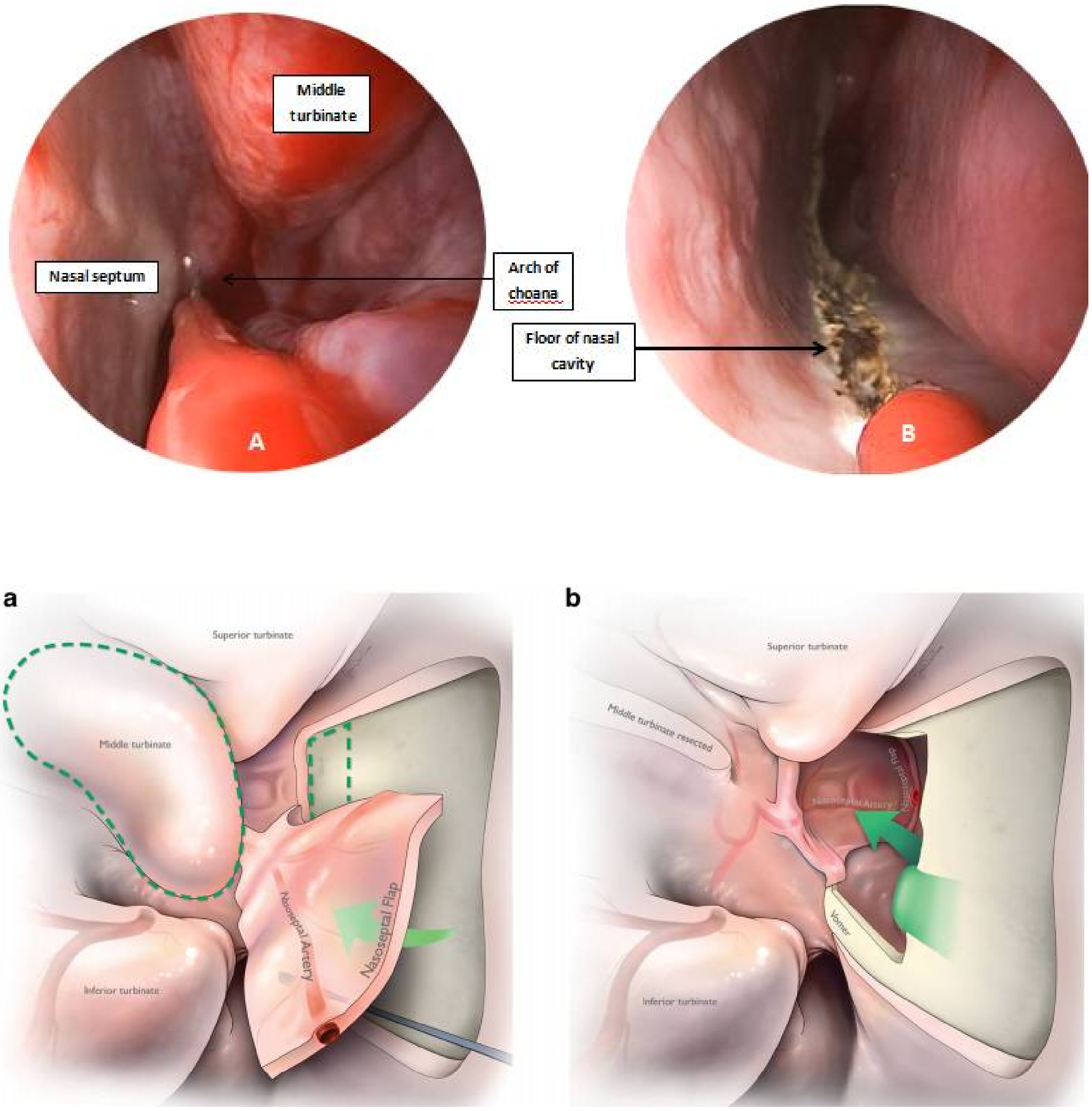

Figure 60: reconstruction of sellar defects with a nasoseptal flap. (A-B) endoscopic view of the harvesting of a right nasoseptal flap starting in the level of choana and running the floor of the nasal fossa. (a) Schematic drawing of the elevation of the NSF from the nasal septum. (b) placement of the NSP into the sellar defect.

4. Complications:

Like in all endonasal surgical procedures, there are rhinological complication to the CS approach including sinusitis, crusting, synechiae, epistaxis, vestibular burns, and orbital injury.

Postoperative CSF leak may be encountered with any approach, as well as subsequent intranial hypotension and meningitis, and particularly the transsellar approach when large dural opening is present, or in the transpterygoid approach when an occult dural entry goes unappreciated.

Beside of theses, the most serious complication during this CS surgery are vascular injuries. Focal venous bleeding is generally controlled with pressure and hemostatic agents, while low-flow arterial bleeding requires control with bipolar cautery.

High-flow arterial bleeding may require immediate embolization for definitive control. Direct injury to the ICA carries a high risk of stroke, although sacrifice may be avoided with the timely application of a covered stent by a neurointerventional radiologist. Pseudoanerysm and dissection of the ICA are additional considerations when the presentation of a cardiovascular event is delayed.

Although dissection of the medial CS theoretically carries decreased risk of CN injury, direct visualization of the area of dissection will help to prevent inadvertent blunt injury or retraction of the neural structures. However, CN might be at risk of injury whenever dissection involves the lateral CS. The abducens nerve is particularly vulnerable because of its more medial course through the lumen of the CS, whereas the other CNs are relatively sheltered within the lateral wall of the CS (82).

Conclusion

The introduction of the endonosal endoscopic approach to the CS allowed a wider exposure of the parasellar region, and offered surgical corridors that were associated with a lower risk of neurovascular injury. Three distinct endoscopic approaches to this structure have been described.

While endonasal endoscopic techniques were linked to a lower rate of operative morbidity and higher rate of resection, a multidisciplinary collaboration between neurosurgeons, radiologists and otolaryngologists is needed, as well as careful preoperative examination of imagery. Neuronavigation and echo-doppler are important adjuncts to CS surgery.

Thorough understanding of the endoscopic anatomy of the CS is crucial in the skull base surgery. Our aim was to add our experience of endoscopic exploration of the CS to the existent studies of the endoscopic anatomy of this structure, and review the endoscopic approaches, their limitations, as well as relevant anatomical landmarks.

Abstracts

Abstract

Title: Cadaveric study of the endoscopic approach of the cavernous sinus

Author: Mouna Youjile

Reporter: Pr Abad Cherif El Asri

Key Words: cavernous Sinus, Cadaveric study, endoscopy

Introduction: CS surgery has always represented a surgical challenge due to the great importance of the surrounding structures and to the high morbidity associated to it. Knowledge of this architecture is essential to perform effective and safe surgery in this region. The introduction of endoscopy in the endonasal transsphenoidal pituitary surgery allowed a wider surgical view, including exposure of the CS and, more recently, to remove tumors located within the CS.

Objective: The aim of this study was to recognize the endoscopic anatomy of the CS and explore the endoscopic endonasal approaches to this structure. This information will facilitate surgical procedures and decrease the rate of surgical complications.

Materials and methods: 3 fresh injected cadavers were studied bilaterally (n = 6). Endoscopic dissections using Karl Storz 0° and 30°, 4 mm, 18 cm, and 30 cm rod lens rigid endoscope were performed in the Skull Base Laboratory at Weill Cornell Medical College in New York USA, to access the CS.

Results: In the 3 cadavers, the CS and superior orbital fissure were exposed with an extended endoscopic endonasal approach. The anteroinferior portion of the CS was exposed by removing the posterior ethmoidal cells and the superior and the middle turbinates (extended endoscopic endonasal transsphenoidal approach). The lateral wall of the CS was exposed by removing the posterior and the anterior ethmoidal cells (endonasal ethmoido-pterygo-sphenoidal approach: far lateral), while the medial wall was exposed by introducing the 30° endoscope through the contralateral nostril (contralateral endoscopic endonasal transsphenoidal approach).

Conclusion: Endoscopic study of the CS in cadaver dissections offers anatomical knowledge that is essential for endoscopic skull base surgery and treatment of various pathologies in this region. In this study, we reviewed the different approaches with an endoscopic view and identify the neurovascular relations.

Résumé

Titre: Etude cadavérique de l'approche endoscopique du sinus caverneux

Auteur: Mouna Youjile

Rapporteur: Pr Abad Cherif El Asri

Mots clés: sinus caverneux, étude cadavérique, endoscopie

Introduction: La chirurgie du **SC** a toujours représenté un défi chirurgical en raison de la grande importance des structures environnantes et de la forte morbidité qui y est associée. La connaissance de cette architecture est essentielle pour effectuer une chirurgie efficace et sûre dans cette région. L'introduction de l'endoscopie dans la chirurgie hypophysaire endonasale transsphénoïdale a permis une vue chirurgicale plus large, y compris l'exposition du **SC** et, plus récemment, la résection des tumeurs situées dans le **SC**.

Objectif: Le but de cette étude était de reconnaître l'anatomie endoscopique du **SC** et d'explorer les approches endonasales endoscopiques de cette structure anatomique. Ces informations faciliteront les interventions chirurgicales et réduiront le taux de complications chirurgicales.

Matériel et méthodes: **3**cadavres frais et injectés ont été étudiés bilatéralement (n = 6). Des dissections endoscopiques utilisant l'endoscope rigide à lentille à tige Karl Storz 0 ° et 30 °, 4 mm, 18 cm et 30 cm ont été réalisées au Laboratoire de la Base du Crane du Collège de Médecine de Weill Cornell à New York, États-Unis, pour accéder au **SC.**

Résultats: Dans les **3** cadavres, le **SC** et la fissure orbitale supérieure ont été exposés avec une approche endonasale endoscopique étendue. La partie antéro-inférieure du **SC** a été exposée en retirant les cellules ethmoïdales postérieures et les cornets supérieurs et moyen (approche endoscopique endonasale transsphénoïdale étendue). La paroi latérale a été exposée en enlevant les cellules ethmoïdales postérieures et antérieures (approche endonasale ethmoïdo-ptérygo-sphénoïdale: latérale), tandis que la paroi médiale a été exposée en introduisant l'endoscope à 30 ° par la narine controlatérale (endoscopie endonasale transsphénoïdale controlatérale).

Conclusion: L'étude endoscopique du **SC** dans les dissections de cadavres offre des connaissances anatomiques essentielles pour la chirurgie endoscopique de la base du crâne et le traitement de diverses pathologies dans cette région. Dans cette étude, nous avons passé en revue les différentes approches du sinus caverneux avec une vue endoscopique en identifiant les relations neurovasculaires.

ملخص

العنوان: دراسة جثة للمقاربة التنظيرية للجيب الكهفي

المؤلف: مونى يوجيل

المشرف: الأستاذ أباد شريف العسري

الكلمات الأساسية: الجيب الكهفي ، تشريح جثة ، التنظير.

مقدمة: لطالما كانت جراحة الجيب الكهفي تمثل تحديًا جراحيًا نظرًا لأهمية التركيبات التشريحية المحيطة والمضاعفات المرتبطة بها. إن معرفة هذه البنية ضروري لإجراء جراحة فعالة وآمنة في هذه المنطقة. أتاح إدخال التنظير الداخلي في جراحة الغدة النخامية عبر الأنف عرضًا جراحيًا أوسع ، بما في ذلك الكشف عن الجيب الكهفي ، ومؤخرًا إزالة الأورام الموجودة داخل الجيب الكهفي.

الهدف: الهدف من هذه الدراسة هو التعرف على التشريح بالمنظار للجيب الكهفي واكتشاف المناهج التنظيرية داخل الأنف لهذا التركيب التشريحي. هذه المعلومات ستسهل العمليات الجراحية وتقلل من معدل المضاعفات الجراحية.

الاساليب والطرق: تم دراسة ثلاث جثث حديثة محقونة ثنائيا (ن=6). التشريح بالمنظار تم باستخدام كارل شتورتس ذو العدسة القضيبية بزاوية 0 ° و 30 ° و 4 مم و18 سم و30 سم في مختبر قاعدة الجمجمة في الجامعة الطبية وايل كورنيل في مدينة نيويورك بالولايات المتحدة الامزيكية للوصول إلى الجيب الكهفي.

النتائج: في الجثث الثلاثة ، تم الكشف عن الجيب الكهفي والشق المداري العلوي من خلال نهج داخلي ممتد بالمنظار. تم الكشف عن الجزء الأمامي السفلي من الجيب الكهفي عن طريق إزالة الخلايا الغربالية الخلفية والتوربينات العلوية والوسطى (نهج تنظيري عبر الأنف و الجيب الوتدي). تم الكشف عن الجدار الجانبي للجيب الكهفي عن طريق إزالة الخلايا الغربالية الخلفية والأمامية (النهج الأنفي الإثمودي - الجناحي - الوتدي: جانبي بعيد) ، بينما تم الكشف عن الجدار الإنسي عن طريق إدخال المنظار الداخلي بزاوية 30 درجة من فتحة الأنف المقابلة (نهج تنظيري عبر الأنف و الجيب الوتدي المقابل).

الخلاصة: توفر الدراسة بالمنظار للجيب الكهفي في تشريح جثة معرفة تشريحية ضرورية لجراحة قاعدة الجمجمة بالمنظار وعلاج الأمراض المختلفة في هذه المنطقة. في هذه الدراسة ، راجعنا الطرق المختلفة للولوج الى الجيب الكهفي بمنظار داخلي وحددنا العلاقات العصبية و الوعائية.

References List

[1] Doglietto, F., Lauretti, L., Frank, G., Pasquini, E., Fernandez, E., Tschabitscher, M., & Maira, G. (2009). *MICROSCOPIC AND ENDOSCOPIC EXTRACRANIAL APPROACHES TO THE CAVERNOUS SINUS. Operative Neurosurgery, 64, ons413–ons422*

[2] Dhandapani, S., Singh, H., Negm, H. M., Cohen, S., Anand, V. K., & Schwartz, T. H. (2016). *Cavernous Sinus Invasion in Pituitary Adenomas: Systematic Review and Pooled*

[3] Demerdash, A., & Tubbs, R. S. (2020). *The Cavernous Sinus. Anatomy, Imaging and Surgery of the Intracranial Dural Venous Sinuses, 135–148.*

[4] Kassam AB, Gardner PA (eds): Endoscopic Approaches to the Skull Base. Prog Neurol Surg. Basel, Karger, 2012, vol 26, pp 119–139

[5] Harris, F. S., & Rhoton, A. L. (1976). *Anatomy of the cavernous sinus. Journal of Neurosurgery, 45(2), 169–180*

[6] Raj, Palaniraj & Smith, Vinayak. (2021). Anatomical Basis of Clinical Manifestations Seen in Cavernous Sinus Syndrome: A Narrative Review. The Open Ophthalmology Journal. 15. 70-78.

[7] https://meetings.ami.org/2018/project/cranial-nerves-within-the-cavernous-sinus/

[8] Alessandra Alfieri, M.D., Hae-Dong Jho, M.D., Ph.D., Endoscopic Endonasal Approaches to the Cavernous Sinus: Surgical Approaches, *Neurosurgery*, Volume 49, Issue 2, August 2001, Pages 354–362

[9] Fernandez-Miranda, J. C., Zwagerman, N. T., Abhinav, K., Lieber, S., Wang, E. W., Snyderman, C. H., & Gardner, P. A. (2018). Cavernous sinus compartments from the endoscopic endonasal approach: anatomical considerations and surgical relevance to adenoma surgery, *Journal of Neurosurgery JNS*, *129*(2), 430-441

[10] Keane JR. Cavernous sinus syndrome. Analysis of 151 cases. Arch Neurol. 1996 Oct;53 (10):967-71.

[11] Bhatkar S, Goyal MK, Takkar A, Mukherjee KK, Singh P, Singh R, Lal V. Cavernous sinus syndrome: A prospective study of 73 cases at a tertiary care centre in Northern India. Clin Neurol Neurosurg. 2017 Apr;155:63-69

[12] Ishikawa H. Clinical anatomy of the cavernous sinus. *Shinkei Ganka (Neuroophthalmol Jpn)* 1996;13:357–63

[13] Yoshihara M, Saito N, Kashima Y, Ishikawa H. The Ishikawa classification of cavernous sinus lesions by clinico-anatomical findings. Jpn J Ophthalmol. 2001 Jul-Aug;45(4):420-4.

[14] Bhatkar S, Goyal MK, Takkar A, Modi M, Mukherjee KK, Singh P, Radotra BD, Singh R, Lal V. Which Classification of Cavernous Sinus Syndrome is Better - Ishikawa or Jefferson? A Prospective Study of 73 Patients. J Neurosci Rural Pract. 2016 Dec;7(Suppl 1):S68-S71.

[15] Toro J, Burbano LE, Reyes S, Barreras P. Cavernous sinus syndrome: need for early diagnosis. BMJ Case Rep. 2015 Mar 27;2015

[16] Fernández S, Godino O, Martínez-Yélamos S, Mesa E, Arruga J, Ramón JM, Acebes JJ, Rubio F. Cavernous sinus syndrome: a series of 126 patients. Medicine (Baltimore). 2007 Sep;86(5):278-281.

[17] Mahalingam HV, Mani SE, Patel B, Prabhu K, Alexander M, Fatterpekar GM, Chacko G. Imaging Spectrum of Cavernous Sinus Lesions with Histopathologic Correlation. Radiographics. 2019 May-Jun;39(3):795-819.

[18] Serioli, Simona et al. “Pituitary Adenomas and Invasiveness from Anatomo-Surgical, Radiological, and Histological Perspectives: A Systematic Literature Review.” *Cancers* vol. 11,12 1936. 4 Dec. 2019

[19] Yang, C., Bao, X. & Wang, R. Role of matrix Metalloproteinases in pituitary adenoma invasion. *Chin Neurosurg Jl* 4, 2 (2018)

[20] Fariselli, L., Biroli, A., Signorelli, A., Broggi, M., Marchetti, M., & Biroli, F. (2016). *The cavernous sinus meningiomas’ dilemma: Surgery or stereotactic radiosurgery? Reports of Practical Oncology & Radiotherapy, 21(4), 379–385.*

[21] Osborn AG. Meningiomas and other nonglial neoplasms. In: Osborne AG, ed. Diagnostic neuroradiology. St Louis, Mo: Mosby-Elsevier Science, 2004; 584–602.

[22] Shaffrey ME, Dolenc VV, Lanzino G, Wolcott WP, Shaffrey CI. Invasion of the internal carotid artery by cavernous sinus meningiomas. Surg Neurol. 1999 Aug;52(2):167-71.

[23] Alhussain ZM, Alharbi SK, Farrash F. Abducens nerve schwannoma of the cavernous sinus: A case report and literature review. Surg Neurol Int. 2020 Nov 25;11:402.

[24] Türe U, Seker A, Kurtkaya O, Pamir MN. Internal carotid plexus schwannoma of the cavernous sinus: case report. Neurosurgery. 2003 Feb;52(2):435-8; discussion 438-9.

[25] Arimoto H, Shirotani T, Nakau H, Hashizume K, Sakai Y, Matsukuma S. Primary malignant lymphoma of the cavernous sinus—case report. Neurol Med Chir (Tokyo) 2000;40(5):275–279.

[26] Ceyhan M, Erdem G, Kanra G, Kaya S, Onerci M. Lymphoma with bilateral cavernous sinus involvement in early childhood. Pediatr Neurol 1994;10(1):67–69.

[27] Huisman TA, Tschirch F, Schneider JF, Niggli F, Martin-Fiori E, Willi UV. Burkitt’s lymphoma with bilateral cavernous sinus and mediastinal involvement in a child. Pediatr Radiol 2003;33(10):719–721.

[28] Hirano H, Tashiro Y, Fujio S, Goto M, Arita K. Diff use large B-cell lymphoma within a cavernous hemangioma of the cavernous sinus. Brain Tumor Pathol 2011;28(4):353–358

[29] Sadruddin S, Medeiros LJ, DeMonte F. Primary T-cell lymphoblastic lymphoma of the cavernous sinus. J Neurosurg Pediatr 2010;5(1):94–97.

[30] Delpassand ES, Kirkpatrick JB. Cavernous sinus syndrome as the presentation of malignant lymphoma: case report and review of the literature. Neurosurgery 1988;23(4):501–504.

[31] Nambiar R, Nair SG. Cavernous sinus syndrome. Proc (Bayl Univ Med Cent). 2017 Oct;30(4):455-456.

[32] Ayer A, Page BR, Lucas JT Jr, Bourland JD, Oliver ER, Tatter SB, Ellis TL, Chan MD. Cavernous sinus metastases treated with gamma knife^{TM} stereotactic radiosurgery. J Radiosurg SBRT. 2014;3(2):131-137.

[33] Post MJ, Mendez DR, Kline LB, Acker JD, Glaser JS. Metastatic disease to the cavernous sinus: clinical syndrome and CT diagnosis. J Comput Assist Tomogr. 1985 Jan-Feb;9(1):115-20.

[34] Wang HY, Chang YL, To KF, Hwang JS, Mai HQ, Feng YF, Chang ET, Wang CP, Kam MK, Cheah SL, Lee M, Gao L, Zhang HZ, He JH, Jiang H, Ma PQ, Zhu XD, Zeng L, Chen CY, Chen G, Huang MY, Fu S, Shao Q, Han AJ, Li HG, Shao CK, Huang PY, Qian CN, Lu TX, Li JT, Ye W, Ernberg I, Ng HK, Wee JT, Zeng YX, Adami HO, Chan AT, Shao JY. A new prognostic histopathologic classification of nasopharyngeal carcinoma. Chin J Cancer. 2016 May 5;35:41.

[35] Abdel Khalek Abdel Razek A, King A. MRI and CT of nasopharyngeal carcinoma. AJR Am J Roentgenol. 2012 Jan;198(1):11-8.

[36] Li, W.-F., Y. Sun, M. Chen, L. Tang, L. Liu, Y. Mao, et al. 2012. Locoregional extension patterns of nasopharyngeal carcinoma and suggestions for clinical target volume delineation. Chin. J. Cancer 31:579–587

[37] Moona MS, Mehdi I. Nasopharyngeal carcinoma presented as cavernous sinus tumour. J Pak Med Assoc. 2011 Dec;61(12):1235-6.

[38] Chidhara SP, Venkateshwaran A. Imaging of Nasopharyngeal Carcinoma with Intracranial Extension. Int J Sci Stud 2014;2(9):117-120.

[39] Huang, C.-C., Fang, F.-M., Chen, H.-C., Hsu, H.-C., Huang, T.-L., Su, Y.-L., & Chang, Y.-C. (2017). *Therapeutic outcome of nasopharyngeal carcinoma with cranial nerve palsy: a single institution experience of 104 patients. OncoTargets and Therapy, Volume 10, 2069–2075.*

[40] Zada, G., Lopes, M. B. S., Mukundan, S., & Laws, E. R. (Eds.). (2016). *Atlas of Sellar and Parasellar Lesions.*

[41] Shi J, Hang C, Pan Y, Liu C, Zhang Z. Cavernous hemangiomas in the cavernous sinus. Neurosurgery. 1999 Dec;45(6):1308-13; discussion 1313-4.

[42] Menon S, Menon RG. Cavernous Carotid Aneurysms: To Do or Not To Do? J Neurosci Rural Pract. 2017 Apr-Jun;8(2):284-287.

[43] Midyett F.A., Mukherji S.K. (2020) Cavernous Carotid Aneurysm. In: Skull Base Imaging. Springer, Cham

[44] Stiebel-Kalish, H., Kalish, Y., Bar-On, R. H., Setton, A., Niimi, Y., Berenstein, A., & Kupersmith, M. J. (2005). *Presentation, Natural History, and Management of Carotid Cavernous Aneurysms. Neurosurgery, 57(5), 850–857*

[45] Seinfeld J, Karim S. Cavernous Sinus Aneurysm. 2021 May 15. In: StatPearls [Internet]. Treasure Island (FL): StatPearls Publishing; 2021 Jan–

[46] Henderson AD, Miller NR. Carotid-cavernous fistula: current concepts in aetiology, investigation, and management. Eye (Lond). 2018 Feb;32(2):164-172.

[47] Adham, Salma et al. “Pathophysiology of carotid-cavernous fistulas in vascular Ehlers-Danlos syndrome: a retrospective cohort and comprehensive review.” *Orphanet journal of rare diseases* vol. 13,1 100. 25 Jun. 2018,

[48] Barrow DL, Spector RH, Braun IF, Landman JA, Tindall SC, Tindall GT. Classification and treatment of spontaneous carotid-cavernous sinus fistulas. J Neurosurg. 1985 Feb;62(2):248-56.

[49] Barrow DL, Spector RH, Braun IF, Landman JA, Tindall SC, Tindall GT. Classification and treatment of spontaneous carotid-cavernous sinus fistulas. J Neurosurg. 1985 Feb;62(2):248-56.

[50] Kim DH, Cho WH, Cho KS, Cha SH. Solitary cavernous sinus neurosarcoidosis mimicking neurosyphilis. J Korean Neurosurg Soc. 2014 Jan;55(1):61-3.

[51] Koffi PN, Ouambi O, El Fatemi N, El Maaquili R. Tuberculome cérébral un challenge diagnostic: à propos d’un cas et mise au point [Cerebral tuberculoma a diagnostic challenge: case study and update]. Pan Afr Med J. 2019 Apr 10;32:176.

[52] Haque, Md & Chowdhury, Forhad & Islam, Md & Khandkar, Ali & Kawsar, Khandkar Ali & Haque, Afm. (2012). Introduction Tuberculomas in the Cavernous Sinus, Temporal Lobe and Basal Subarachnoid Spaces. Journal of Medicine. 13.

[53] Abdolhoseinpour H, Abolghasemi S, Jangholi E, Naghi Tehrani KH. Isolated Oculomotor and Abducens Nerve Palsies as Initial Presentation of Cavernous Sinus Tuberculoma: Case Report and Literature Review. World Neurosurg. 2018 Sep;117:413-418.

[54] Konar, Mithun & Ghosh, Taraknath. (2016). Tuberculoma of Cavernous Sinus - An Atypical Presentation of Neurotuberculosis with Review of Existing Literature. International Journal of Scientific Research. 5. 85 - 88.

[55] Iaconetta G, Stella L, Esposito M, Cappabianca P. Tolosa-Hunt syndrome extending in the cerebello-pontine angle. Cephalalgia. 2005 Sep;25(9):746-50.

[56] Amrutkar C, Burton EV. Tolosa-Hunt Syndrome. [Updated 2020 Aug 10]. In: StatPearls [Internet]. Treasure Island (FL): StatPearls Publishing; 2021 Jan-.

[57] Carreón E, Muñiz S, Di Capua D, Porta-Etessam J. Tolosa-Hunt syndrome with spontaneous remission and recurrence. Neurologia. 2018 Jan-Feb;33(1):68-70.

[58] Kline LB, Hoyt WF The Tolosa-Hunt syndrome *Journal of Neurology, Neurosurgery & Psychiatry* 2001;71:577-582.

[59] Nadarajah, J., Madhusudhan, K. S., Yadav, A. K., Chandrashekhara, S. H., Kumar, A., & Gupta, A. K. (2015). *MR imaging of cavernous sinus lesions: Pictorial review. Journal of Neuroradiology, 42(6), 305–319.*

[60] deShazo RD, O'Brien M, Chapin K, Soto-Aguilar M, Gardner L, Swain R. A new classification and diagnostic criteria for invasive fungal sinusitis. Arch Otolaryngol Head Neck Surg. 1997 Nov;123(11):1181-8.

[61] Knosp E, Steiner E, Kitz K, Matula C. Pituitary adenomas with invasion of the cavernous sinus space: a magnetic resonance imaging classification compared with surgical findings. Neurosurgery 1993;33(4):610–617; discussion 617–618

[62] Case courtesy of Assoc Prof Frank Gaillard, Radiopaedia.org, rID: 71524

[63] https://radiopaedia.org/articles/knosp-classification-of-cavernous-sinus-invasion-by-pituitary-macroadenomas

[64] Kamran Munawar, Gopi Nayak, Girish M. Fatterpekar, Chandra Sen, David Zagzag, Elcin Zan, Mari Hagiwara, Cavernous sinus lesions, Clinical Imaging, Volume 68, 2020, Pages 71-89, ISSN 0899-7071

[65] Hirsch WL, Sekhar LN, Lanzino G, Pomonis S, Sen CN. Meningiomas involving the cavernous sinus: value of imaging for predicting surgical complications. AJR Am J Roentgenol. 1993 May;160(5):1083-8.

[66] https://operativeneurosurgery.com/doku.php?id=cavernous_sinus_meningioma_classification

[67] Yang, CC., Chen, TY., Tsui, YK. *et al.* Primary marginal zone B-cell lymphoma of the cavernous sinus: a case report and review of the literature. *BMC Med Imaging* 21, 25 (2021).

[68] Gagliardi, D., Faravelli, I., Villa, L., Pero, G., Cinnante, C., Brusa, R., … Corti, S. (2018). *Bilateral Cavernous Carotid Aneurysms: Atypical Presentation of a Rare Cause of Mass Effect. A Case Report and a Review of the Literature. Frontiers in Neurology,*

[69] Henderson AD, Miller NR. Carotid-cavernous fistula: current concepts in aetiology, investigation, and management. *Eye (Lond)*. 2018;32(2):164-172

[70] Weerasinghe D, Lueck CJ. Septic Cavernous Sinus Thrombosis: Case Report and Review of the Literature. *Neuroophthalmology*. 2016;40(6):263-276.

[71] Kim DH, Cho WH, Cho KS, Cha SH. Solitary cavernous sinus neurosarcoidosis mimicking neurosyphilis. *J Korean Neurosurg Soc*. 2014;55(1):61-63.

[72] Abuzayed B, Tanriover N, Gazioglu N, Ozlen F, Cetin G, Akar Z. Endoscopic anatomy and approaches of the cavernous sinus: cadaver study. Surg Radiol Anat. 2010 Jun;32(5):499-508.

[73] https://www.karlstorz.com/cps/rde/xbcr/karlstorz_assets/ASSETS/3331211.pdf

[74] https://images.app.goo.gl/Q1Aqxo8LdJyDEJwR6

[75] De Divitiis, E., Esposito, F., Cappabianca, P., Cavallo, L. M., & de Divitiis, O. (2009). *Extended endoscopic endonasal transsphenoidal approach to supra-parasellar tumors. Cavernous Sinus, 75–86*

[76] Frank G, Pasquini E. Endoscopic endonasal cavernous sinus surgery, with special reference to pituitary adenomas. Front Horm Res. 2006;34:64-82

[77] Dolenc, V. V., & Rogers, L. (Eds.). (2009). *Cavernous Sinus.*

[78] https://www.jnjmedicaldevices.com/en-EMEA/product/anspach-eg1-electric-system

[79] http://www.mizuhomedical.co.jp/products/?id=1461299942-673127

[80] Brain Shift in Neuronavigation of brain tumours: A Review - Scientific Figure on ResearchGate.

[81] https://entokey.com/endoscopic-pituitary-surgery-in-the-cavernous-sinus/

[82] McCoul, E. D., Anand, V. K., & Schwartz, T. H. (2011). *Endoscopic approaches to the cavernous sinus. Operative Techniques in Otolaryngology-Head and Neck Surgery, 22(4), 263–268.*

[83] Cavallo, L. M., Cappabianca, P., Galzio, R., Iaconetta, G., de Divitiis, E., & Tschabitscher, M. (2005). *Endoscopic Transnasal Approach to the Cavernous Sinus versus Transcranial Route: Anatomic Study. Operative Neurosurgery, 56, 379–389.*

[84] Cappabianca, P., Cavallo, L. M., de Divitiis, O., & Esposito, F. (Eds.). (2016). Midline Skull Base Surgery.

Serment d'Hippocrate

Au moment d'être admis à devenir membre de la profession médicale, je m'engage solennellement à consacrer ma vie au service de l'humanité.

- *Je traiterai mes maîtres avec le respect et la reconnaissance qui leur sont dus.*
- *Je pratiquerai ma profession avec conscience et dignité. La santé de mes malades sera mon premier but.*
- *Je ne trahirai pas les secrets qui me seront confiés.*
- *Je maintiendrai par tous les moyens en mon pouvoir l'honneur et les nobles traditions de la profession médicale.*
- *Les médecins seront mes frères.*
- *Aucune considération de religion, de nationalité, de race, aucune considération politique et sociale ne s'interposera entre mon devoir et mon patient.*
- *Je maintiendrai le respect de la vie humaine dès la conception.*
- *Même sous la menace, je n'userai pas de mes connaissances médicales d'une façon contraire aux lois de l'humanité.*
- *Je m'y engage librement et sur mon honneur.*

قسم أبقراط

بسم الله الرحمان الرحيم

أقسم بالله العظيم

في هذه اللحظة التي يتم فيها قبولي عضوا في المهنة الطبية أتعهد علانية:

- بأن أكرس حياتي لخدمة الإنسانية .
- وأن أحترم أساتذتي وأعترف لهم بالجميل الذي يستحقونه .
- وأن أمارس مهنتي بوازع من ضميري وشرفي جاعلا صحة مريضي هدفي الأول .
- وأن لا أفشي الأسرار المعهودة إلي .
- وأن أحافظ بكل ما لدي من وسائل على الشرف والتقاليد النبيلة لمهنة الطب .
- وأن أعتبر سائر الأطباء إخوة لي .
- وأن أقوم بواجبي نحو مرضاي بدون أي اعتبار ديني أو وطني أو عرقي أو سياسي أو اجتماعي .
- وأن أحافظ بكل حزم على احترام الحياة الإنسانية منذ نشأتها .
- وأن لا أستعمل معلوماتي الطبية بطريق يضر بحقوق الإنسان مهما لاقيت من تهديد .
- بكل هذا أتعهد عن كامل اختيار ومقسما بالله .

والله على ما أقول شهيد .

المملكة المغربية
جامعة محمد الخامس بالرباط
كلية الطب والصيدلة
الرباط

سنة : 2021
أطروحة رقم: 171

دراسة جثة للمقاربة التنظيرية للجيب الكهفي

أطروحة

قدمت ونوقشت علانية يوم : / /2021

من طرف

السيدة مونى يوجيل

المزدادة في 21 شتنبر 1995 بمكناس

لنيل شهادة

دكتور في الطب

الكلمات الأساسية : الجيب الكهفي؛ تشريح جثة؛ التنظير

أعضاء لجنة التحكيم:

السيد ميلودي كزاز أستاذ في جراحة الدماغ والأعصاب	**رئيس**
السيد عباد الشريف العسري أستاذ في جراحة الدماغ والأعصاب	**مشرف**
السيد ياسر أرخا أستاذ في جراحة الدماغ والأعصاب	**عضو**
السيد عادل بلهاشمي أستاذ في جراحة الدماغ والأعصاب	**عضو**
السيد محمد زلاغ أستاذ في أمراض الأنف والأذن والحنجرة	**عضو**